An Investigation

of the

PROFILES OF BURSTS

OF SOLAR RADIO NOISE

A thesis presented for the degree of

Master of Science

of Rhodes University

by

P.A.T.Wild B.Sc.(Hons.) Rhodes.

Physics Dept.,
Rhodes University,
GRAHAMSTOWN.

December 1959.

CONTENTS.

Contents (cont.)

The Rhodes University Radio Telescopes.

On the left is the 300 Mc/s broadside array: on the right is the 125 Mc/s helix mounted above the apparatus shack.

FRONTISPIECE

HISTORY OF THE PROJECT.

At the beginning of 1957 Dr. E. F. Stack Forsyth of the Physics Dept., Mr. W. Shuter (M. Sc. student) and Mr. J. O. Speedy (C. S. I. R. Technical Assistant) commenced the construction of the first channel of a three-channel swept-frequency radio receiver for the study of solar noise. Due to difficulties experienced with the construction of the swept-frequency receiver, it was decided in mid-year to construct a single-frequency receiver as an interim measure, in order to obtain results during the I. G. Y.

By the end of the year the receiver was completed: it comprised a wide-band helical antenna, superheterodyne receiver tuned at 125 Mc/s, and cathode-ray display. The latter was continuously photographed on 35mm. film. The antenna and the shack housing the receiver are shown in the Frontispiece.

In January 1958, L. M. G. Poole and the author commenced the construction of a similar receiver to operate at a frequency of 300 Mc/s. During the early part of the year a windmill tower was dismantled, transported to the site of the 125 Mc/s receiver, and reassembled there. Work on the component amplifiers of the receiver was begun, and the antenna mounting

was constructed at the University Engineering workshops.

Considerable difficulty was experienced in constructing a reliable preamplifier to operate at 300 Mc/s, and this delayed the project to such an extent that it was not until the end of the year that the receiver, except for the preamplifier, was completed.

In February 1959 Poole took on the post of C.S.I.R. Technical Assistant, and his contributions to the project, in this capacity, are designated by "Poole (T/A)".

During the early part of 1959 Dr. Stack-Forsyth designed and built a preamplifier which operated satisfactorily; final testing and matching of the antenna was now possible, and the "time-tape" machine for control of the antenna drives was devised, constructed and tested, together with power supplies and regulators for the new preamplifier.

The first daily record of solar radiation at a frequency of 300 Mc/s was obtained on 24/6/59. After several records had been obtained it was decided to boost the gain of the receiver by construction of an additional I.F. stage.

The projects originally envisaged were the following:

Poole: A study of the "thermal component" of solar radio noise and of "enhanced radiation", and correlation with visual solar phenomena.

Wild: A study of "noise storms" and "outbursts" of solar radio noise, and correlation with visual solar phenomena.

By the time the equipment was operating it was decided that more worthwhile projects could be undertaken by converting the 125 Mc/s receiver to 150 Mc/s and thus obtaining simultaneous records on two frequencies of which one was the first harmonic of the other.

Poole (T/A) commenced the construction of a 150 Mc/s preamplifier and first detector unit, but by September this was not yet completed. The author therefore decided to revert to a single-frequency project, namely the study of noise storm profiles at a frequency of 300 Mc/s. The results of this study are presented in the following pages.

NOTE ON THE DIVISION OF LABOUR.

The contributions of each member of the team to the research project are listed below:

P.A.T.Wild. Design, construction and adjustment of preamplifier Mk.I. and preamplifier Mk.II. Construction and adjustment of H.T. and L.T. regulators for the preamplifier (later discarded). Completion of E.H.T. supply designed by Shuter. Construction of C.R.O. Design, construction and adjustment of transistor-regulated L.T. supplies for the preamplifier. Design, construction and testing of noise-diode calibrating unit. Construction and adjustment of additional stage for the I.F. amplifier. Shack-mast wiring.

Part construction and testing of antenna. Part construction of mast. Part calculation and manufacture of "time tapes".

L.M.G.Poole. Design, construction and adjustment of I.F. amplifier and D.C. amplifier. Construction and adjustment of Mk.IV preamplifier. Interwiring in the apparatus shack. Design of antenna drive. Extension of camera drive. Design, construction and adjustment of balun transformer.

Part construction of mast. Part construction and testing of antenna.

Dr. E.F.Stack-Forsyth: Design and construction of preamplifier Mk.III and preamplifier Mk.V. General supervision in the constructional phase of the project.

L.M.G.Poole (T/A): Part construction of Mk.V preamplifier. Part calculation and manufacture of "time-tapes". Additions to the transistor-regulated L.T. power-supplies. Reconstruction of I.F. amplifier. Operation and maintenance of the equipment.

ACKNOWLEDGEMENTS.

The author is indebted to the following:

Dr. E.F.Stack-Forsyth for directing the research, and particularly for generously giving up his free time to help in the constructional phase of the work.

Prof. J.A Gledhill for helpful criticism and advice at all times.

Mr A.R.Scanlen and Mr G. Walters of the Physics Dept. Workshop for assistance and advice with regard to the construction of the antenna and camera drives.

Mr J.West of the Engineering Workshop for construction of the antenna mounting and drive systems, and for help and advice in mounting these on the mast.

The C.S.I.R. for a research grant and bursary during 1958.

SUMMARY.

Chapter I. The general characteristics of solar radiation at metre wavelengths are described, with reference to data published in the literature. A brief description of some aspects of solar physics relevant to the study of solar noise is given, and the literature relating to the correlation of radio effects with solar disturbances is reviewed.

Chapter II. A concise description of the apparatus constructed for the continuous recording of the flux density of solar radio noise at a frequency of 300 Mc/s is given, with some mention of difficulties experienced, and how these were overcome. Full circuit diagrams of electronic apparatus, and illustrative photographs, are supplied.

Chapter III. The development of theories of the origin and propagation of solar noise radiation is historically reviewed, and the success of each theory in explaining or predicting observed phenomena, is assessed. A working model is chosen from among these theories, and reasons for its adoption are given.

Chapter IV. Observations made by the author of solar radiation at a frequency of 300 Mc/s are described,

together with a description of the objects and methods of analysis of the records.

Chapter V. Phenomena observed by the author are compared with those observed by other workers. It is concluded that storm bursts are caused by transients similar to those producing Type II and Type III bursts, and a model for the production of storm bursts is tentatively suggested.

Chapter VI. Suggestions for further research, including suggestions for methods of testing the author's conclusions, are made.

CHAPTER ONE

INTRODUCTION.

A. GENERAL CHARACTERISTICS OF SOLAR RADIATION AT METRE WAVELENGTHS.

In the years since about 1945, much evidence has been collected concerning the radio-frequency radiation emitted by the sun.

Payne-Scott (1) showed in 1949 that the radiation at metre wavelengths could be roughly classified as "circularly polarized" and "not circularly polarized" radiation.

Wild and McCready (2), using a receiver operating continuously over the range 70 to 130 Mc/s, found that the radiation consisted of a background varying slowly with time, on which were superimposed sudden increases in intensity, or "bursts" of radiation. They were able to classify these bursts according to properties of their dynamic spectra, as follows.

Spectral Type I. "Storm Bursts".

These are short-lived bursts superimposed on a high slowly-varying background continuum; the whole disturbance is termed a "noise storm", and may last for hours or even for days.

This type of burst is characterised by its narrow spectrum (of the order of a few Mc/s wide), and by the fact that the frequency of maximum intensity remains approximately constant throughout the life-time.

Storm bursts have been shown by Komesaroff (3) to exhibit strong circular polarization, and may be identified with Payne-Scott's "circularly polarized radiation".

Spectral Type II "Outbursts".

The spectrum of this type shows a distinct low-end cut off frequency, which drifts gradually towards lower frequencies, at a rate of about $\frac{1}{4}$ (Mc/s) sec^{-1} The bursts last for several minutes. They may be identified with the so-called "outbursts" defined by Payne-Scott (1) as those bursts typically associated with solar flares (see Section C).

Komesaroff (3) has shown that these bursts are probably unpolarized.

Spectral Type III "Isolated Bursts".

This type of burst is characterised by a rapid drift of the frequency of maximum intensity towards lower frequencies. The rate of drift is of the order of 20 (Mc/s) sec^{-1} The life-times of such bursts are of the order of a few seconds. Payne-Scott (1)

included these bursts in the class of "not-circularly polarized radiation" and they have been thought to be unpolarized.

Komesaroff (3) has shown that, while some of these bursts appear to be unpolarized, many exhibit strong elliptical polarization.

Wild, Murray and Rowe (4) have demonstrated the existence of harmonic pairs in this type of burst, giving rise to the "double-humped" bursts commonly detected on single-frequency records.

New Spectral Types.

"Inverted-U" Bursts. Maxwell and Swarup (5) have published details of a spectral type in which the frequency of maximum intensity decreases with time, reaches a minimum value, and then increases with time.

The bandwidths of the bursts are of the order of 20 Mc/s, and life-times are of the order of 3-10 secs.

"Reverse-Drift Pairs". A new type of burst, which has been called a "reverse-drift pair" or simply "reverse pair", has been identified by Roberts (6). These bursts consist of two short-lived features which drift rapidly to higher frequencies,

in contrast to the negative drift of spectral types II and III.

Appearance on Single-Frequency Records.

Spectral types I, II and III have characteristic forms enabling them to be recognised immediately even on single-frequency records. Plate A shows examples of all three types observed by the author on a frequency of 300 Mc/s.

Type I ("Storm bursts") appear as rapid intensity fluctuations continuing for hours or days, and accompanied by a general increase in the background level.

Type II ("Outbursts") occur sporadically, and consist of rapid intensity fluctuations superimposed on a high background level. They last for a few minutes.

Type III ("Isolated bursts") occur singly or in small groups. They have a characteristic shape, namely a fairly rapid linear rise portion, and a decay portion which has been shown by several workers, (1,7) to be roughly exponential. The characteristic "double-humped" bursts also fall into this class.

B. A Model of the Solar Atmosphere.

In order to understand the postulated mechanisms

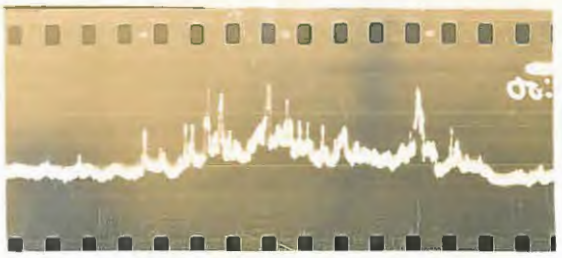

Noise storm, showing a large number of Type I (storm) bursts.

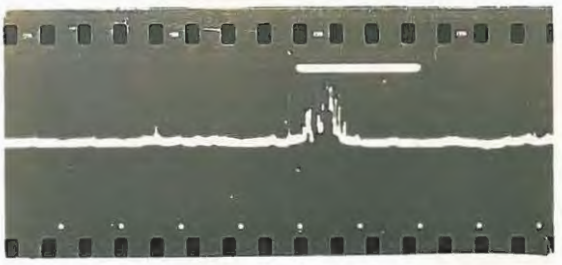

A rather short-lived, moderately intense, Type II burst (outburst).

A typical single-peak Type III burst (isolated burst.)

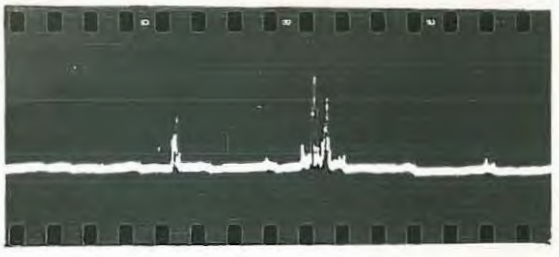

Two complex Type III bursts, each consisting of several peaks.

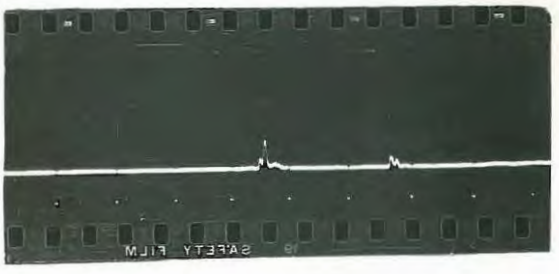

A reversed double-humped burst, followed by a very small double-humped burst.

PLATE A

for the productions of the various types of solar radio bursts, it is necessary that we should describe the chief features of the sun's atmosphere. The outer portion of the sun is divided into three main layers, as follows:

White light is emitted from a thin shell a few hundred kilometres deep and of radius 696,000 km., called the "photosphere". The photosphere is taken as the limit of the sun's disc, and the radius of the photosphere is taken as one solar radius. Photospheric temperatures are of the order of 6000° K.

The photosphere is surrounded by a shell about 10,000 k.m. deep, called the "chromosphere". Temperatures in the chromosphere are somewhat in doubt.

The "corona", the outermost region of the solar atmosphere, stretches from the chromosphere to a distance of many solar radii. It has a characteristic shape at sunspot minimum but becomes very disturbed and less regular in shape at sunspot maximum. The temperature in the corona varies with distance in an unknown manner, and is generally taken as constant (about a million degrees) for the inner corona.

More information is available with regard to the distribution of electron densities in the corona. Baumbach, assuming spherical aymmetry, has developed an expression revised by Allen (8), relating the

electron density (N) to the distance from the centre of the sun in solar radii (r).

$$N = (1.55\ r^{-6} + 2.99\ r^{-16})10^{14} m^{-3}.$$

Some important constants of these regions are listed in Table I.

C. SOLAR DISTURBANCES

Sunspots. These are the most prominent of solar disturbances. They are dark areas on the photosphere with temperatures about 1000°K lower than their surroundings. Individual sunspots appear in an unpredictable manner, but statistically their incidence is governed by the well-known 11-year cycle. Strong magnetic fields are known to be associated with sunspots. Figure 1:1 shows the variation of sunspot numbers between 1935 and 1953. Figure 1:2 illustrates the 22-year cycle which is associated with the reversal of polarity of bipolar sunspots.

Prominences. Consisting of elevated masses of gas extending from the chromosphere high up into the corona, prominces are sometimes transitory, but may have life-times of several weeks.

Flares. A flare is an area in the chromosphere which, in the space of a few minutes, becomes much brighter. After about twenty minutes the brightness returns

TABLE I

	Photosphere	Chromosphere	Corona
Temperature	$6000^{\circ}K$	$\sim 10^{4}\,^{\circ}K$	$\sim 10^{6}\,^{\circ}K$
Radius	$R_{\odot}$ 6.96×10^{8} m.	$R_{\odot} + 10^{7}$ m.	many $\times R_{\odot}$
Electron density	$\sim 10^{13}$ cm.$^{-3}$	$\sim 10^{9}$ cm.$^{-3}$	varies with distance from sun's centre

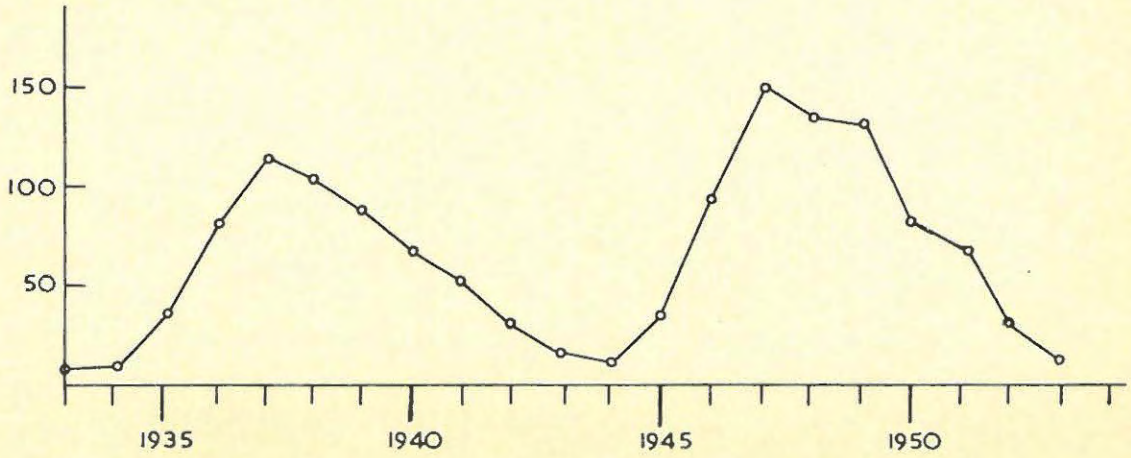

FIGURE 1:1

Sunspot numbers over about twenty years, illustrating the 11 year cycle.
(Reproduced from Ellison: "The Sun and its Influence")

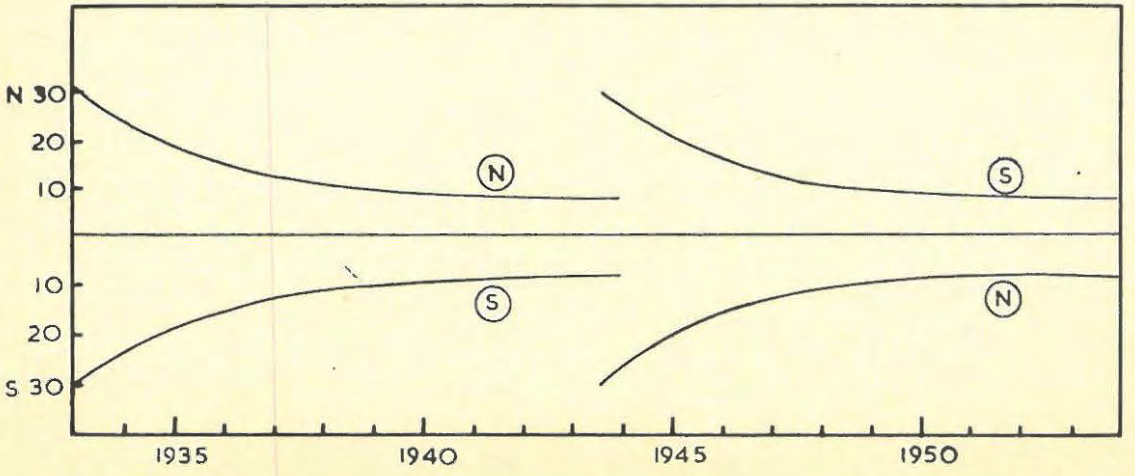

FIGURE 1:2

Approximate mean sunspot latitudes over about twenty years. Letters within circles denote the polarity of the leading (westerly) member of bipolar sunspots. One complete "twenty-two-year cycle" is shown. (Reproduced from Ellison: "The Sun and its Influence")

to normal. Flares vary in size and brilliance and are roughly classified into three degrees of importance.

Sudden changes in the ionization of the ionosphere, magnetic storms and aurorae occur after a solar flare: where time-delays between the solar and terrestrial events are observed, these may be explained in terms of a stream of solar corpuscles emitted during a flare with velocities of the order of 10^5 km/sec. The arrival of this stream at the earth is regarded as the cause of the terrestrial disturbance.

D. RELATION OF BURSTS TO SOLAR EVENTS.

The following is a brief summary of attempts recorded in the literature to relate solar bursts of the various types to visual solar phenomena.

Wild and McCready (2) showed that noise storms were associated with the incidence of sunspots, while three out of five large outbursts observed, coincided approximately with the start of a flare or sudden radio communication fade-out. They reported no correlation between isolated bursts and other phenomena.

Giovanelli and Roberts (9) observed 18 outbursts: for 13 of these, the optical disturbance responsible for the burst was identified: in two cases there

were alternative identifications: in the remaining three cases the optical records were unsatisfactory.

All but two of the identified disturbances were chromospheric flares.

Loughhead, Roberts and McCabe (10) investigated 300 flares and found that 20% were accompanied by Type III bursts. More than 60% of the bursts recorded occurred during the life-time of a flare, usually near the beginning. The probability of a burst accompanying a flare was found to be greater for the larger flares, and for flares having "surges" associated with them.

Giovanelli (11) has related the occurrence of isolated bursts to "flare-puffs". Some flares are of an explosive character, expanding rapidly at or near the outbreak of the flare. This expansion or "puff" is clearly defined in space and time. More diffuse and indefinite expansions are not included as "puffs".

Out of a total of 27 flare-puffs examined, 18 were found to coincide with Type III bursts to within $\pm$ 2 minutes.

Maxwell and Swarup (5) in discussing the "inverted U" bursts identified by them, show that their occurrence is related to solar flares. All but 6 of 29 such bursts observed, coincided with flares to within

about 5 minutes; these six apparently were not related to any optical phenomena.

Dodson, Hedeman et al. (12, 13, 14, 15).

From a comprehensive set of observations taken at the McMath-Hulbert Observatory (University of Michigan), Dodson, Hedeman et al. have studied in detail the relation of the H_α flare-brightening to radio disturbances at frequencies of 200 Mc/s and 2800 Mc/s. The following conclusions, inter alia, were reached:

(a) 200 Mc/s

(i) 78% of all flares observed were associated with 200 Mc/s events.

(ii) The radio events often consisted of an outburst followed by a storm. The outburst corresponded to the early portion of the flare, and the storm to the latter portion of the flare life-time.

(iii) The percentage correlation was independent of flare importance, and of the position of the flare on the solar disc.

(iv) Outburst times coincided with the times of ejection of high velocity particles near the beginnings of flares.

(v) Sudden ionospheric disturbances only occurred for flares larger than a certain

"threshold" size. These disturbances coincided with the beginnings of flares.

(b) 2800 Mc/s.

(i) Sudden ionospheric disturbances showed a high correlation with flares having associated 2800 Mc/s events.

(ii) A 2800 Mc/s disturbance was found to occur only when a flare or subflare was in progress.

(iii) Flare-burst correlations exhibited some dependence on flare importance and position.

The various types of burst together with distinguishing features and solar events with which they are correlated, are listed in Table II.

E. FLUX DENSITY OF SOLAR RADIATION AT METRE WAVE-LENGTHS.

The steady background or "thermal" component at metre wavelengths has a flux density of the order of 1×10^{-21} watts m^{-2} $(c/s)^{-1}$. Increases in flux density by a factor of 1000 may occur during large outbursts and storms. Isolated bursts represent an increase of flux density by a factor of about 100.

In designing the equipment for detecting this radiation, it is therefore necessary that it should be sensitive enough to record a signal of flux density 1×10^{-20} watts m^{-2} $(c/s)^{-1}$.

Class of Burst	Polarization	Occurrence	Visual Correlation	Dynamic Spectrum			
				Type	Bandwidth	Duration	Remarks
Storm Bursts	Strong Circular	During Noise Storms	Sunspots	I	Narrow	Seconds	No frequency drift
Outbursts	Probably Unpolarized	Sporadic	Flares	II	Broad	Minutes	Slow drift to lower frequencies
Isolated Bursts	Sometimes Strong Elliptical	Sporadic	Flare Puffs	Diverse including III	Broad	Seconds	Rapid drift to lower frequencies
Inverted U Bursts	?	Sporadic	Flares	—	Fairly Broad	Seconds	Rapid negative and positive drift
Reverse Pairs	Probably not Strongly Polarized	Rare Sporadic	—	—	Broad	Less than a second	Fairly rapid drift to higher frequencies

TABLE II

BLOCK DIAGRAM OF RECEIVER

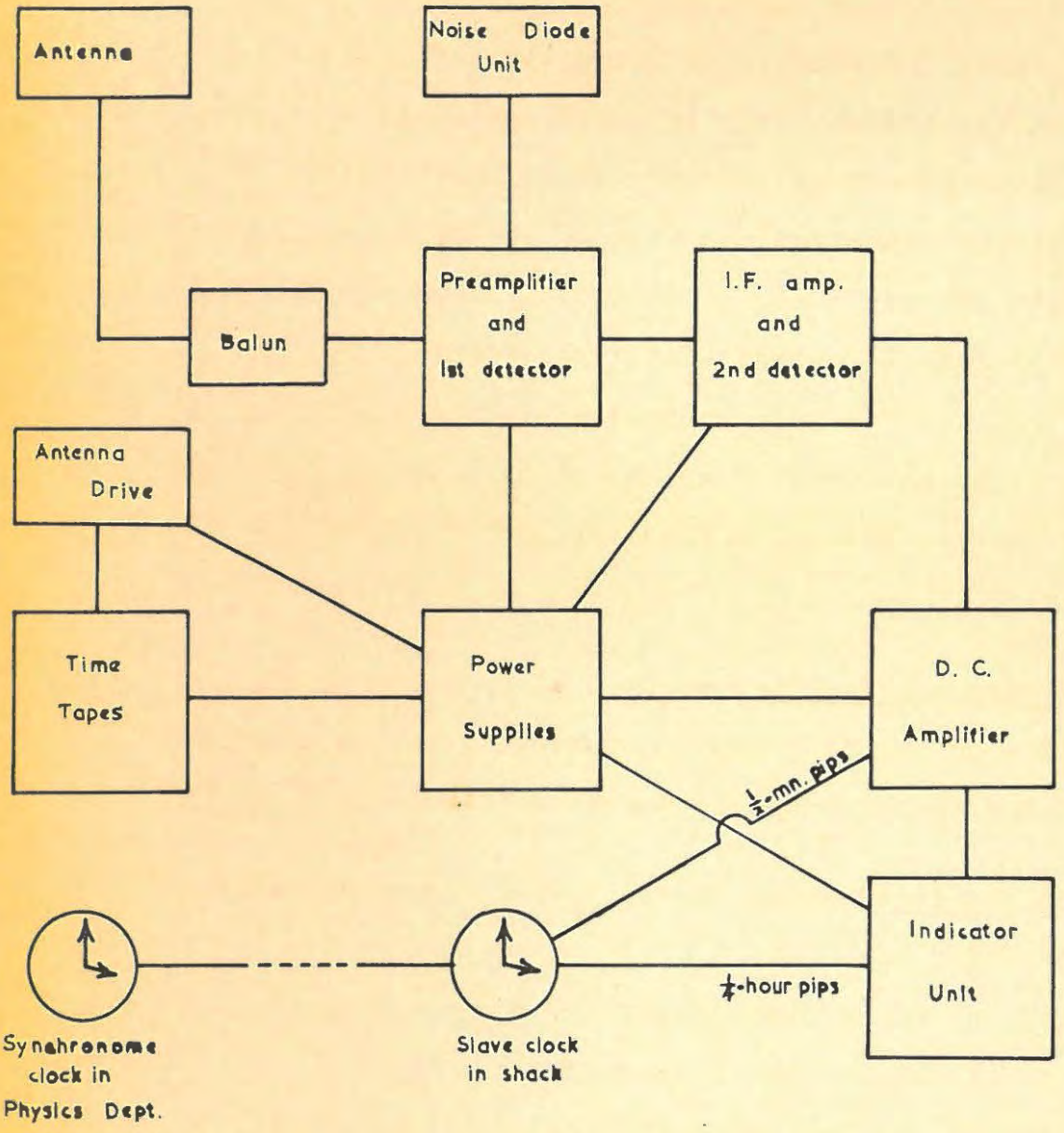

FIGURE 2:1

CHAPTER II.

THE EQUIPMENT.

The essentials of the equipment used to record continuously the intensity of solar radiation at a frequency of 300 Mc/s are illustrated in Fig. 2:1. The apparatus was situated in Grahamstown, C.P. South Africa.

Geographical Co-ords: Latitude: S. 33°18'39''.

Longitude: E. 26°31'08''.

The equipment consists of three basic elements: an antenna system, a receiver, and a recording device.

The antenna system consisted of an array of dipoles on an alt-azimuth mounting, with a suitable "balun transformer" to match to 50Ω co-axial cable.

The receiver was of the super-heterodyne type and consisted of:

(i) a 300 Mc/s preamplifier, first detector and first 30 Mc/s I.F. amplifier

(ii) second I.F. amplifier and second detector

(iii) a D.C. amplifier.

The recording device consisted of a C.R. oscilloscope with its Y-plates connected to the output of the D.C. amplifier. A photographic film moving at a constant speed in the x direction gave a

continuous record of the variation of the intensity of the incoming signal with time. Since losses along a transmission line increase with frequency, it is advantageous to make the lead from the antenna to the preamplifier and first detector as short as possible. The preamplifier was therefore housed on the mast together with the drive motors. All other equipment was housed in the "apparatus shack". (See Frontispiece).

1. The Antenna.

The antenna consisted of a broadside array of dipoles arranged, as shown in Fig. 2:2, in six groups of three. The dipoles consisted of 48cm. lengths of copper tubing insulated from their wooden supports by polystyrene blocks. The dipole supports were mounted on a wooden frame of dimensions 10'x8', across which copper wires were stretched to form a reflecting screen.

The dipole interconnections were originally made with twin-feeder lines consisting of heavy-gauge copper wire separated at intervals by polystyrene blocks. This was found to be clumsy and unsatisfactory and these lines were replaced by 300Ω twin-feeder tape.

Using the array as a transmitting antenna, the feeder tapes were roughly matched by attach-

ing "stubs." This was done with the antenna at ground level. Final matching was carried out with the antenna mounted on the mast. A 300 Mc/s transmitter was set up about a mile from the mast: the received signal passed through all stages of the receiver and the positions and lengths of the stubs were altered to give the best gain together with the best polar diagram.

The gain of the antenna relative to a single dipole was measured and was found to be of the expected magnitude. The polar diagrams for rotation of the antenna in both the horizontal and vertical planes, are given in Fig. 2:23. The polar diagrams were obtained as follows: a constant-output 300 Mc/s transmitter was placed about a mile from the antenna and the antenna was rotated in the horizontal and vertical planes in turn. The D.C. amplifier output voltage was then plotted against the angle of the antenna.

Antenna parameters.

(i) Beam-width to half-power points.

Vertical sweep	12°
Horizontal sweep	10°

(ii) Gain.

The "directive gain" (g) of an antenna may

be defined as the ratio of the power absorbed in the direction of maximum gain, to the average power absorbed over all antenna orientations.

We may calculate "g" from the polar diagram of the antenna as follows. Since the polar diagrams in the two principal planes of the antenna are very similar, we assume for simplicity that the three-dimensional polar diagram may be obtained by rotating Fig 2:2(b)(i) about the direction of maximum gain.

By the theorem of reciprocity we may consider our antenna as transmitting instead of receiving. Let us suppose that equal power inputs to the given antenna and to an isotropic radiator give rise to peak values of field strength of OP and OE respectively in a direction specified by the angle θ.

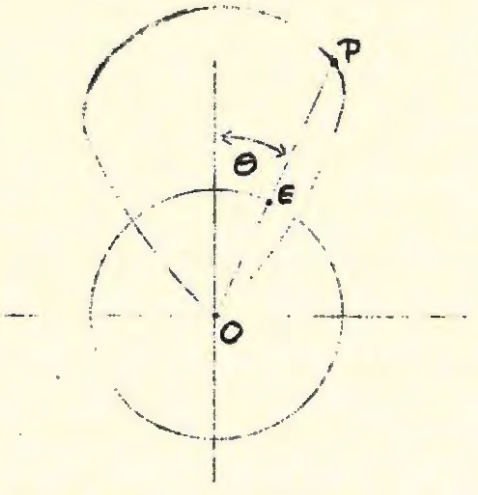

The Antenna.

In the direction θ, the flux density will be given by

$$\frac{(OP)^2}{2 \times 120\pi}$$

where 120π is the permittivity of free space.

Thus the total flux through the annulus shown will be

$$\frac{(OP)^2}{240\pi}\cdot(2\pi r\sin\theta)(r\Delta\theta)$$

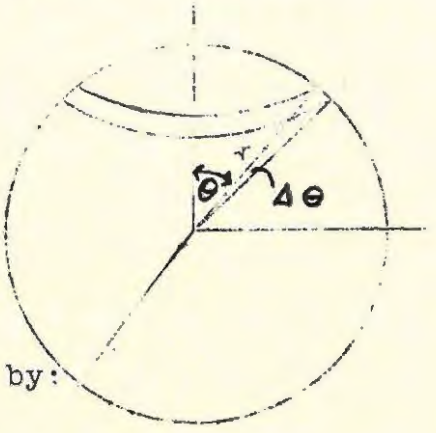

The total flux in all directions will be given by:

$$F_a = \sum\frac{(OP)^2}{240\pi}\cdot 2\pi r^2\sin\theta\,\Delta\theta$$

$$= \frac{2\pi r^2}{240\pi}\Delta\theta\sum(OP)^2\sin\theta \quad \ldots\ldots\ldots(a)$$

where $\Delta\theta$ is a small (finite), constant angular interval.

The Isotropic Radiator.

The total flux in all directions is given by

$$F_i = \frac{(OE)^2}{240\pi}\cdot 4\pi r^2 \quad \ldots\ldots\ldots\ldots\ldots(b)$$

Since the total power inputs to the two systems are the same, we may equate the expressions (a) and (b).

We then obtain the relation

$$(OE)^2 = \tfrac{1}{2}\Delta\theta\sum(OP)^2\sin\theta \quad \ldots\ldots\ldots\ldots\ldots(c)$$

The directive gain, "g", is then given by

$$g = \frac{(OP)^2_{max}}{(OE)^2} \quad \ldots\ldots\ldots\ldots\ldots\ldots(d)$$

This may be expressed in decibels by means of

the relation

$$G(db)=10 \log_{10} g .$$

(iii) Effective Area.

The "effective area" of an antenna (A) is related to the directive gain by the expression

$$g = \frac{4\pi A}{\lambda^2}$$

$$\text{Thus } A = \frac{g\lambda^2}{4\pi}$$

(iv) Summary.

Beamwidth	11°
g	76.4
G(db)	18.8db
A	6.1sq.m.

(v) Note: Equation (d) was derived by Dr. Stack-Forsyth and the author. Similar derivations may be found in Shelkunoff and Friis; "Antennas: theory and practice".

2. The Balun Transformer.

This was constructed by Poole according to a design by Roberts (16) for a broadband coaxial balun. It has the function of matching a balanced line (i.e. the twin-feeder tape) to an unbalanced line (i.e. coaxial cable). The principle of construction of the balun is indicated in Fig. 2·3.

The balun consists of a short length of co-axial cable placed parallel to the cable intended to carry the signal, received by the antenna, to the preamplifier. This short section is a little more than an eighth of a wavelength long, and a small hole is drilled in it at H, so as to cut the inner conductor exactly one-eighth of a wave-length from the top end. The two sections of cable are separated by a polystyrene rod.

The two inner conductors are connected at the top end, as shown; the twin-feeder tapes from the three banks of dipoles are connected to "a" and "b", which are terminals soldered onto the outer shielding of the two sections of cable. The two outer shields are connected at the lower end of the balun by means of a strip of perforated metal soldered to these shields.

By variation of the thickness of the poly-styrene rod, the separation of "a" and "b" is adjusted until the input impedance is a pure re-sistance of 100Ω, thus matching to the three 300Ω tapes connected in parallel at "a" and "b".

This impedance of 100Ω is transformed by the $\frac{\lambda}{8}$ line to an impedance of 50Ω, which matches to the 50Ω coaxial line.

THE ANTENNA

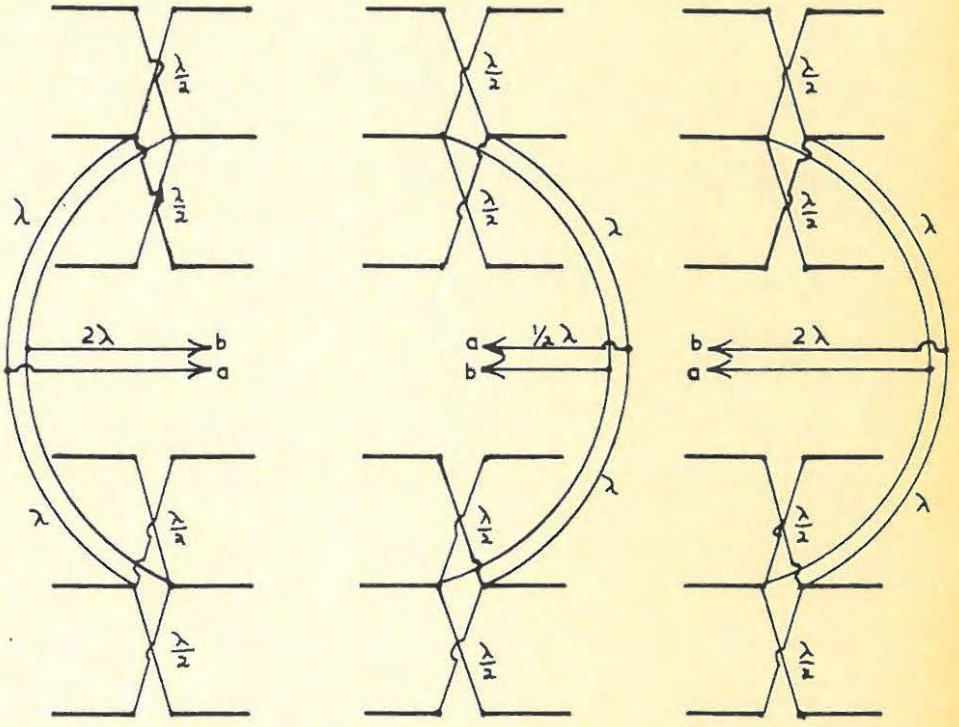

FIGURE 2:2A

POLAR DIAGRAMS

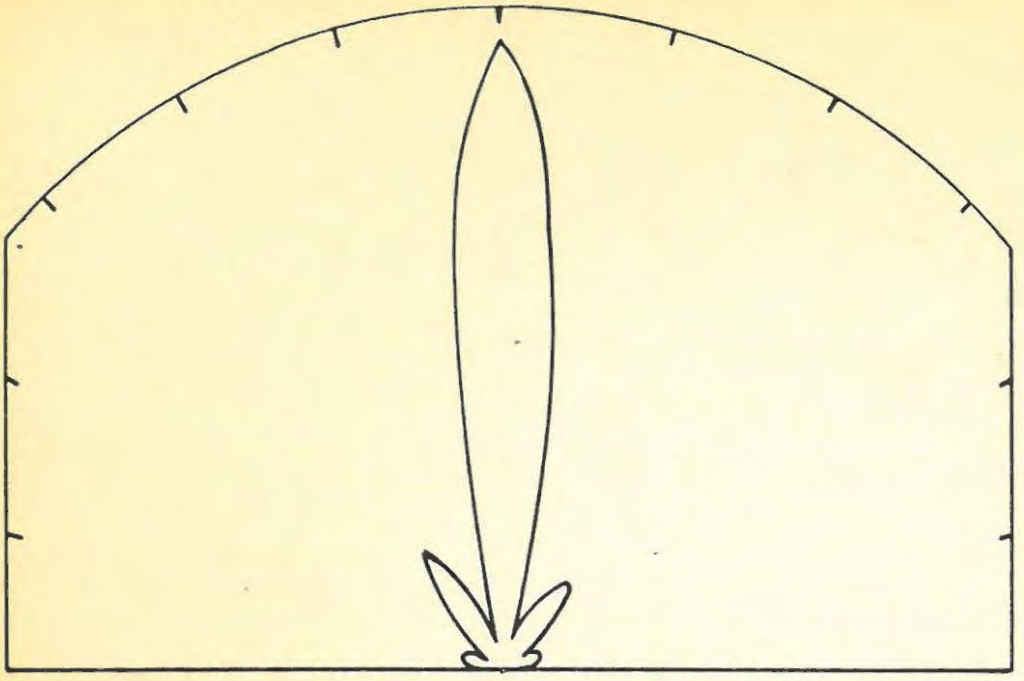

1. horizontal sweep

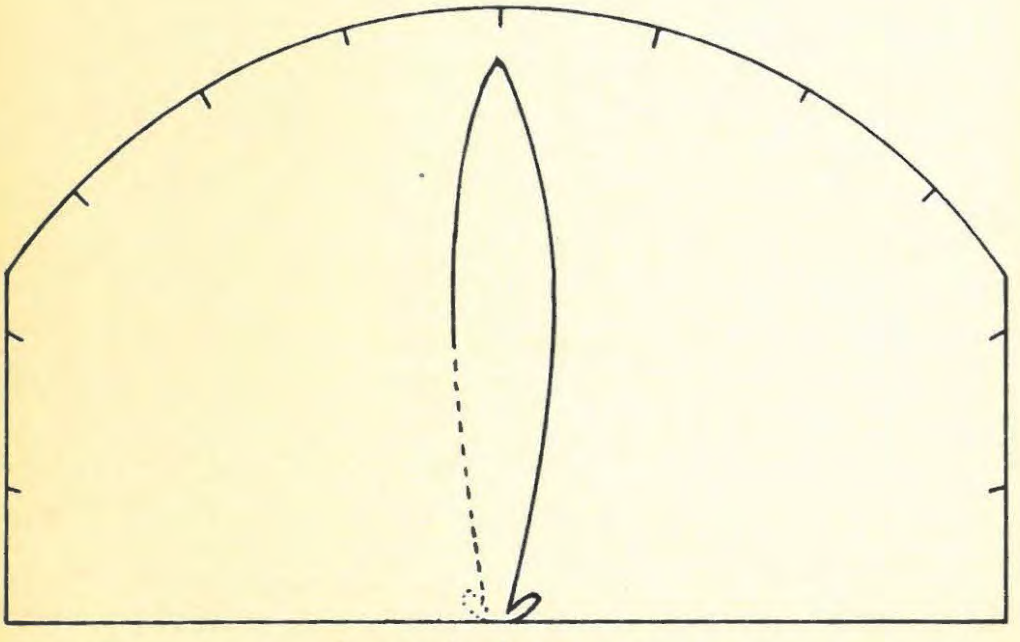

2. vertical sweep

FIGURE 2:2B

BALUN TRANSFORMER

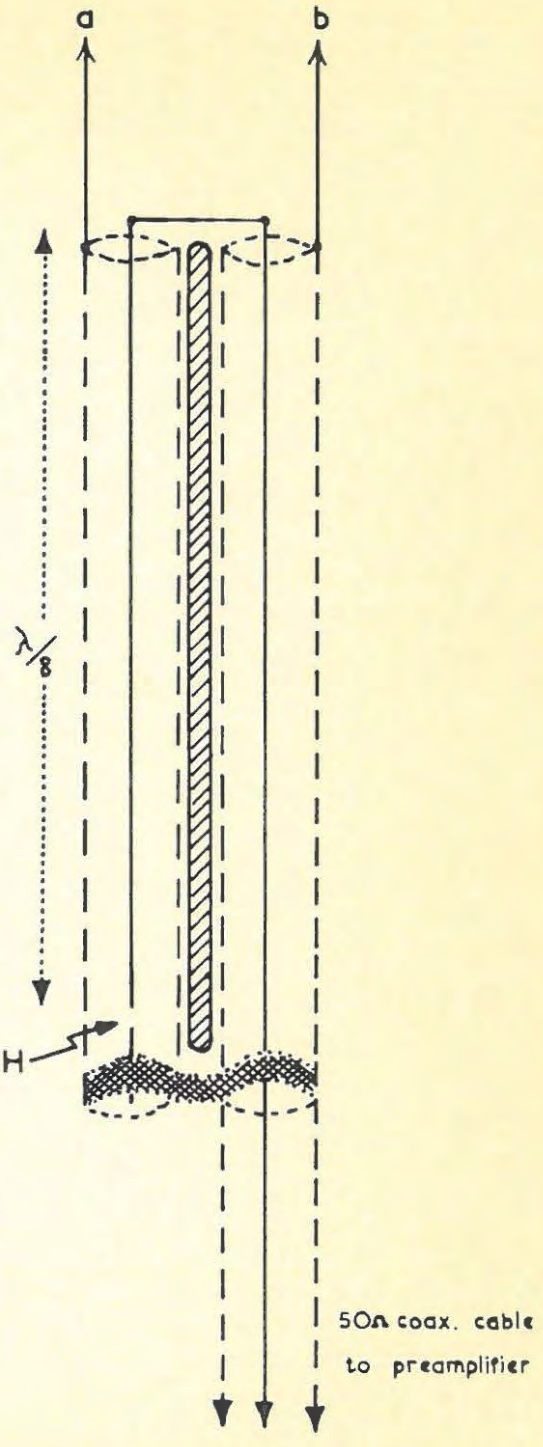

FIGURE 2:3

3. The Antenna Drive.

The antenna was attached to an alt-azimuth mounting, i.e. a mounting which can be moved

(a) in the horizontal plane.

(b) in the vertical plane.

The drives are independent, and each is designed in such a way that, once actuated by the making of a contact, it will turn the antenna mount through a fixed angle and then automatically switch itself off. Each drive consists of a fractional H.P. electric motor connected through two 150:1 reduction gears to the appropriate drive shaft.

Since the projections of the sun on the horizontal and vertical planes travel at varying angular speeds during the day, it is necessary that the frequency of actuation of the two drives should vary during the day.

This was accomplished by the use of the "time Tape" machine shown in plate B. This machine was devised by the author and Poole, and consists of two lengths of 35 mm. film running on a sprocket driven from the camera drive.

Each film runs over a brass drum. Holes punched in the film allow a spring-loaded contact to make momentary connection with the drum.

PLATE B

Azimuth drive. Reference to Fig. 2:4 shows how the making of this contact activates a relay A, causing switches B and C to close. Even after the time-tape contact has been broken, the relay remains closed owing to the current flowing by way of B and D.

This condition is maintained until the rear end of the piston arm, having made one complete revolution, opens switch D momentarily. Switches B and C are then opened; the momentum of the motor carries the piston arm past D, which closes once more.

Thus the whole system is reset for the next cycle. During this whole operation the ratchet wheel has been pulled round one tooth.

Since there are 19 teeth on the ratchet wheel, this represents a rotation of the antenna mount of

$$\frac{1}{19} \times \frac{1}{150} \times 360^{\circ} = 0.126^{\circ}.$$

Altitude drive . (see Fig. 2:5).

When the time-tape contact is made, relay L is activated and closes switches M and N. The time-tape contact breaks but L remains activated, due to the current flowing by way of M and P.

After completing one revolution, the arm K closes switch S. The 10 µf-condenser, which has been charged through a rectifier from the mains,

is then discharged through the relay O. P is momentarily opened, M and L open, and the system has been reset for the next cycle. During the whole operation the antenna has been rotated through an angle of

$$\frac{1}{150} \times 360^{\circ} = 2,4^{\circ} .$$

The direction of rotation of the drive motor is reversed manually at noon by means of the reversing key.

Reliability.

After some adjustment the switching-off mechanisms were found to operate reliably. The time-tape machine exhibited various faults and "teething troubles", which were gradually eliminated. The whole system then operated with fair reliability.

Calculations for Time Tapes.

(i) The azimuth of the sun, measured from due South (A), at any time "t" hours after midnight is given by Godfray (17) as

$$A = \cot^{-1} \frac{\tan \delta \cos \phi \cos h}{\sin h}$$

where δ is the declination of the sun from the equinox position (taken as positive in summer).

AZIMUTH DRIVE

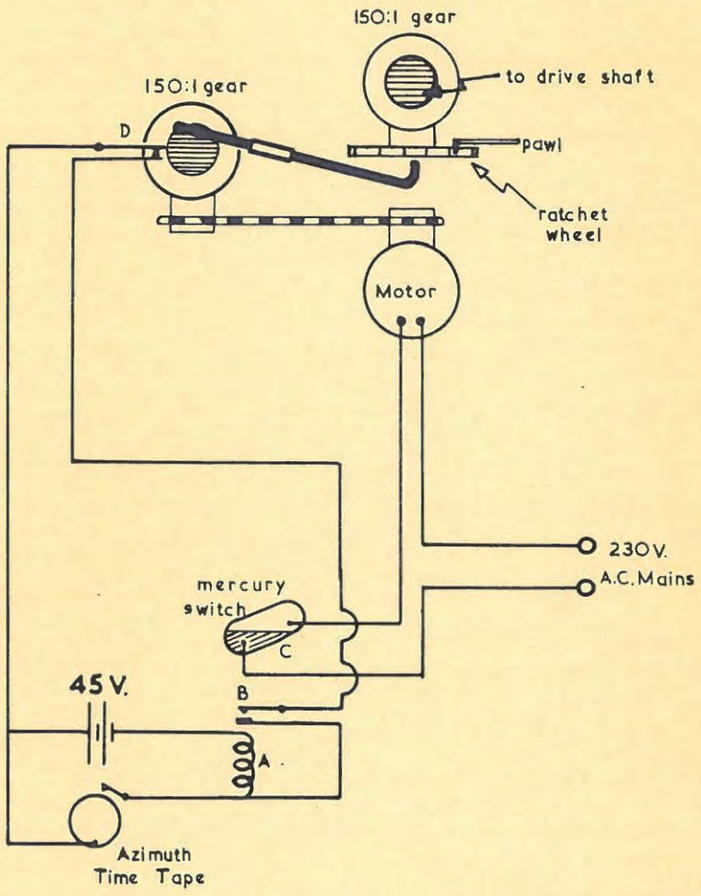

FIGURE 2:4

ALTITUDE DRIVE

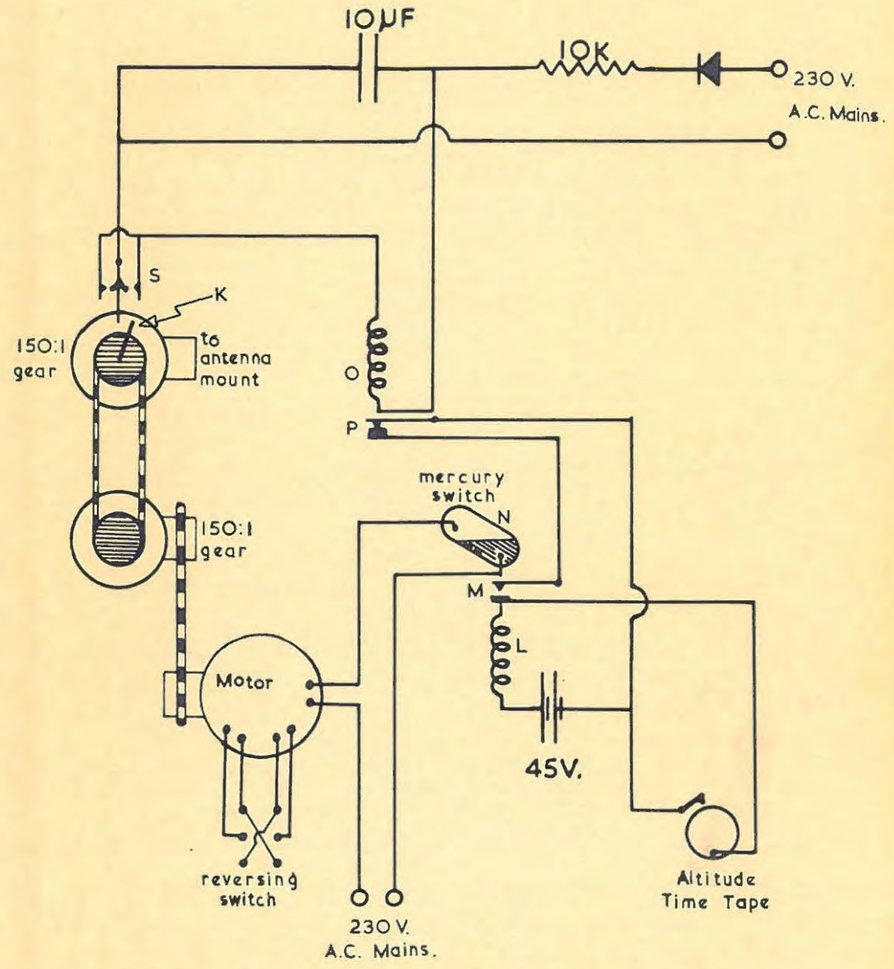

FIGURE 2:5

ϕ is the latitude of the place of observation,

h is the hour angle of the sun measured from midnight, = 15 t where t is the number of hours after midnight.

A set of graphs of A vs. h for various values of δ was constructed.

(ii) The azimuth of the sun (A) is related to the altitude of the sun ($90-\alpha$) by the expression

$$A = \cos^{-1} \frac{\sin \delta - \cos \alpha \sin \phi}{\sin \alpha \cos \phi}$$

where δ and ϕ have their previous meanings

α is the "zenith Distance" of the sun, i.e. (90° - Altitude above horizon).

Thus a set of graphs of A vs. ($90 - \alpha$) was constructed for various values of δ.

(iii) By combining the graphs constructed in (i) with those obtained in (ii) it was possible to set up a third set of graphs, in this case plotting altitude vs. time.

Thus knowing the angle through which the antenna was turned every time the drive mechanism was activated, it was possible to calculate at what times the punched holes should appear on the tape. The tapes were found to run at a speed of almost exactly 1 foot in 5 minutes, making calibration extremely simple.

Working life of Tapes.

It was found that a tape designed for a

given value of δ was adequate for three weeks on either side of the date corresponding to that value of δ. Since all of the tapes can be used twice during the course of the year, only five different tapes are required for each drive system.

4. Preamplifier (Mk. I).

Built by the author, this amplifier comprised a cascode R.F. amplifier tuned to 300 Mc/s, first detector, and three I.F. amplification stages stagger-tuned around a central frequency of 30Mc/s.

It was found that the wiring capacitance and inductance was too large to allow the R.F. stage to tune to 300 Mc/s.

This amplifier was then abandoned and the author proceeded to build the

5. Preamplifier (Mk II).

This was a modified version of a design quoted in the Radio Amateur's Handbook (18). The circuit is shown in Fig. 2:6, and a view of the amplifier is shown in plate C.

A crystal ground down by the author to a frequency of 9.165 Mc/s was used to control the frequency of the local oscillator. This frequency was then doubled to 18.33 Mc/s, trebled to 55.0 Mc/s, trebled to 165 Mc/s and finally doubled to

PREAMPLIFIER

MK II

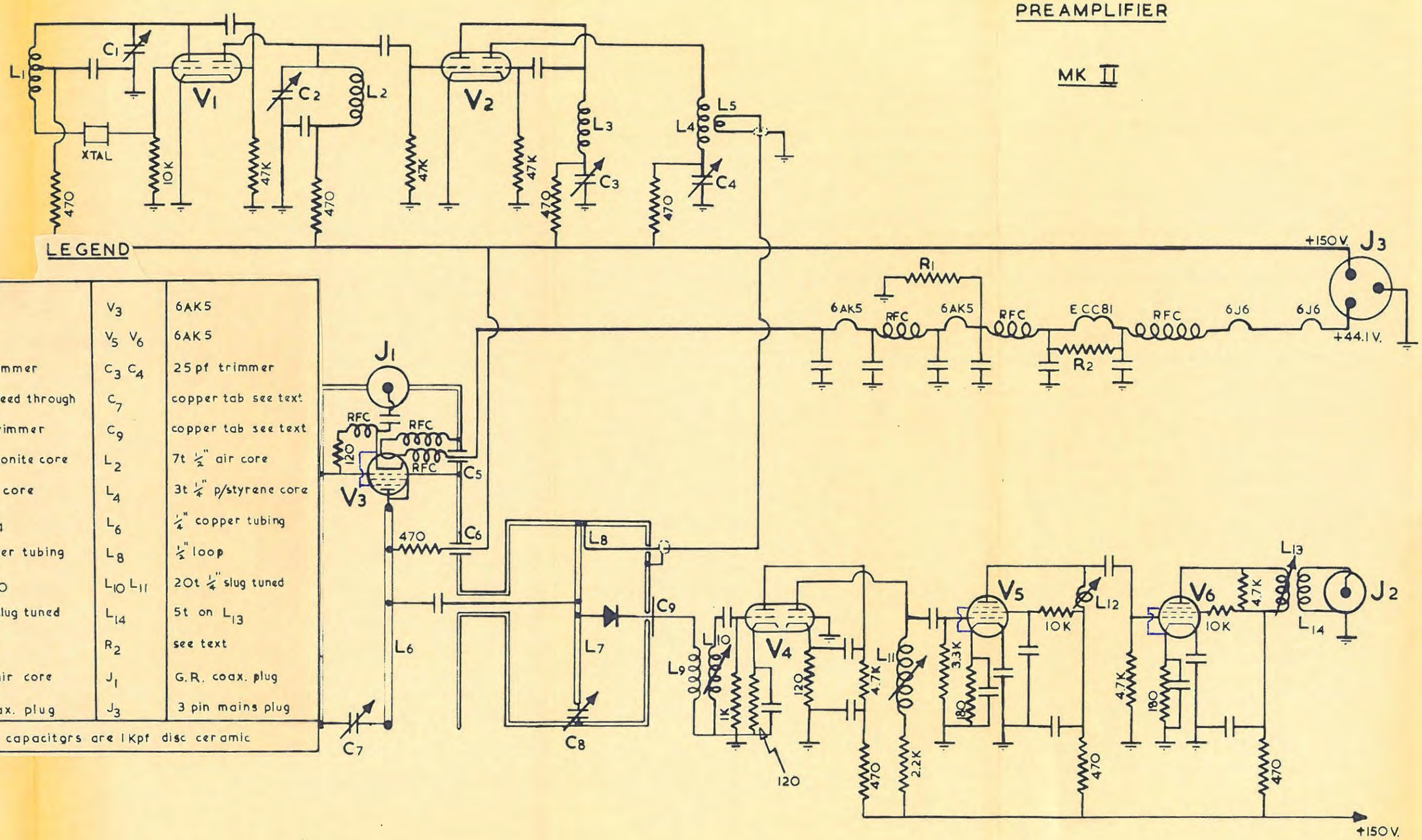

V_1 V_2	6J6	V_3	6AK5
V_4	ECC 81	V_5 V_6	6AK5
C_1 C_2	25pf trimmer	C_3 C_4	25 pf trimmer
C_5 C_6	500pf. feed through	C_7	copper tab see text
C_8	2–5pf trimmer	C_9	copper tab see text
L_1	15t ½" ebonite core	L_2	7t ½" air core
L_3	3t ½"air core	L_4	3t ¼" p/styrene core
L_5	1t on L_4	L_6	¼" copper tubing
L_7	¼" copper tubing	L_8	½" loop
L_9	5t on L_{10}	L_{10} L_{11}	20t ¼" slug tuned
L_{12} L_{13}	20t ¼" slug tuned	L_{14}	5t on L_{13}
R_1	see text	R_2	see text
R.F.C.	15t ¼" air core	J_1	G.R. coax. plug
J_2	Pye coax. plug	J_3	3 pin mains plug

All unmarked capacitors are 1Kpf disc ceramic

FIGURE 2:6

330 Mc/s.

The R.F. amplifier consisted of a pentode with a tuned-line anode load. The signal and local oscillator output were mixed in a crystal, and the resultant 30 Mc/s signal was fed to the I.F. triple which had been transferred, component by component, from the preamplifier Mk. I.

Adjustment.

The R.F. amplifier was tuned and was found to have a voltage gain of 18 db. with a rather narrow bandwidth of about ½ Mc/s. The I.F. section was then tuned and adjusted. Local oscillator power however, was very poor, and after some attempts had been made to improve it, Dr. Stack-Forsyth decided to undertake himself the construction of

6. Preamplifier Mk. III.

This amplifier employed cylindrical coaxial lines, plunger-tuned, for the R.F. amplifier, mixer, and local oscillator. It was found to be unstable, partly due to poor connections made by the plungers.

7. Preamplifier Mk. IV.

This consisted of the R F. and mixer stages from the Mk. II amplifier, and the local oscillator

and I.F. section of the Mk. III amplifier. This amplifier was not a success: the patch-work nature of the amplifier led to instability and unreliability in operation.

Dr. Stack-Forsyth thus commenced the construction of

8. Preamplifier Mk. V.

As will be seen from the circuit diagram (Fig. 2:7) and the view of the exterior of the amplifier (plate D) the Mk. V preamplifier embodies many of the features of the Mk. II amplifier, built by the author. A conventional 165 Mc/s oscillator and doubler circuit replaces the crystal-controlled local oscillator of the Mk. II amplifier, and tuned coaxial lines are used for R.F., local oscillator and mixer stages. The bandwidths of the R.F. amplifier and local oscillator stages were brought up to about 1 Mc/s by means of the "damping" resistors connected across the ends of the tuned lines.

This amplifier has been found to operate satisfactorily and is the one incorporated in the receiver.

FIGURE 2:7 PREAMPLIFIER MK. V

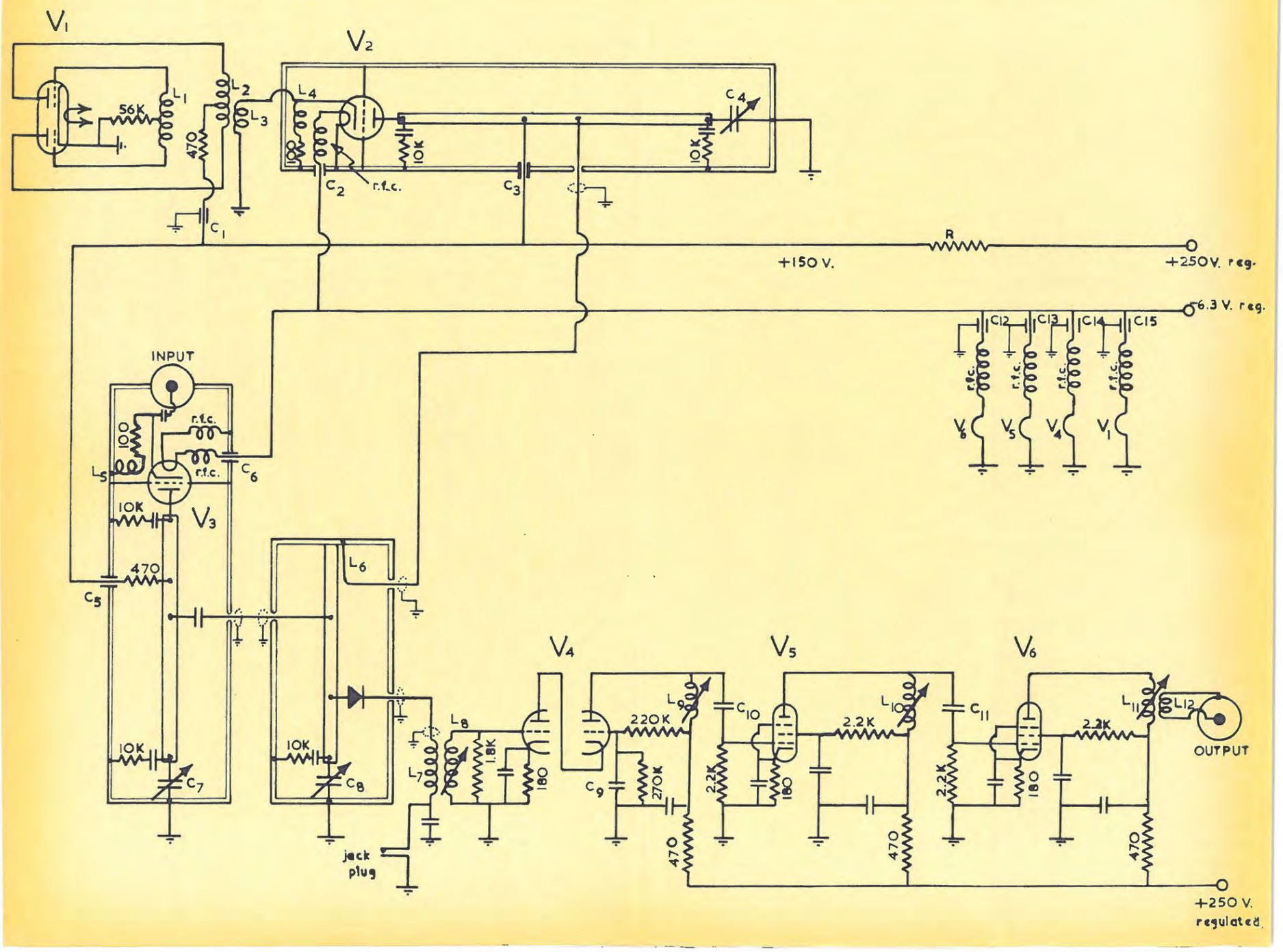

LEGEND

V_1	6J6	V_2	6AJ4
V_3	6AJ4	V_4	ECC 81
V_5	EF92	V_6	EF92
L_1	4t $\frac{1}{4}$" slug tuned	L_2	4t $\frac{1}{4}$" slug tuned
L_3	3t round L_2	L_4	5t $\frac{1}{4}$"
L_5	5t $\frac{1}{4}$"	L_6	$\frac{1}{2}$" loop
L_7	5t on L_8	L_8	20t $\frac{1}{4}$" slug tuned
$L_9 L_{10} L_{11}$	20t $\frac{1}{4}$" slug tuned	L_{12}	5t round L_{11}
C_1 C_2 C_3	470 pf. feed through	C_5 C_6	470pf. feed through
C_4 C_7 C_8	copper disk see text	$C_{10} C_{11}$	3kpf ceramic
$C_{12} C_{13}$	470pf. feed through	C_{14} C_{15}	470pf feed through
r.f.c.	15t.	R	3.3K

All unmarked capacitors are 1kpf disc ceramic

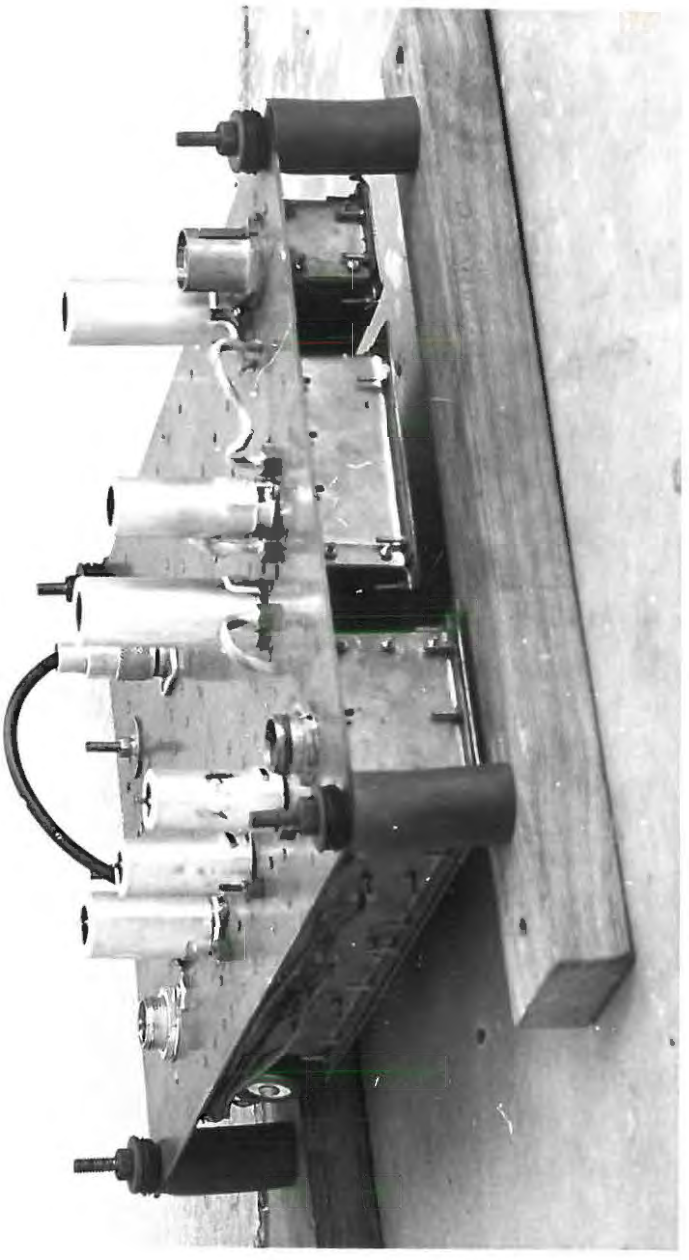

PLATE D

Preamplifier Parameters.

Gain	40 db.
Bandwidth	1 Mc/s
Central Frequency	300 Mc/s
Intermediate frequency	30 Mc/s

9. Regulators for Preamplifier Power Supplies.

It is essential that the preamplifier parameters should not be affected by changes in mains voltage, since such changes will be subjected to amplification by the whole receiver. Regulators are therefore necessary for both H.T. and L.T. supplies. The same argument applies with nearly equal force to the I.F. amplifier, and in some measure to the D.C. amplifier.

H.T. and L T. regulators for the preamplifier power supplies were constructed and adjusted by the author. However, in order to supply the parallel-fed filaments of the Mk.V preamplifier it was necessary to construct regulators capable of handling a much larger filament current.

Using a design by Keller (19) as a basis, a regulator was designed, constructed and tested by the author and was found to regulate almost perfectly for as much as a 15% change in supply voltage.

The circuit is shown in Fig 2:8, and a general view of the regulator is shown in plate E.

The 250V. A.C. Mains voltage is converted to about 20 V. by a transformer with a high-amperage secondary winding. This alternating voltage is rectified by means of a selenium rectifier; smoothing is achieved by using a 1000 µF electrolytic condenser. This voltage is applied to the collector of the transistor: a drop in this voltage alters the base current in such a way that the voltage drop between collector and emitter falls. The output voltage thus remains constant.

Safety Devices. Damage may be caused to the transistor if the base-collector voltage becomes too large. Switches A and B are arranged so that no voltage can be applied to the base unless the supply voltage is also switched on to the collector. The relay S disconnects the base from the reference supply in the event of a power failure.

Two of the regulators were used for the pre-amplifier, the third being used for the I.F. amplifier.

10. I.F. Amplifier.

As originally constructed by Poole, this consisted of a stagger-tuned triple centred at a

LEGEND.

A_1 A_2 A_3	double pole single throw.
B_1 B_2 B_3	single pole single throw.
C	1000 μF electrolytic.

TRANSISTOR REGULATED L.T. SUPPLIES

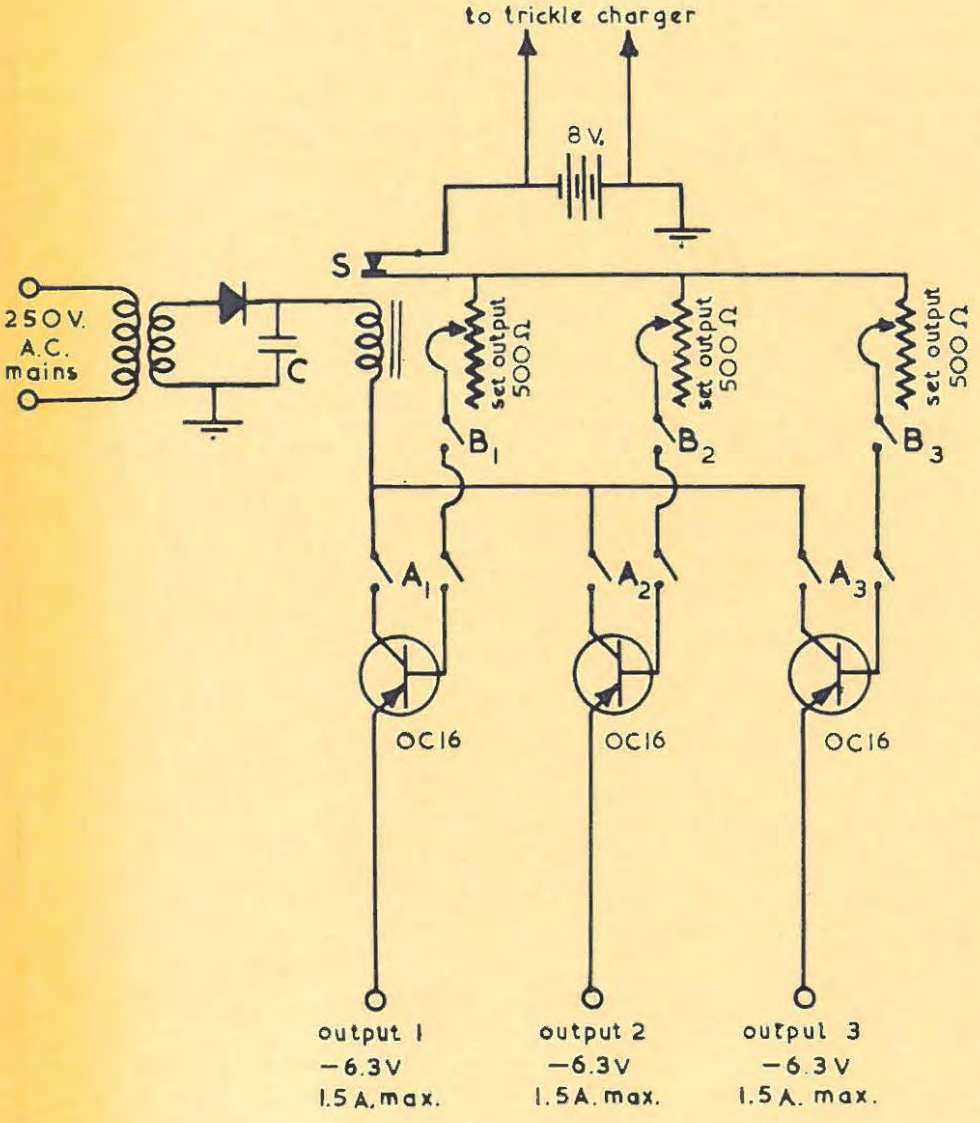

FIGURE 2:8

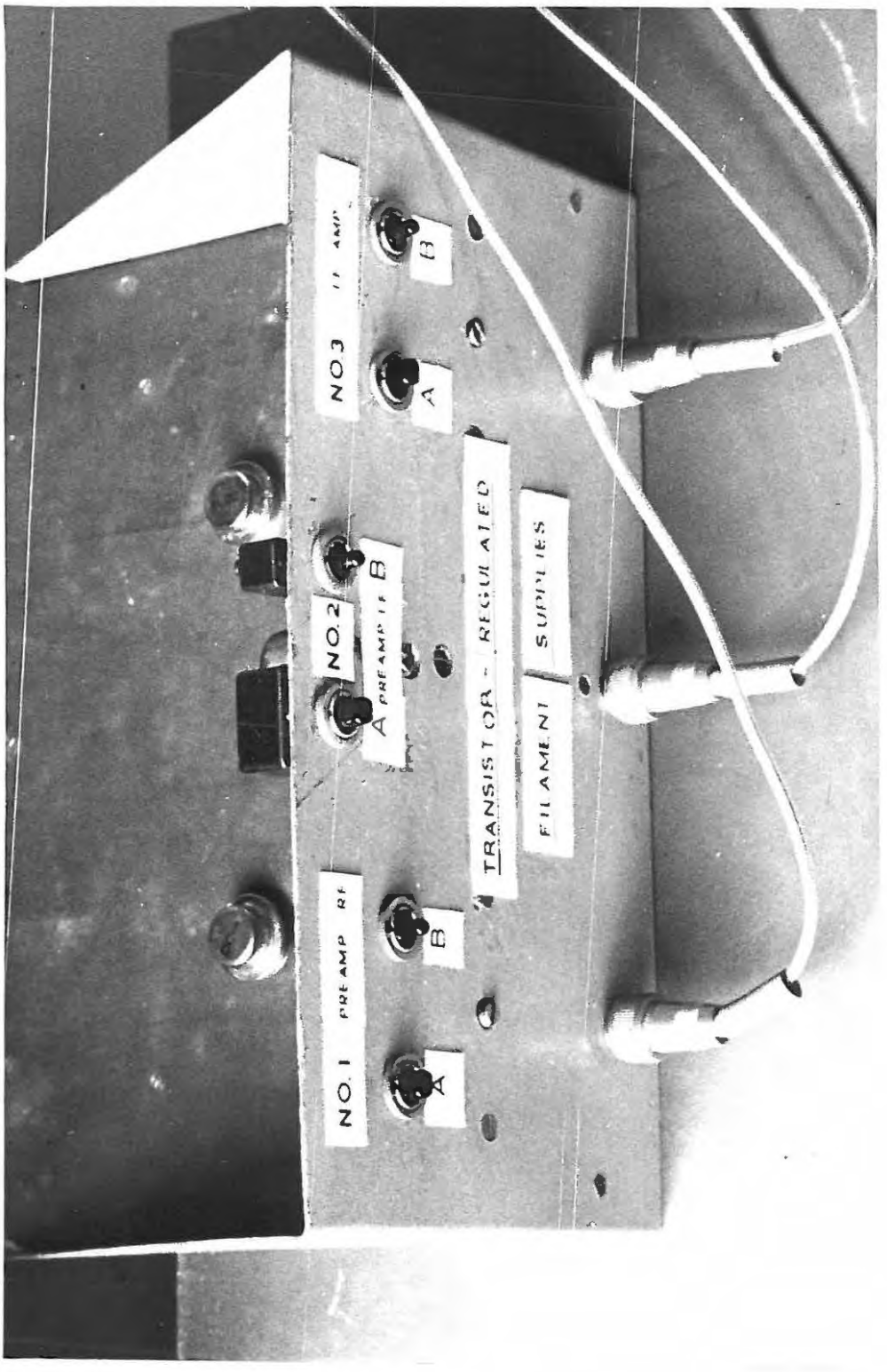

PLATE E

frequency of 30 Mc/s and a diode detector, with cathode-follower monitors at input and output.

An additional 30 Mc/s stage was constructed by the author to boost the gain of this amplifier, after preliminary tests of the complete receiver had indicated that there was not enough gain.

Final parameters of this amplifier were:

Central frequency	30 Mc/s
Bandwidth	1.5 Mc/s
Gain	60 db.

The varying D.C. output voltage from this amplifier is applied to the

11. D.C. Amplifier.

This is a three stage difference amplifier, with a maximum voltage gain of about 45 db. The circuit is shown in Fig.2:9.

Initial adjustments.

When no signal is being fed into the amplifier, the "high" and "low" output voltages should be equal, and of a suitable magnitude for connection to the Y plates of the oscilloscope (in this case 140 volts). The following procedure is adopted to accomplish this:

(i) Set switches "B","E" and "I" to "adjust".

(ii) Set potentiometer "A" for balance at the output.

(iii) Set switch "B" at "operate".

(iv) Adjust potentiometer "C" for balance at the output.

(v) Adjust output level to about 140 V. by means of potentiometer "D".

(vi) Set switch "E" to "operate".

(vii) Set output level to exactly 140 V. by means of potentiometer "F".

(viii) Set potentiometers "G" (coarse) and "H" (fine) for balance at output.

Operating adjustments.

Controls "G" and "H", the gain control "J" and the filter and attenuator selector switches are situated on the front panel and further adjustments are made when the amplifier is mounted in position on its rack.

We now choose suitable filter and attenuator settings.

The set-noise voltage generated in the pre-amplifier input circuit is amplified by the pre-amplifier and I.F. amplifier. The resultant steady voltage is balanced out at the D.C. amplifier input by means of a voltage of opposite sign; the magnitude of this balancing voltage is determined

by the setting of the "buck-out control".

Thus

(ix) Set switch "I" to "operate".

(x) Adjust the buck-out control for balance at the output.

Under the actual operating conditions, the following steps are taken:

(xi) Set "G" and "H" so that the amplifier is <u>out of balance</u> at the output by -45 volts. (oscilloscope spot moves down to the bottom of screen).

(xii) Adjust the buck-out control so that a small set-noise signal is applied to the amplifier. The output voltage moves towards balance (new reading say -35 volts). (Oscilloscope spot moves up about 1/5 of screen height). The latter adjustment is made in connection with the time-mark system. (see p. 33).

By setting the amplifier out of balance as in (11), the full height of the oscilloscope screen is employed. A signal applied to the input causes the amplifier to move towards balance (spot moves towards centre of screen) and then out of balance in the opposite direction (spot moves above centre of screen).

FIGURE 2:9

D.C. AMPLIFIER

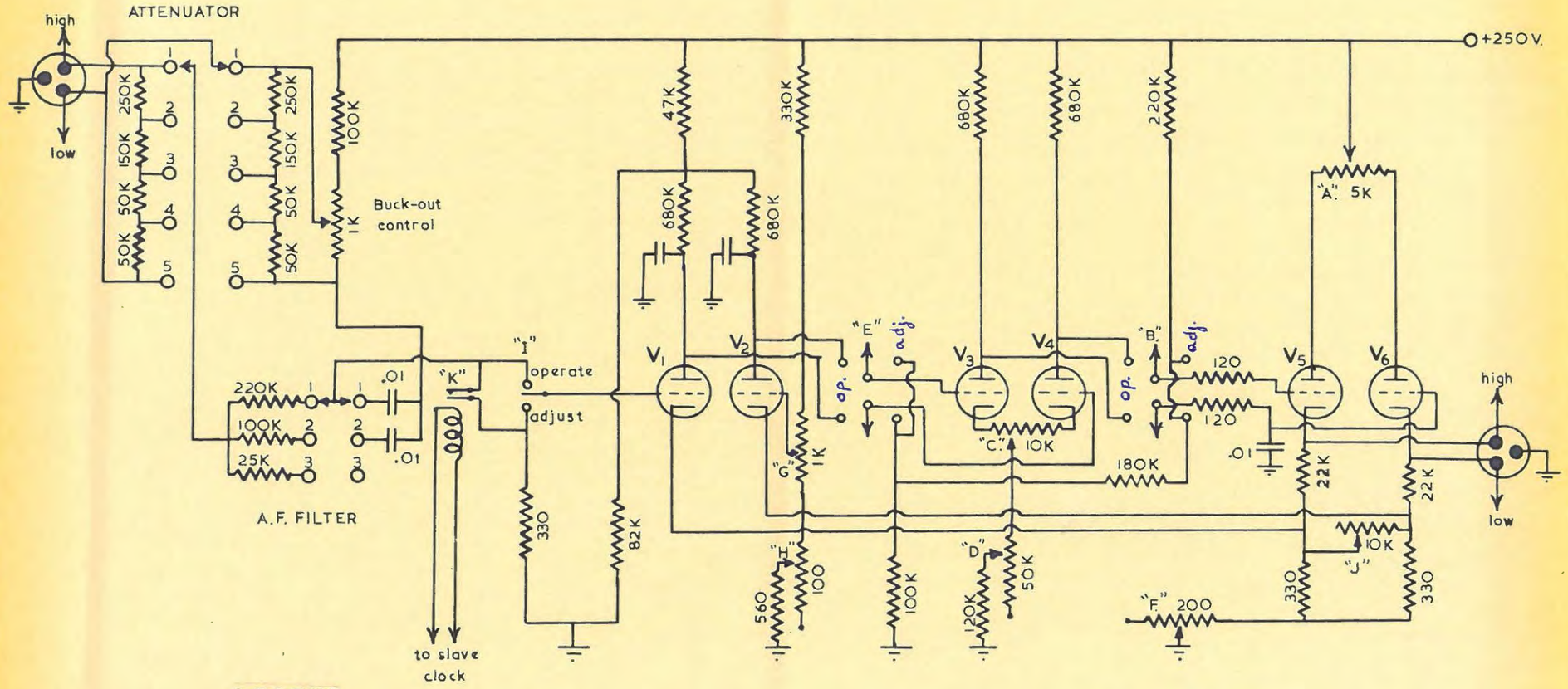

LEGEND

V_1 V_2 V_3 V_4 V_5 V_6 : All EC92 triodes
All unmarked capacitors: 1kpf ceramic

Parameters of the D.C. Amplifier.

(a) Attenuator settings and the resulting fraction of the input applied to the amplifying stages:

Setting	Fraction
1	1
2	1/2
3	1/5
4	1/10
5	0

(b) Range of frequencies accepted for various settings of the A.F. filter:

Setting	Range (c/s)
1	0-880
2	0-200
3	0-50

12. The C.R.O. and associated Power Supply.

Plate F shows a view of the front panel of the oscilloscope constructed by the author. The camera is shown in position.

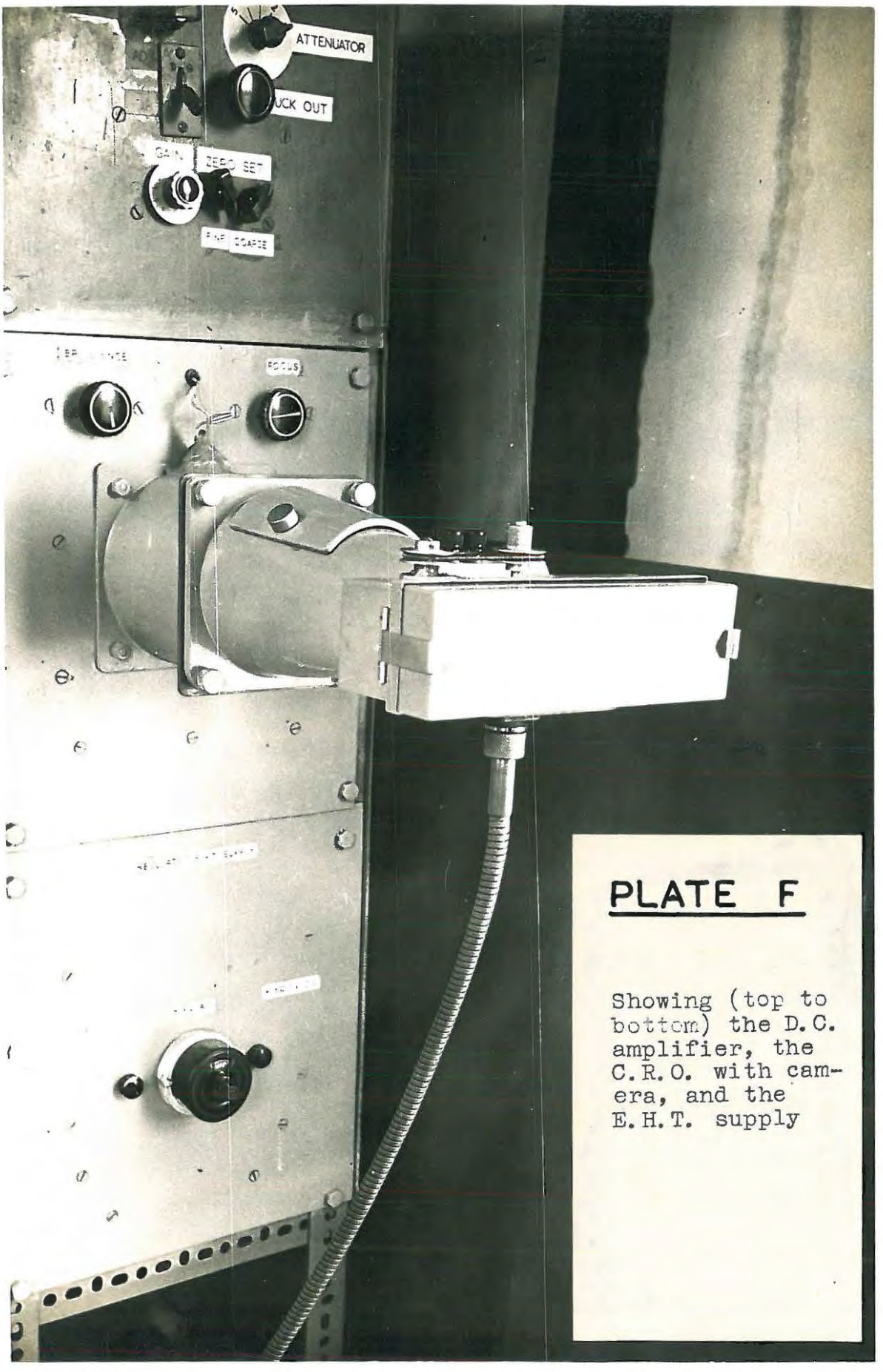

PLATE F

Showing (top to bottom) the D.C. amplifier, the C.R.O. with camera, and the E.H.T. supply

The circuits of the regulated E.H.T. supply and the oscilloscope are illustrated in Fig. 2:10. The former was designed and partly constructed by W.L. Shuter, and was completed and tested by the author. Considerable attention had to be paid to insulation. Where necessary, tube bases were mounted on ebonite blocks to prevent sparking from pins to the chassis.

Regulation was efficient for 15% mains changes above and below the operating value of 235 volts.

13. Noise-diode calibration unit.

Some difficulty was experienced in finding a conventional-type "noise-diode" which would be useful

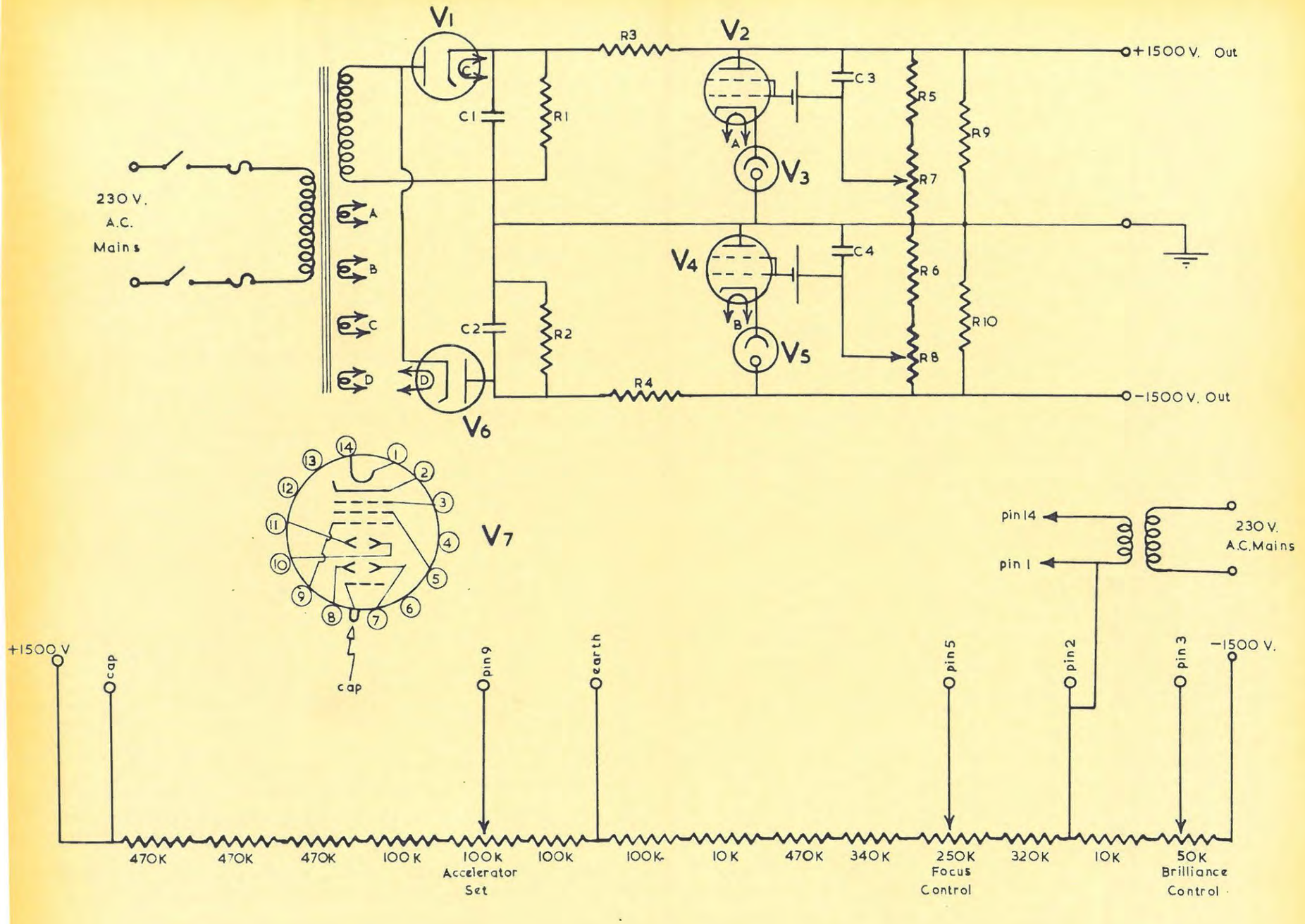

FIGURE 2:10 OSCILLOSCOPE & E.H.T. SUPPLY

LEGEND

R1 & R2	3.3M+3.3M+3.3M+3.3M	C3	0.1μF 1500V. D.C. wkg.
R3 & R4	100K+67K+67K+67K	C4	0.01μF 2500V. D.C. wkg.
R5 & R6	470K+470K	V_1 & V_6	2X2
R7 & R8	500K carbon pot.	V_2 & V_4	807
R9 & R10	470K+470K+470K	V_3 & V_5	90C1
C1 & C2	0.25UF 2500V. D.C. wkg.	V_7	5 ADP 11 C.R.T.

useful at 300 Mc/s. Coaxial diodes, though more suitable, were too expensive, and it was decided to use a CV 2398 tube. This is an inexpensive tube useful up to 500 Mc/s, although it cannot be used for absolute calibrations above about 200 Mc/s.

As it was not proposed to investigate the absolute flux density of solar radiation incident on the antenna, this disadvantage was not considered important.

The plate load circuit was tuned to 300 Mc/s by adjustment of L (see Fig. 2:11), and the output was matched to 50Ω coaxial cable. The resistor R served both as a voltage-dropping resistor and a monitoring device, the two "monitor" leads being connected to a meter in the apparatus shack.

The filament leads were connected to a series combination of accumulators, rheostat and ammeter in the apparatus shack.

Calibration.

The noise unit was used to check

(1) the linearity of the receiver

(2) that the gain of the receiver remained constant from day to day.

In order to perform a calibration, the antenna plug is removed from the preamplifier, and replaced

NOISE DIODE UNIT

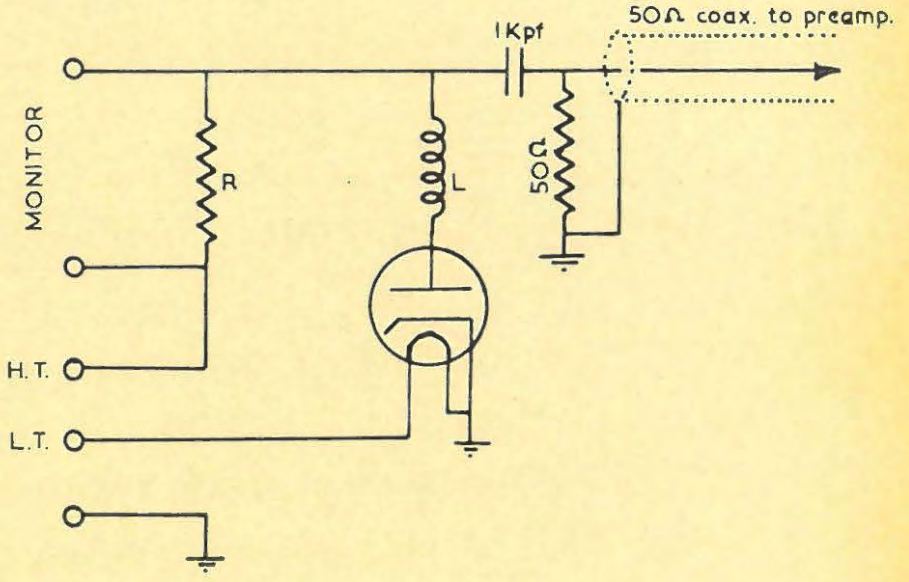

FIGURE 2:11

by the noise-diode output plug. The filament current is then set in the shack at various suitable values, and for each of these values, the readings obtained on the noise-diode plate current meter and the voltage appearing at the output of the D.C. amplifier are noted. The camera shutter is opened for a few seconds each time, giving a vertical line of dots if the film is stationary, or a series of short "stripes" if the film is moving.

A plot of oscilloscope deflection vs. noise-diode plate current then indicates whether the response of the amplifier is linear: if it is, the slope of this line is a measure of the gain.

14. Time Markers.

Every half minute a pulse is sent to the "master relay" in the shack from the synchronome clock in the Physics Dept. This pulse is used to operate a slave clock in the shack, and also to short-circuit momentarily the input of the D.C. amplifier. (see relay and switch "K" in Fig. 2:9).

Thus if the D C. amplifier is operated slightly above its zero (by suitable setting of the "buck-out" control) the spot moves down to the zero line every half-minute. Plate G shows a strip of recording film with half-minute pips.

PLATE G

The heavy stripe at the top of the record marks the quarter-hour. A contact on the slave clock makes one half-minute before the quarter-hour and breaks one half-minute after. During this one-minute interval a spot of light focussed on the recording film is switched on, producing the black stripe.

Thus the half-minute pip corresponding to the centre of the stripe marks the actual time of the quarter-hour.

15. Existing apparatus.

The following is a brief list of the most important apparatus existing in the shack and used by the author and Poole.

L.T. and H.T. Power supplies.

LT and HT Regulators for the I.F. amplifiers.

LT and HT Regulators for the D.C. amplifiers.

Camera Drive (extended by Poole).

Monitor panel, partly connected.

In addition the 125 Mc/s radio telescope built by Shuter and Stack-Forsyth, comprising Helical Antenna, preamplifier, I.F. amplifier, D.C. amplifier and Cathode Ray display was in existence and largely operative. Poole (T/A) later converted this for use at 150 Mc/s.

16. Operation and Maintenance.

As soon as the apparatus showed signs of running reliably, the author left most of the maintenance and operation to Poole (T/A). The author, however, operated the apparatus during the period 19/8/59 to 26/8/59 and is thoroughly familiar with all aspects of its operation.

CHAPTER THREE.

THE ORIGIN AND PROPAGATION OF SOLAR BURSTS.

Before discussing the observations made by the author of solar noise bursts at a frequency of 300 Mc/s, it is necessary that we should review the theories which have been put forward by various workers to account for the production of solar radio-frequency radiation, and explain its propagation through the solar atmosphere on its way to the Earth.

A. HISTORY.

Ryle and Vonberg (20). In a relatively early paper (1948), M. Ryle and D.D. Vonberg reported observations of solar radiation at frequencies of 80 Mc/s and 175 Mc/s. They found that the intensity of the radiation corresponded to that given out by a black body at a much greater temperature than the 6000°K estimated for the chromosphere. The minimum intensity was in fact calculated as corresponding to a source temperature of 10^6 °K for a source subtending an angle of $\frac{1}{2}^\circ$. On this basis, temperatures of 10^8 °K or 10^9 °K would have to be realised above sunspots in order to account for the intensity of the received radiation.

Interferometric measurements later showed that radio sources associated with sunspots subtended an

angle on the average of only 10' of arc. This corresponded to a source temperature of 2×10^9 ^oK for bursts in the 175 Mc/s band.

Ryle (21) attempted in the same year to explain the existence of these very high temperatures in localized areas of the corona. He pointed out that the sun's permanent magnetic field, in conjunction with the non-uniform rotation of solar surface matter, could produce a high potential difference between the poles and the equator. This would be sufficient in the quiet sun to produce discharge currents capable of maintaining temperatures of the order of $10^6 - 10^8$ ^oK. In the vicinity of strong sunspot magnetic fields, temperatures of the order of 10^{10} ^oK appeared likely.

Assuming that the radiation was produced by a thermal mechanism in this way, bursts could be attributed to sudden changes in the equivalent temperature of localized areas, due to mechanical changes in the surface matter.

Taking Appleton's (22) theory of the passage of radiation through an electron gas in a magnetic field as a basis, Ryle applied the magneto-ionic theory to conditions obtaining in areas above sunspots. Thus he was able to show the existence of three regions in such an area capable of absorbing a given frequency. Since regions of high absorption are regions of high

radiating power, we have therefore three regions capable of radiating a given frequency.

It was shown that radiation from the region of maximum absorption could only be propagated towards the centre of the sun. The remaining two regions absorbed circularly polarized radiations of opposite sense. Since the intensity of the radiation from these two source regions would in general be different, the received radiation would be detected as being circularly polarized, with the sense of the more intense component.

Westfold (23) pointed out in 1949 that Appleton's classical theory applied only to plane waves in a uniformly ionized medium in a uniform magnetic field. Even the Hartree and Booker modifications of this theory assumed stratification of all electro-magnetic properties of the medium.

This set of idealized conditions does not hold in the corona; for instance, the refractive index depends on the direction of propagation as well as on the electron density, and the use of Snell's law is not justified.

Westfold showed that if a set of reference axes is chosen such that one axis is parallel to the magnetic field (rather than to the direction of propagation), a new form of the equation for the complex

refractive index of the medium can be obtained. This led to the result that three types of "plasma" oscillation* in the medium could exist; the resultant radiations would exhibit right-handed, left-handed and linear polarization. The linearly polarized component would have its magnetic vector directed along the direction of the magnetic field.

Collisions in the plasma would tend to damp the oscillations, and Westfold was able to predict exponential damping constants of the order of $\frac{1}{4}\nu$ to $\frac{3}{4}\nu$, where ν is the collision frequency in the plasma.

Ryle (24) summarised early attempts to explain the production of solar radio-frequency radiation in terms of

(a) thermal processes.

(b) non-thermal processes, i.e. those involving coherent oscillations of electrons.

He pointed out that while theories of plasma oscillations accounted for plasma levels having a natural frequency of oscillation fo given by

* "Plasma oscillations": In electric discharge tubes, a uniform region of an ionized gas in which electron and positive -ion concentrations are equal, is sometimes called a "plasma". Under certain conditions oscillations of the ions and electrons (independent of the conditions of an external circuit) may be set up.

$$f_o^2 = \frac{Ne^2}{\pi m}$$

where N is the electron density

e is the electronic charge (esu)

m is the electronic mass,

these theories did not explain how these oscillations were excited, or the mechanism of propagation of the radiation. Where such explanations were attempted, they were confined to the consideration of plasma oscillations in discharge tubes.

Under these conditions

(i) the dimensions of the medium are very much smaller than one wave-length (in vaccuo) of the emitted radiation.

(ii) the electrons and ions are constrained to follow a highly ordered motion

(iii) the gradients of electron density and magnetic field are large.

None of these conditions holds in the solar corona.

Some workers had attempted to explain the radiation in terms of ionic plasma oscillations. Ryle pointed out that the frequency of such an oscillation would be given by the equation

$$(f_o^2)_I = \frac{Ne^2}{\pi M}$$

where N is the ion density

and M is the ionic mass.

Such oscillations would have a low frequency, but Ryle made the tentative suggestion that radiation of this order of frequency travelling through an electron plasma could cause excitation of the plasma. This might be a possible explanation of the occurrence of bursts.

Jaeger and Westfold (25) calculated the trajectories, equivalent path and absorption of radiation in the range 20 Mc/s - 100 Mc/s. Their work was based on the following idealized picture of the corona.

(i) No magnetic field.

(ii) Spherical symmetry.

(iii) electron densities were taken as being given by the Baumbach-Allen formula.

(iv) The collision frequency was taken as being given by

$$\nu = 42\ N\ T^{-3/2}$$

(The constant 42 is due to Smerd and Westfold and is an average value of a function which is nearly constant throughout the corona).

N is the electron density.

T is the equivalent electron temperature.

Figure 3:1 shows a set of trajectories calculated in this way.

Double-humped bursts of solar noise were explained as echo effects. The time delay and intensity ratio

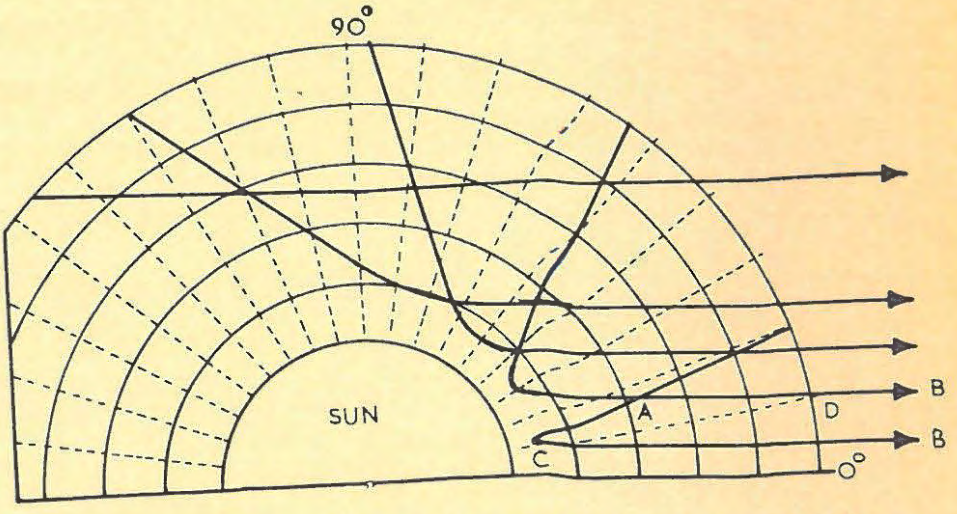

Ray trajectories in the solar corona at a frequency of 100 Mc/s. (Jaeger and Westfold (25)).

FIGURE 3:1

between signals arriving at the Earth after traversing alternative paths such as ACB and ADB (fig. 3:1) were calculated. These were found to agree reasonably with experimental observations, if interpreted as follows: for small source angles (i.e. for sources near the centre of the solar disk), the intensity ratio would be large and the burst would be recorded as single-peaked. For large source angles (i.e. for sources beyond the limb), the peak intensities would be nearly equal but the time delay would be very small and the burst would be recorded as single-peaked. For intermediate source angles the time delay and the intensity ratio would be such that a double-humped burst would be detected.

Jaeger and Westfold (26) have attempted to describe the observed phenomena in terms of a transient produced by a concentrated disturbance at a level of plasma frequency fo. They found the exact solutions of a number of transient problems on the linear propagation of radiation in a homogeneous medium (a) without, and (b) in the presence of, a magnetic field.

It was possible to show that such a transient would give rise to radiation of all frequencies greater than or equal to f_o, but none less than f_o. Their work predicted that the intensity of the radiation would fall off according to an inverse square or

fourth power law:

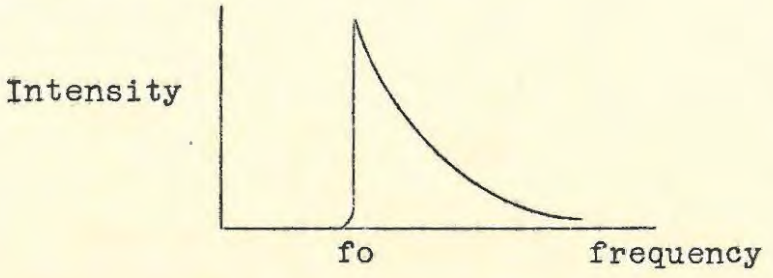

Experimental results at 60 and 85 Mc/s showed an inverse square variation.

The intensity at a given frequency should then decay exponentially with time, the decay constant being equal to the collision frequency . (Experimental observations show that the decay is exponential, and the decay constants are of the same order as ν). Assuming the equation

$$\mu = (1 - \frac{f^2}{f_o^2})^{1/2}$$

for the refractive index at a level of plasma frequency fo for radiation of frequency f, the excess of equivalent path over distance traversed for a ray passing radially outwards from a height ρ (in units of the base of the corona) to infinity, was calculated. The Baumbach-Allen formula for the electron density N and the Smerd-Westfold expression for the collision frequency ν were also assumed.

It was then possible to calculate the expected time delays between direct and echo radiation (see Fig. 3:1) and also the ratios of their intensities.

The time delays were found to agree with those observed in double-humped bursts. However intensity ratios of between 5 and 27 were predicted for the two peaks of double-humped bursts at frequencies around 80 Mc/s; these are very much higher than the ratios observed at these frequencies.

Smerd (27).

Magneto-ionic theory defines three dimensionless quantities x,y and z as follows:

$$x = \frac{fo^2}{f^2}$$

$$y = \frac{f_H}{f}$$

$$z = \frac{\nu}{2\pi f}$$

where f is the frequency of a wave being propagated through the medium

fo is the natural frequency of plasma oscillations at a given level in the medium $= (\frac{e^2N}{\pi m})^{1/2}$ sec.$^{-1}$ (see p. 40).

fH is the electron gyro-frequency at that level, given by

fH = 2.8 x 10^6H sec.$^{-1}$

(where H is the strength of the magnetic field)

ν is the collision frequency.

Points of zero refractive index in the solar atmosphere may then be shown to occur when

$x = 1$ (ordinary ray)

$x = 1 \pm y$ (extraordinary ray).

Neglecting the condition $x = 1 + y$, since it appeared that no radiation could escape from this level, Smerd calculated the heights at which levels of zero refractive index occurred in the corona for radiation of different frequencies. (see Fig. 3:2). Each such level represents a "stop-band" through which radiation of the corresponding frequency cannot be transmitted.

Thus radiation at any frequency f will not be transmitted unless it originates at a height in the corona where the plasma frequency fo is less than or equal to f. In other words it must be produced at a height in the corona greater than or equal to the height of the "stop-band" for the frequency f.

Wild, Murray and Rowe (28), using a swept frequency receiver, observed that outbursts frequently occurred in what appeared to be harmonic pairs, with characteristic features at a frequency f being duplicated at a frequency approximately equal to 2f. The dynamic spectrum of a typical harmonic pair is shown in Fig. 3:3.

The following points required explanation:

FIGURE 3: 2

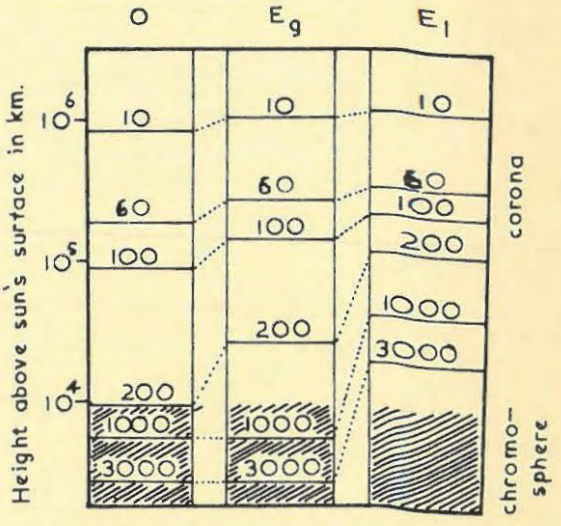

Levels of zero refractive index in the solar atmosphere at different radio frequencies. The levels are shown at 30° latitudes and drawn for the ordinary ray, extraordinary ray in the general magnetic field and the extraordinary ray in a 3600 oersted field above a large sunspot. Numbers on lines give the wave frequency in Mc/s.

(Reproduced from Smerd (27).)

FIGURE 3:3

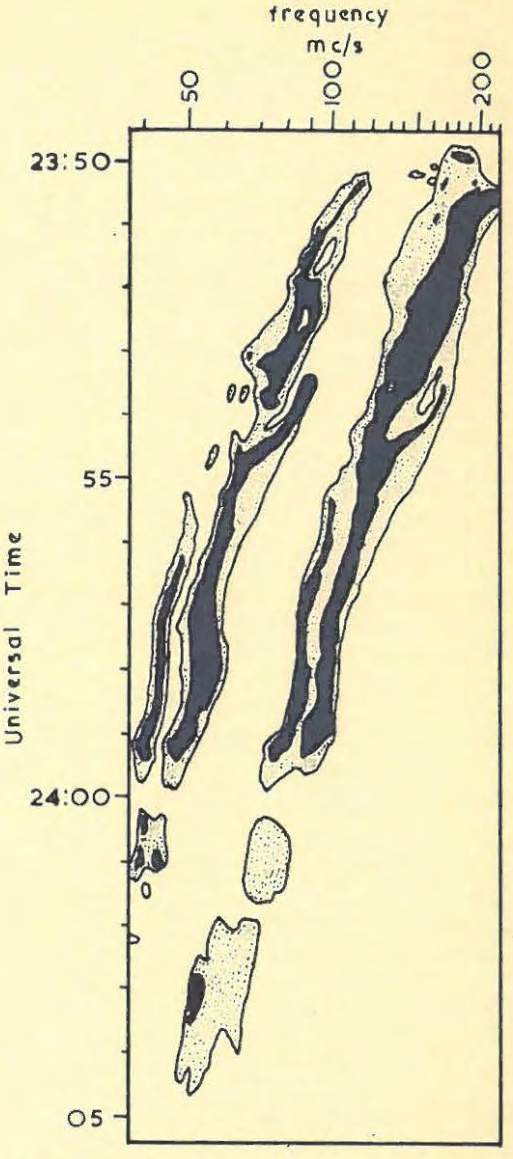

Calibrated Dynamic Spectrum of an outburst, showing a well-defined harmonic poir. The intensity contours correspond to levels of approximately 5 and 20 X 10^{-21} watts $m^{-2}(c/s)^{-1}$

Wild Murray & Rowe (4).

(i) the frequency ratio was consistently just less than 2, (i.e. 1.90 -- 1.99).

(ii) intensity of the second harmonic was frequently equal to or even greater than that of the fundamental.

The authors attempted to explain these anomalies as follows:

(i) If a band of radiation of central frequency f_o is produced at the level in the corona having a natural plasma frequency f_o, the lower half of the band will be cut off. Thus the peak frequency f will appear to be a little higher than fo, and the ratio $\frac{2\ fo}{f}$ will be a little less than 2.

(ii) the second harmonic will tend to be attenuated less since it is further from its level of zero refractive index.

Fig. 3:4 shows how such differential absorption may explain the observed results.

Wild and his colleagues, assuming this model, used Smerd's (26) table of plasma frequencies for different heights in the corona to convert their records of frequency vs. time to plots of "height in the corona" vs. time. The sharp low-end cut-off frequency of the lower-frequency burst was used as the frequency of the fundamental.

A linear plot was obtained, (see Fig. 3:5) which

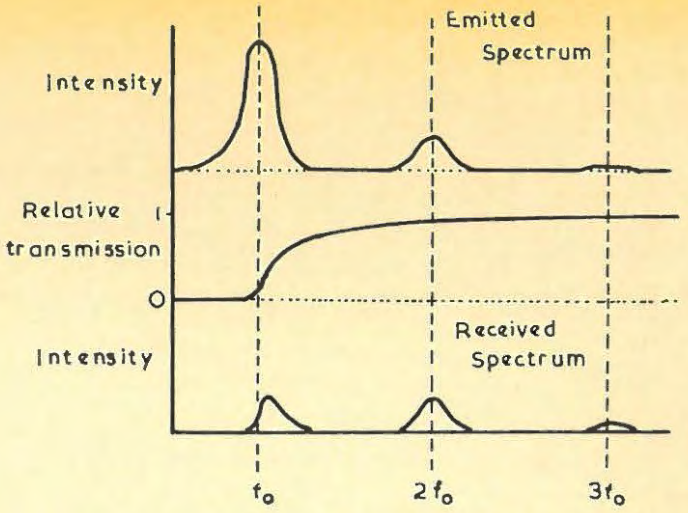

The effect of absorption in the solar atmosphere on harmonics originating at the f_o level. Wild, Murray & Rowe (4).

FIGURE 3:4

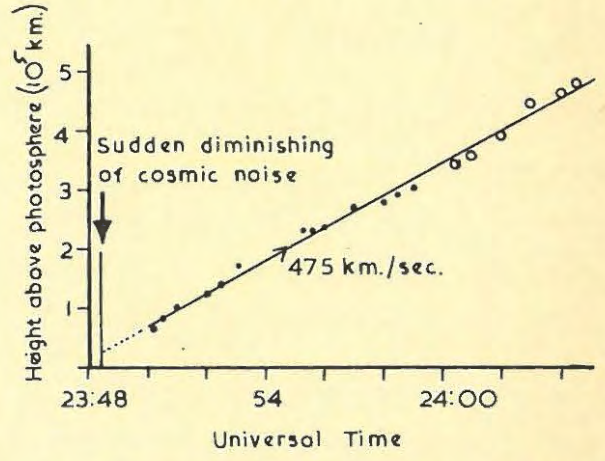

Variation with time of the height of the source of an outburst. Heights are derived from the cut-off frequency of the lower band (black dots) or half the frequency of the upper band (circles). Wild Murray & Rowe (4).

FIGURE 3:5

may be interpreted as representing a source travelling outwards through the corona with a constant speed of the order of several hundred kilometres / sec. The time delays between the onset of a solar flare and the onset of various terrestrial disturbances lead to source velocities of the order of 300 - 3000 km/sec.

The authors point out that the higher velocities can easily be explained in terms of the known asymmetry of the corona, for heights in the corona are derived from an assumed spherical electron-density distribution. Variations from spherical symmetry will therefore cause our estimate of the distance travelled by a source in a given time to be incorrect.

Wild, Roberts and Murray (29) carried out similar work on Type III bursts, and deduced source velocities of the order of 5×10^4 km./sec. The time delay between the onset of a flare and the arrival of such a source stream at the Earth would correspond to the time delay between the start of the flare and the sudden cosmic ray increase at the Earth.

The authors hesitated to propose that protons ejected at the time of flares were the source of these cosmic ray increases since protons with velocities of this order would have relatively low energies.

In all cases extrapolation of the source-posi-

tion graph to the time of the start of the flare gave an original source position within 10^5km. of the photosphere, i.e. at the base of the corona. (see Fig. 3:5).

Kruse, Marshall and Platt (30) showed that synchrotron radiation by non-relativistic electrons spiralling up out of sunspots could cause solar radiation. The speed of the electrons (v) relative to the velocity of light (c) is limited by the observed characteristics of the radiation:

(i) the observed ratio of peak intensities of harmonic pairs of outbursts gives $v/c \leq 0.2$.

(ii) the temperature above a sunspot is estimated at 10^4 ^oK.

This gives $v/c \geq .0018$

Values of v/c of this order give a third harmonic which would be of too low an intensity to be recorded on existing apparatus. This would explain the fact that no third or higher harmonics have been detected in experimental observations.

Taking a value of $v/c = .02$, the calculated intensity of radiation at a frequency of 100 Mc/s, as measured on Earth, would be of the order of 2×10^{-19} watts m^{-2} $(c/s)^{-1}$. This is in good agreement with experiment.

Westfold (31) reverts to the theory of excitation of plasma oscillations by streams of particles ejected from the sun during flares.

He has explained the "slow" Type II velocities as those of the shock waves accompanying such a particle stream, rather than the velocities of the particles themselves.

In the presence of local magnetic fields of a few hundred gauss (easily realisable in the corona), the shock-wave velocity takes on a magneto-hydrodynamic component. The resultant velocity would then take on a value of the order of those estimated for Type III burst sources.

Such a shock wave would fit the Jaeger-Westfold transient model described on pp. 42, 43.

Roberts (6) in discussing the "reverse drift pair" bursts observed by him, mentions in a footnote that the Australian radio-astronomers had by that time (1958) discarded the "echo" theory of the production of double-humped bursts. These were attributed rather to a source moving outwards and causing excitation of the f level and a short time later of the f/2 level. It was suggested that the decay portions of Type III bursts might be explained in terms of the reduction of the effect of the exciting source,

rather than in terms of the natural decay of plasma oscillations.

B. SUMMARY.

We have seen that many of the observed characteristics of solar noise radiation may be explained on various hypotheses, and it is difficult to make a choice between these based on information available at present.

Type III bursts are now generally accepted as being produced in the following manner: some sort of transient disturbance, (probably associated with a stream of solar corpuscles emitted at the time of a micro-flare or flare-puff), moves outwards through the corona and excites successive plasma levels. A single-frequency receiver tuned to a frequency f will record a peak as the disturbance passes through the plasma level of natural frequency f. Some seconds later the transient excites the f/2 level, which radiates at frequencies f/2, f, 3f/2, etc. Thus a further peak appears on the receiver. Making the simplifying assumptions that the source moves radially outwards through a corona which

(i) is spherically symmetrical,

(ii) has an electron-density distribution given by

the Baumbach-Allen formula, we may deduce the speed of the exciting source.

The decay of the plasma oscillations may be attributed either to a collision effect (which would predict an exponential decay constant equal to the collision frequency ν), or to the reduction in the effect of the exciting disturbance. The latter explanation is favoured since it accounts for the facts that

(i) the decay constant is of the same order as, but is not equal to, the collision frequency.

(ii) "reversed" bursts are recorded fairly frequently. These are "mirror images" of the usual Type III burst, i.e. they have a roughly exponential rise portion and a rapid linear decay portion. Reversed double-humped bursts have the first peak smaller than the second, indicating a source moving inwards towards the centre of the sun. Clearly such reversed bursts cannot be explained in terms of the natural decay of plasma oscillations, since these would decay in a manner independent of the motion of the source.

Type II bursts are explained in a similar manner; we may suppose that plasma oscillations are set up in this case by a rapid succession of transients of the

same general form as those producing Type III bursts.

Despite the availability of a very considerable quantity of observational data concerning sunspots, we find ourselves still somewhat vague as to what conditions actually obtain in the vicinity of a sunspot. Theories of solar radio emission from sunspots are therefore rather exploratory in nature. Type I bursts are known to be correlated with sunspots - they have been explained in terms of both thermal and coherent oscillation sources.

According to Smerd, noise storm radiation at a frequency f must be generated above the "stop-band" for that frequency in the corona. It will therefore be emitted from the same regions in the corona as Type II and III radiation which have the same frequency, and which are propagated in the same mode.

It will therefore be interesting to investigate whether the complex storm profiles can be shown to be the sum of a large number of bursts having the typical shape of Type III bursts. The result of this investigation will allow us to suggest which is the most likely mechanism for the production of storm bursts.

CHAPTER FOUR.

OBSERVATIONS OF SOLAR NOISE AT A FREQUENCY OF 300 Mc/s, AND METHODS OF ANALYSIS.

During the period 24/6/59 to 17/11/59, 95 records of the flux density of solar radio noise at a frequency of 300 Mc/s were obtained. Each of these represented approximately 7 hours of continuous recording.

Altogether 385 hours of recording film were suitable for analysis. The records were projected (magnification about 16x) onto graph paper and the intensity contours of bursts were carefully plotted.

Further analysis was then carried out on these plots.

A. LINEARITY OF RECEIVER.

Before any analysis of the records could be usefully undertaken, it was necessary to find the manner in which the deflection of the oscilloscope spot, as measured on the film, varied with the input signal.

Every few days a noise diode calibration was performed (see p. 32). In a temperature-limited diode, the intensity of the noise signal generated in the

plate circuit is proportional to the plate current. By varying the filament voltage we may set the plate current at suitable values. A plot of "noise-diode plate current" vs. "deflection of spot on film" thus gives a true representation of the response of the amplifier.

Practically every plot thus constructed approximated very closely to a straight line. Variations from linearity, where they did occur, were not consistent and could therefore be attributed to slight errors in setting and reading the plate current, and in the measurement of spot deflections.

Some typical plots of this type are shown in Fig. 4:1.

Thus we may take the response of the receiver as being linear,

i.e. the variation of the height of the photographic trace above the baseline is an accurate representation of the variation of flux density at the antenna.

B. Isolated Bursts.

As a preliminary measure, isolated (Type III) bursts recorded by the apparatus were analysed. The objects of this analysis were as follows:

(i) to check that these bursts had the characteristics observed by other investigators at similar frequencies.

FIGURE 4:1

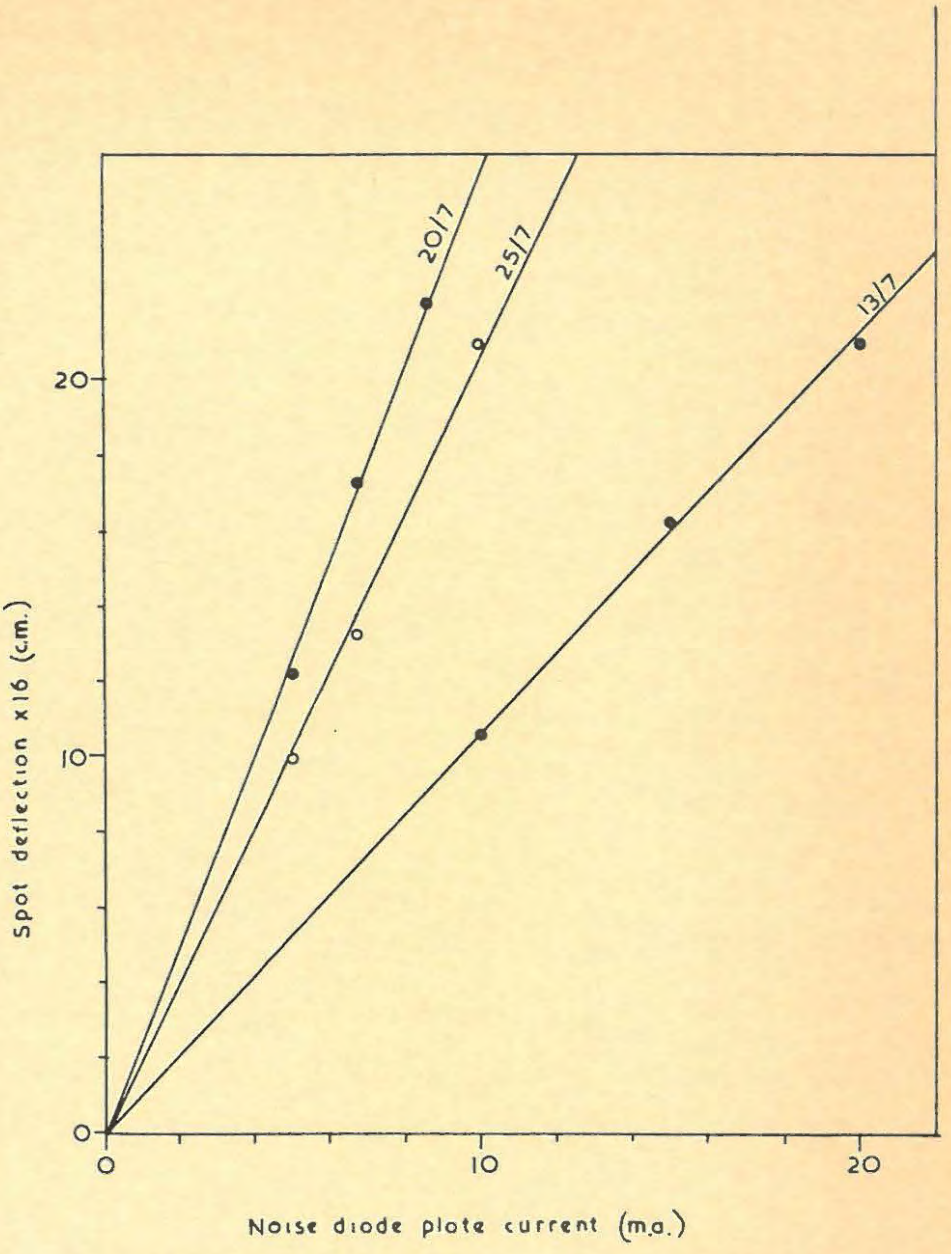

Typical noise diode calibration plots, for three different gain settings.

(ii) to attempt to ascertain the type of function giving the best agreement with observed decay portions, e.g. exponential, $I^{1/n}$, etc.

(iii) to find an average value of the "decay constant" for these bursts and to compare this value with the average value for storm bursts.

For the purposes of analysis, isolated bursts were classified into three sub-types as follows:

(i) Single-peaked.

(ii) Double-humped.

(iii) Complex, i.e. groups of three or more single peak bursts occurring in rapid succession.

These three subtypes have been designated by the letters S,D and X respectively.

In analysing the decay portions of these bursts, the position of the start of the decay portion was chosen somewhat arbitrarily to coincide with the peak of the burst. The perpendicular dropped from the peak to the baseline intersects it at a point which is assigned the time value t = 0.

The intensity (arbitrary units) at various values of t was then read off. Plots of $\log_{10}I$, $I^{\frac{1}{2}}$, $I^{\frac{1}{4}}$, $I^{-\frac{1}{2}}$ and $I^{-\frac{1}{4}}$ vs. t were constructed for the first few bursts. The plots of both $\log_{10}I$ and of $I^{\frac{1}{4}}$ vs. t approximated fairly closely to straight lines: the

remaining plots were definitely not linear.

The exponential plots fitted the observed decay portions slightly better than the plots of $I^{\frac{1}{4}}$, and thereafter only the exponential function was plotted. The slope of this plot (in units of $sec.^{-1}$) was calculated in each case. This slope is the "decay constant" k in the expression

$$I = I_0 \, e^{-kt}$$

which we shall assume to be a representation of the decay portion of the burst.

Fig. 4:2 shows a typical single-peak isolated burst and the resultant plots obtained.

The life-times of bursts (measured between points of quarter-maximum intensity) were also calculated: in the case of double-humped bursts the time delay between the two peaks was measured and the intensity ratio of the peaks was calculated.

The results of this analysis are summarised in tables III, IV, V and VI.

C. STORM BURSTS.

It was hoped to show that complex storm profiles could be interpreted as the sum of a large number of bursts, each having the typical shape of an isolated burst.

In order that a storm section could be analysed into component bursts in this way, it was necessary

56a

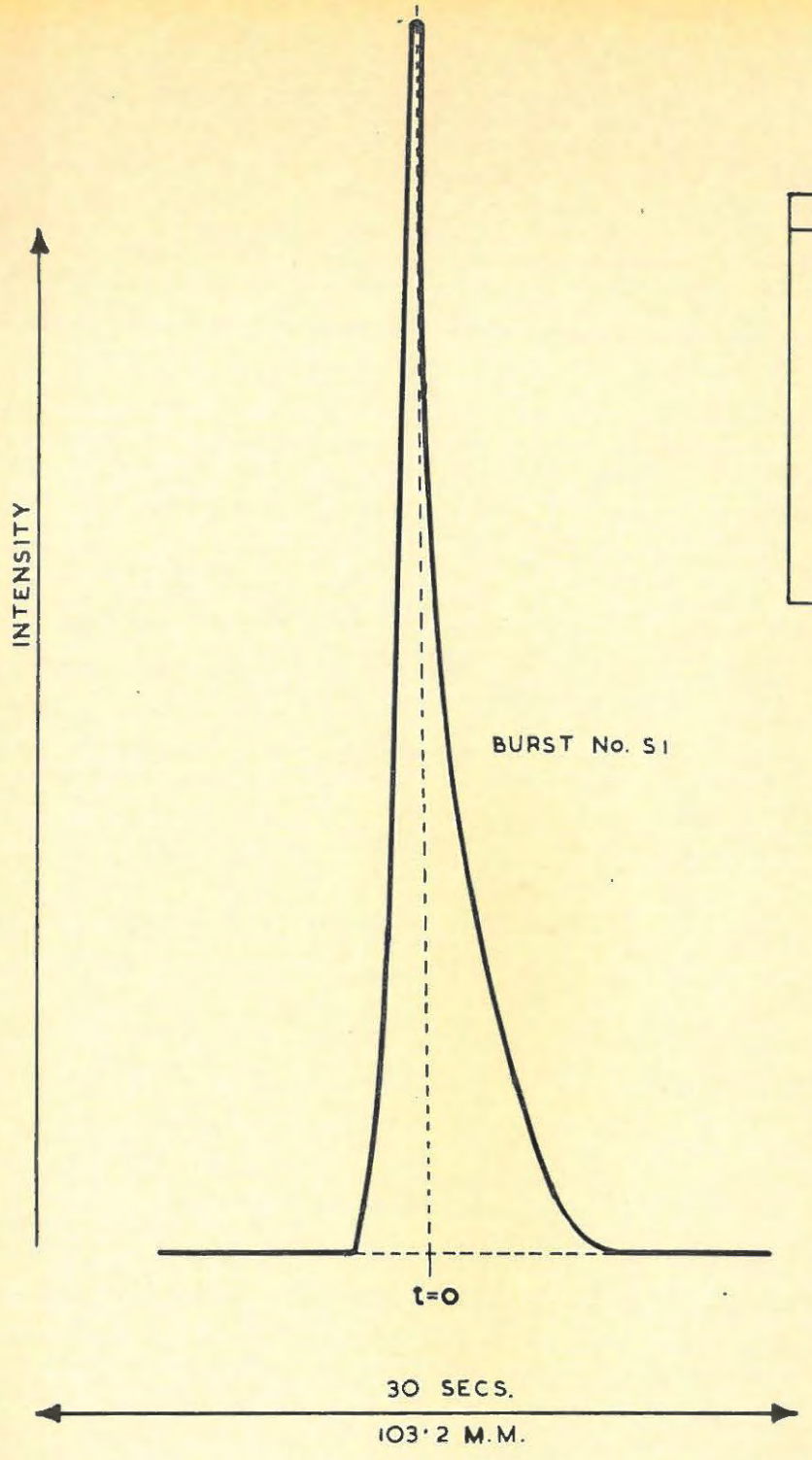

t mm.	I cm.
0	16.75
2	7.7
4	6.2
6	4.7
8	3.85
10	2.9
12	2.2
14	1.5

FIGURE 4:2

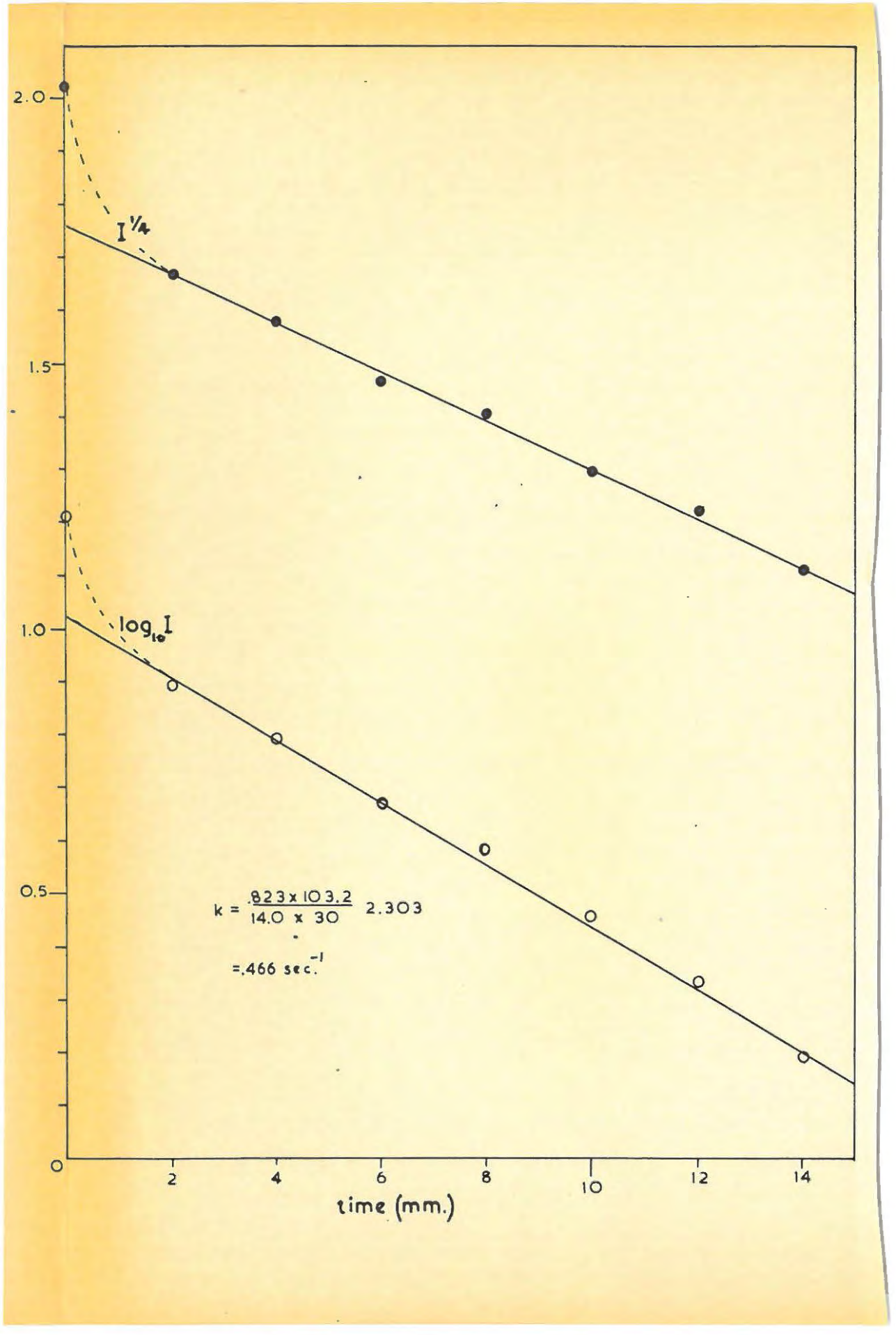
2.0
1.5
1.0
0.5
0
$I^{1/4}$
$\log_{10} I$
$k = \frac{.823 \times 103.2}{14.0 \times 30} \; 2.303$
$= .466 \text{ sec.}^{-1}$
2
4
6
8
10
12
14
time (mm.)

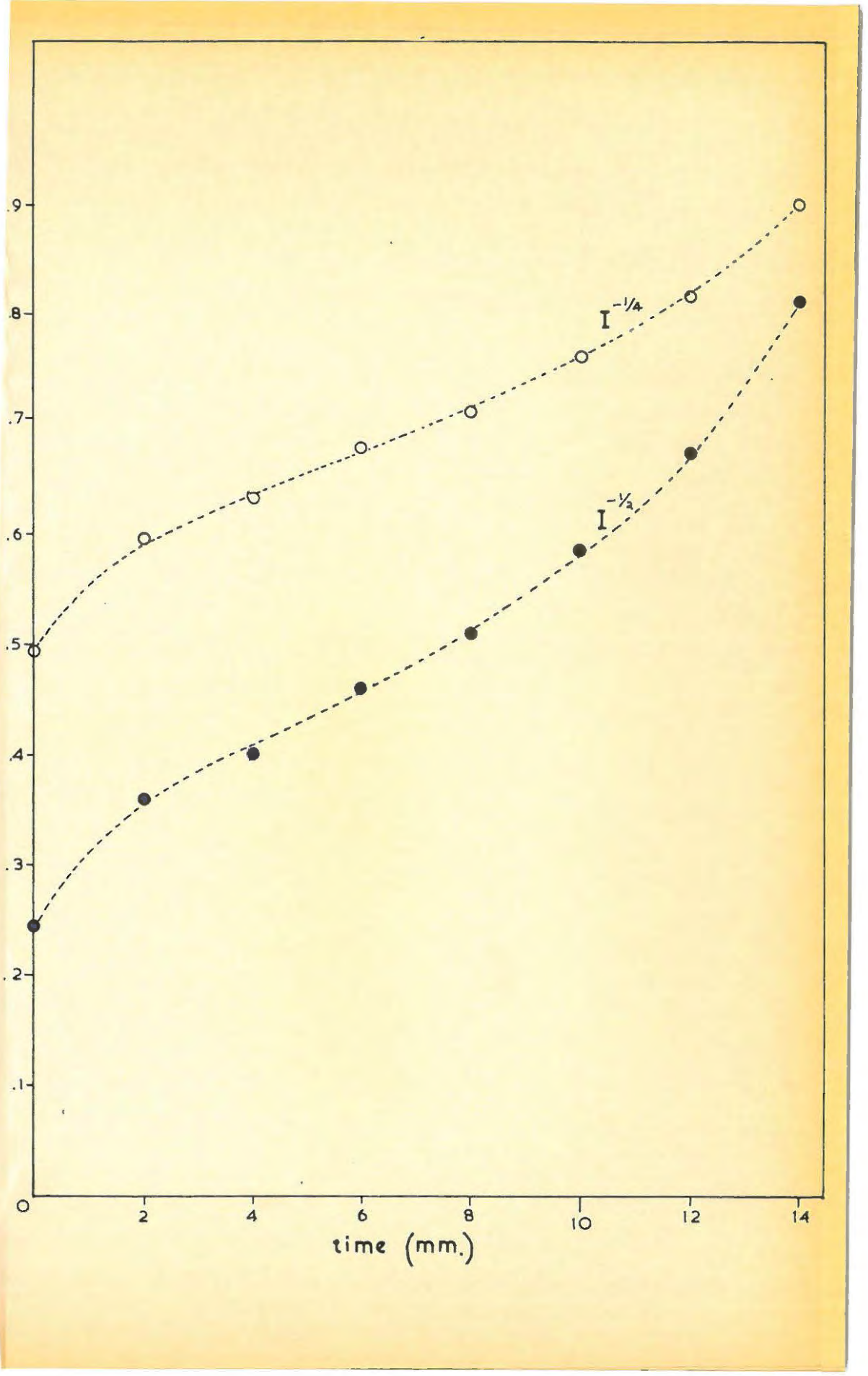
.9
.8
.7
.6
.5
.4
.3
.2
.1
0
2
4
6
8
10
12
14
time (mm.)
$I^{-1/4}$
$I^{-1/3}$

TABLE III

TYPE III (ISOLATED) BURSTS RECORDED BY THE AUTHOR ON A FREQUENCY OF 300 Mc/s.

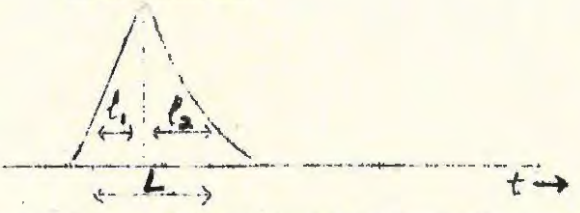

Rdd. No.	Bst. No.	Date	Universal Time	Decay Const. "k" $sec.^{-1}$	Lifetimes (secs) t_1	t_2	L	Remarks.
P 8	S 1	8.7.59	12.33	.47	1.50	2.20	3.70	
P13	S 2	13.7.59	09.18	2.88	.28	.70	.98	
"	S 3	"	09.22	1.45	.43	1.15	1.58	R
"	S 4	"	11.07	1.37	.60	.41	1.01	
P14	S 5	14.7.59	08.39	2.38	.26	.65	.91	R
P19	S 6	25.7.59	11.40	.60	2.14	2.53	4.67	
P36	S 7	22.8.59	09.30	.93	.64	1.63	2.27	
"	S 8	"	13.55	1.86	.43	.72	1.20	
		Average Values		1.61	.79	1.25	2.04	

Bursts marked "R" are "reversed", i.e. they appear to have exponential rise portions and linear decay portions. In each of these cases the time scale has been reversed and the burst analysed in the usual way.

TABLE IV

DOUBLE-HUMPED ISOLATED BURSTS RECORDED BY THE AUTHOR ON A FREQUENCY OF 300 Mc/s.

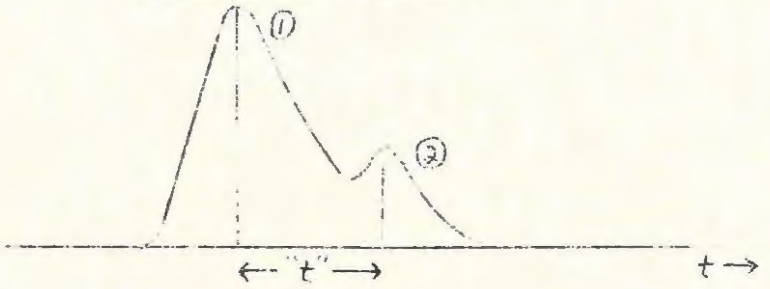

Rcd. No.	Bst. No.	Date.	Universal Time.	Decay consts.		"t" secs.	Velocity of source 10^4 km/sec.	Rem-arks.
				"k_1" $sec.^{-1}$	"k_2" $sec.^{-1}$			
P 8	D 1	8.7.59	11.20	.79	.50	6.44	.44	
P11	D 2	11.7.59	09.31	2.40	1.43	.55	5.10	
P13	D 3	13.7.59	10.59	.94	1.40	2.59	1.10	R
P14	D 4	14.7.59	08.13	3.11	4.94	.52	5.39	R
P23	D 5	30.7.59	10.20	.52	.58	1.81	1.57	
P31	D 6	14.8.59	12.20	1.37	1.04	2.80	1.02	
P35	D 7	21.8.59	11.18	1.05	1.68	2.59	1.10	R
P36	D 8	22.8.59	13.55	3.43	2.17	1.91	1.49	
		Average Values		1.71	1.71	2.40	2.15	

Bursts marked "R" are "reversed", i.e. they appear to have exponential rise portions and linear decay portions. In each of these cases the time scale has been reversed and the burst analysed in the usual way.

TABLE V.

DOUBLE-HUMPED ISOLATED BURSTS RECORDED BY THE AUTHOR ON A FREQUENCY OF 300 Mc/s.

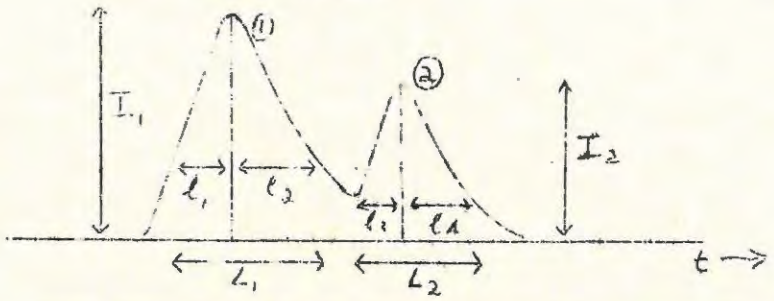

Rcd. No.	Bst. No.	Lifetimes (secs.)						$\frac{I_1}{I_2}$	Remarks.
		"l_1"	"l_2"	"L_1"	"l_3"	"l_4"	"L_2"		
P 8	D 1	.68	1.92	2.60	2.69	3.00	5.69	.683	
P11	D 2	1.09	.27	1.36	.96	.96	1.92	1.97	
P13	D 3	1.37	1.58	2.95	-	1.15	-	2.52	R
P14	D 4	.26	.26	.52	.26	.39	.65	1.96	R
P23	D 5	.90	1.81	2.71	.78	2.31	3.09	1.93	
P31	D 6	1.22	1.10	2.32	.95	1.46	2.41	2.39	
P35	D 7	1.44	1.29	2.73	.36	.72	1.58	2.83	R
P36	D 8	.72	.48	1.20	.60	.76	1.36	1.53	
Average Values.		.96	1.09	2.05	1.05	1.34	2.39	1.98	

Bursts marked "R" are "reversed", i.e. they appear to have exponential rise portions and linear decay portions. In each of these cases the time scale has been reversed and the burst analysed in the usual way.
Blanks appear in the above table where it was not possible to measure the lifetime of a burst.

TABLE VI

COMPLEX ISOLATED BURSTS RECORDED BY THE AUTHOR ON A FREQUENCY OF 300 Mc/s.

Rcd. No.	Bst. No.	Date.	Universal Time.	Decay Const. "k" sec.$^{-1}$	Lifetimes (secs.) t_1	t_2	L	Remarks.
P 8	X1 a	3.7.59	09.23	1.93	.86	.57	1.43	
	b			.90	.86	1.57	2.43	
	c			.65	1.14	2.28	3.42	R
	d			.90	2.28	1.71	3.99	
P 8	X2 a	3.7.59	12.40	.94	.71	1.42	2.13	
	b			.73	1.72	.43	2.15	
P 8	X3 a	3.7.59	13.32	.43	.29	2.86	3.15	R
	b			1.64	1.14	.14	1.28	
P 8	X4 a	3.7.59	13.33	.71	.57	1.72	2.29	
	b			2.11	1.00	.86	1.86	
	c			.85	.43	.58	1.01	
P40	X5 a	27.8.59	09.35	1.75	.75	1.00	1.75	R
P36	X6 a	3.11.59	12.05	1.04	.68	2.04	2.72	
	b			1.51	1.70	1.87	3.57	
P39	X7 a	6.11.59	08.29	2.30	.65	.91	1.56	
	b			1.95	1.04	.91	1.95	
		Average Values		1.27	.99	1.30	2.29	

Peaks marked "R" are "reversed". The time scale has been reversed in analysing such bursts.

that the following conditions should be satisfied:

(i) the bursts should not follow too closely on one another, otherwise each burst will mask the decay portion of the preceding burst.

(ii) the complex profile should return to, or near to, the baseline several times in the selected portion, so that "starting points" for analysis were available.

The analysing procedure consisted of the following main steps.

(i) Find a suitable "starting point" where a considerable portion of a burst is unmasked by nearby bursts.

(ii) Check that the decay portion of this burst is exponential, and plot by extrapolation the complete decay portion.

(iii) Subtract the intensity thus calculated from the total observed intensity, at various points.

(iv) By extrapolation complete the new burst, portions of which have been obtained in step (iii).

This process is continued until as much as possible of the complex storm contour has been analysed into component bursts.

This procedure was carried out on four sections of storm records, two at 300 Mc/s and two at 125 Mc/s (125 Mc/s records were kindly made available by

Dr. Stack Forsyth for this purpose.)

The results of this analysis are shown in Figs. 4:3 to 4:6. In each case Fig. (a) is the complex profile and Fig. (b) shows the component burst shapes deduced by the author. Arrows indicate places where the complex profile could not be analysed into component peaks.

The complex and deduced profiles have been drawn separately for clarity, but have been arranged in such a way that they may be conveniently superposed.

The exponential decay constant of each component burst was calculated and the average value of "k" for each of the two frequencies was found.

Contact prints of the actual storm records analysed appear in plate H.

FIGURE 4:3A

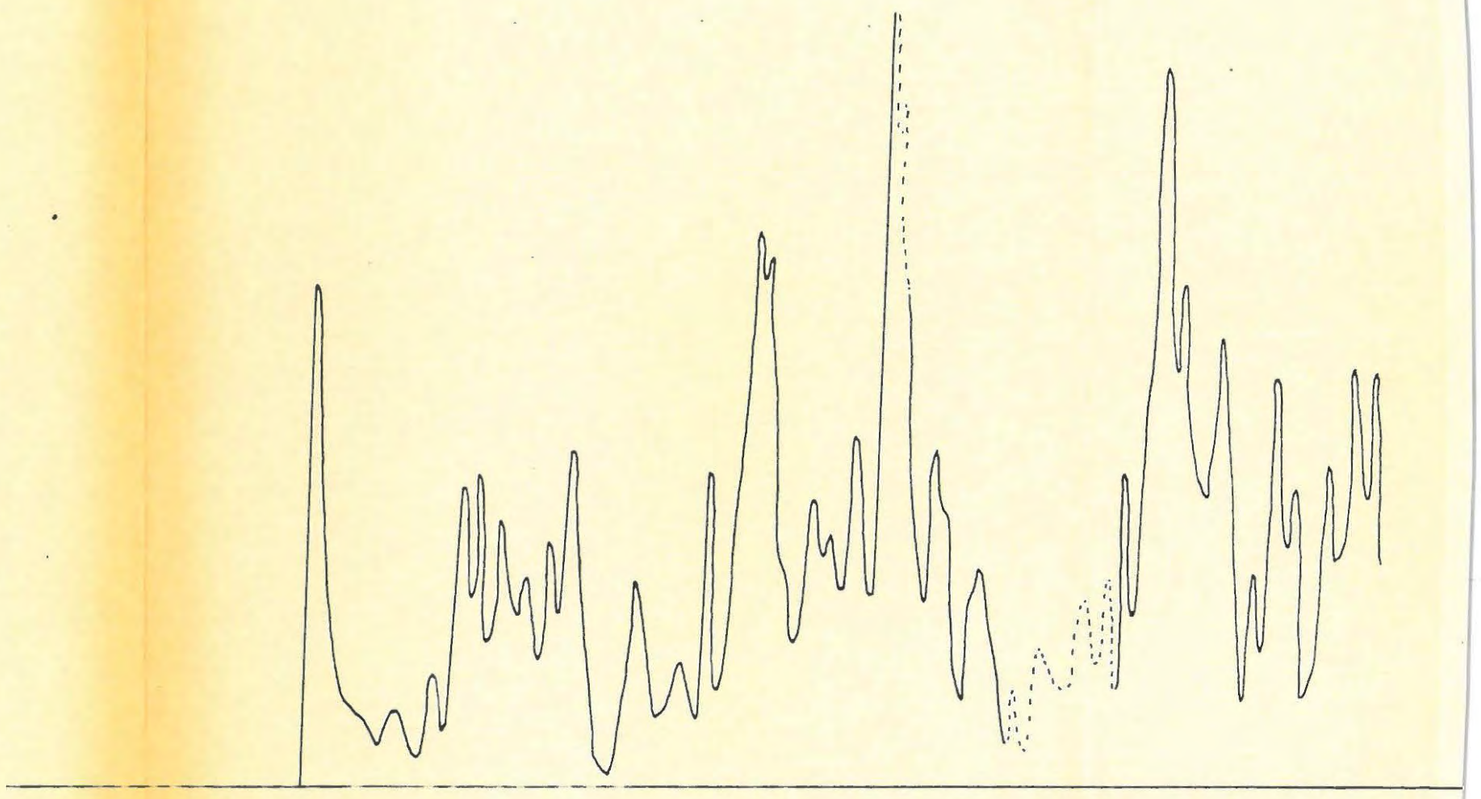

FIGURE 4:3B

Record Number	P 14
Date	14.7.59
Frequency	300 Mc/s
Number of bursts	27
$k_{av.}$	2.82 sec.$^{-1}$

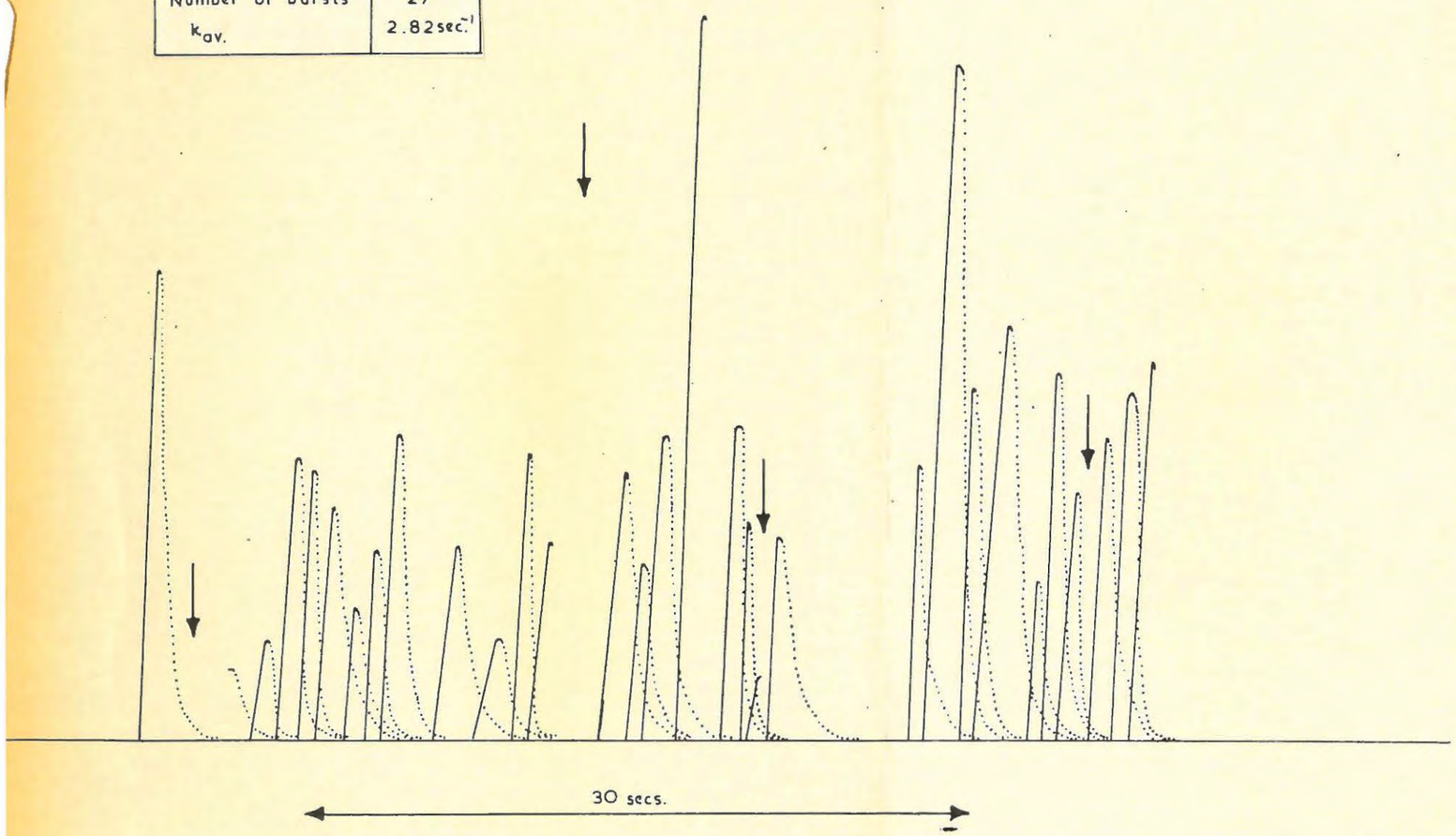

FIGURE 4:4 A

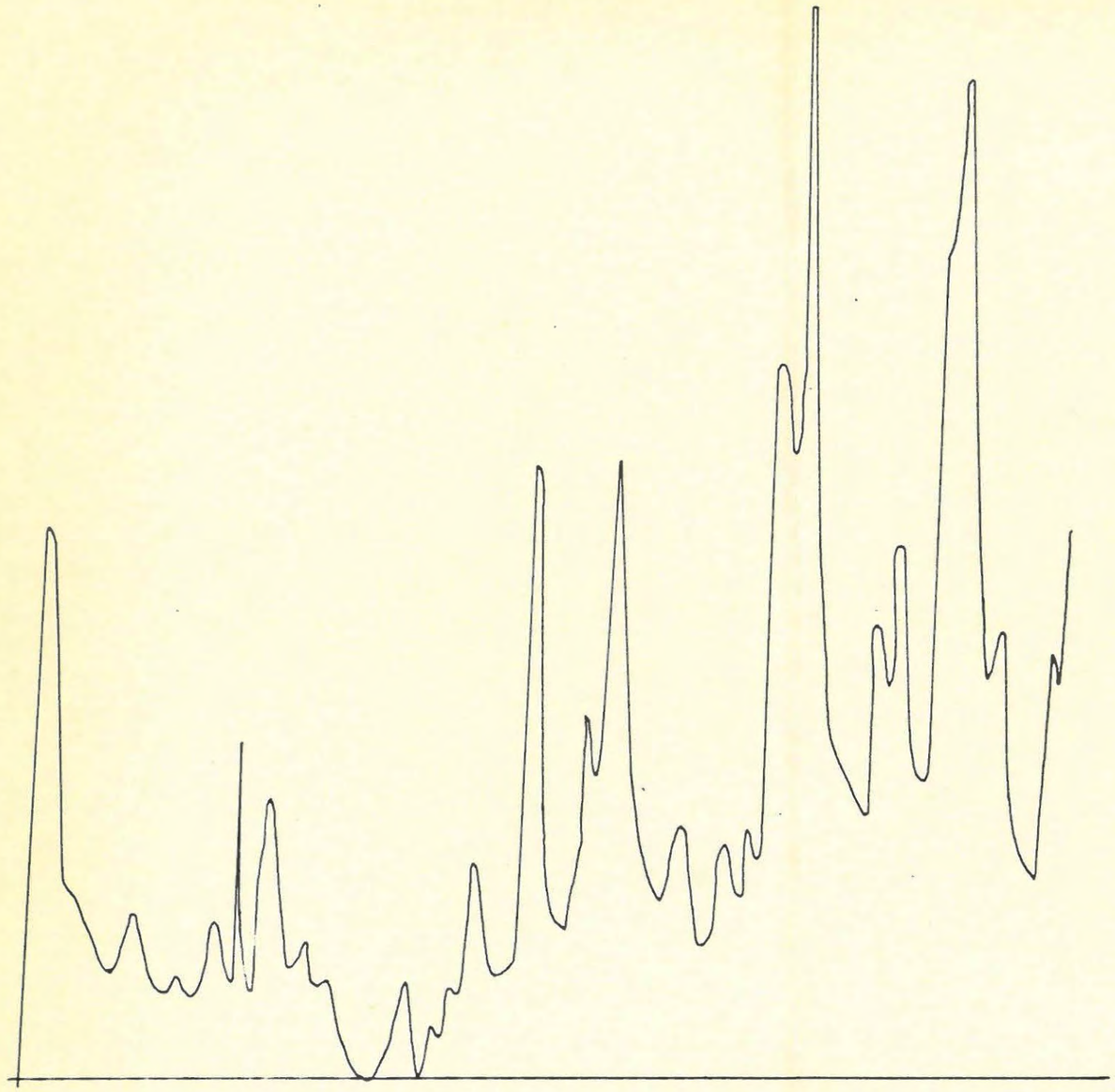

FIGURE 4:4B

Record No.	P 14
Date	14.7.59
Frequency	300 Mc/s
Time (U.T.)	11:40
Number of bursts	29
$k_{av.}$	2.99 $sec.^{-1}$

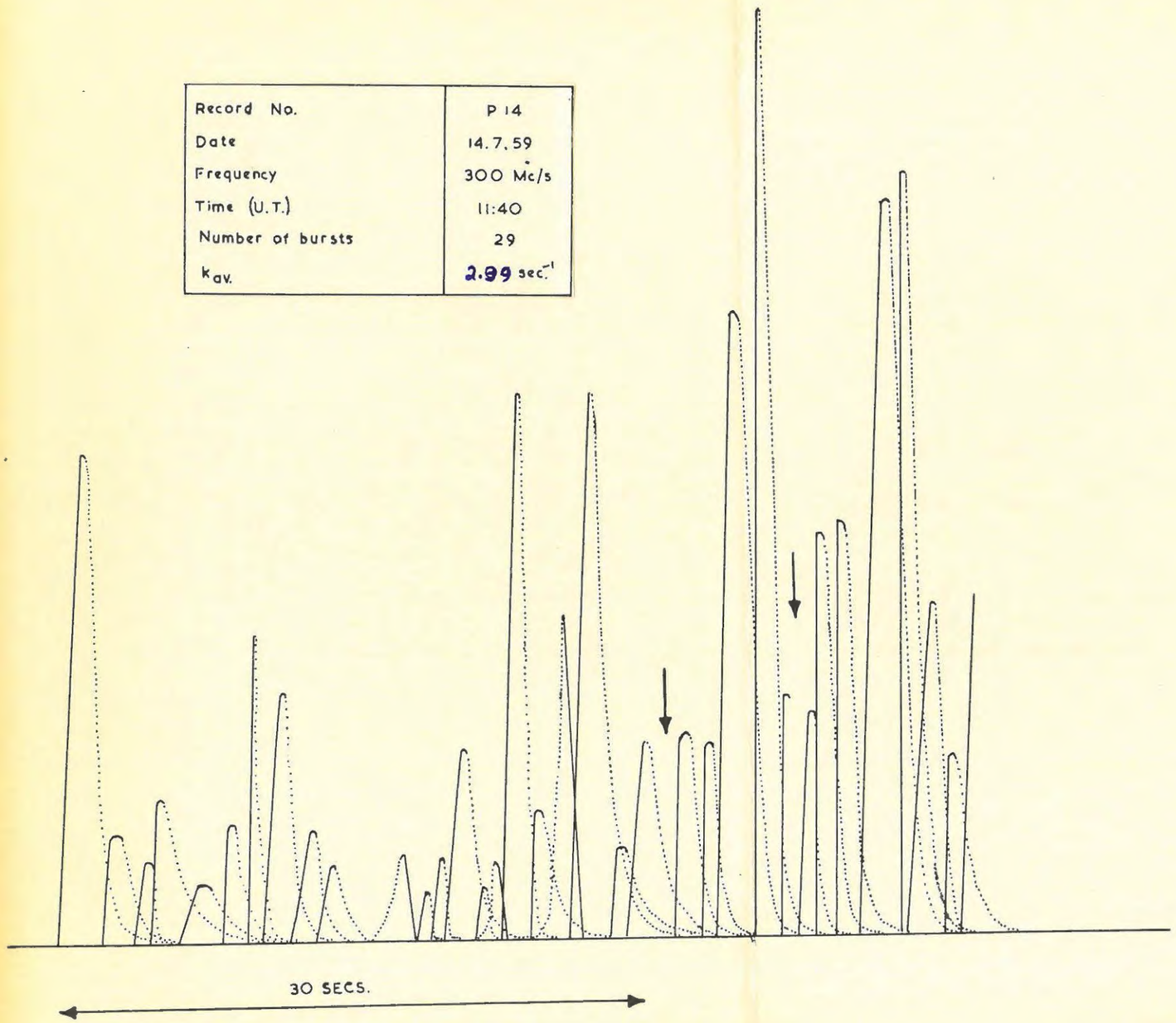

FIGURE 4:5A

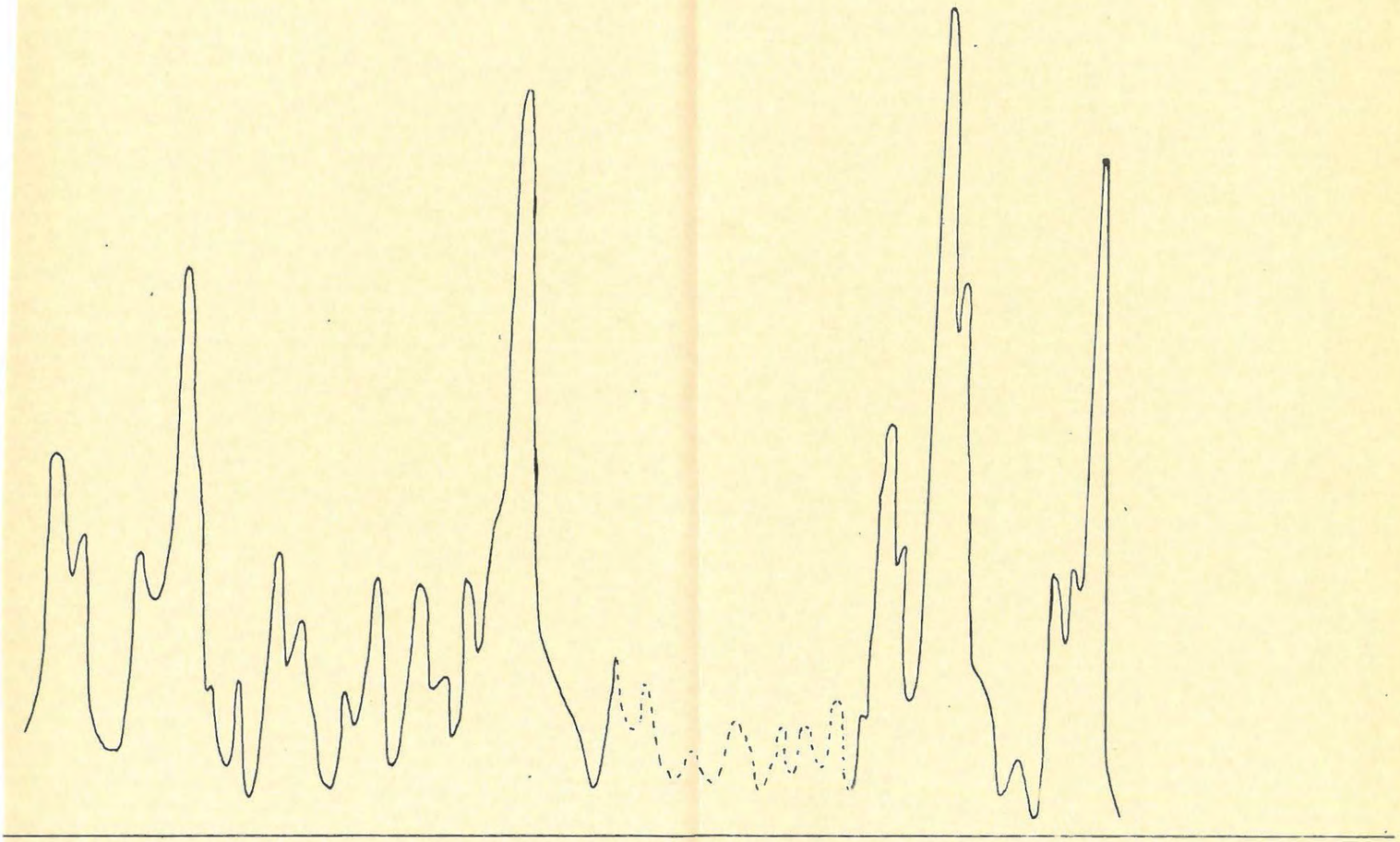

FIGURE 4:5 B

Record No.	B 33
Date	3.7.58
Time (U.T.)	09:34
Frequency	125 Mc/s.
Number of bursts	19
$k_{av.}$	2.68 sec.$^{-1}$

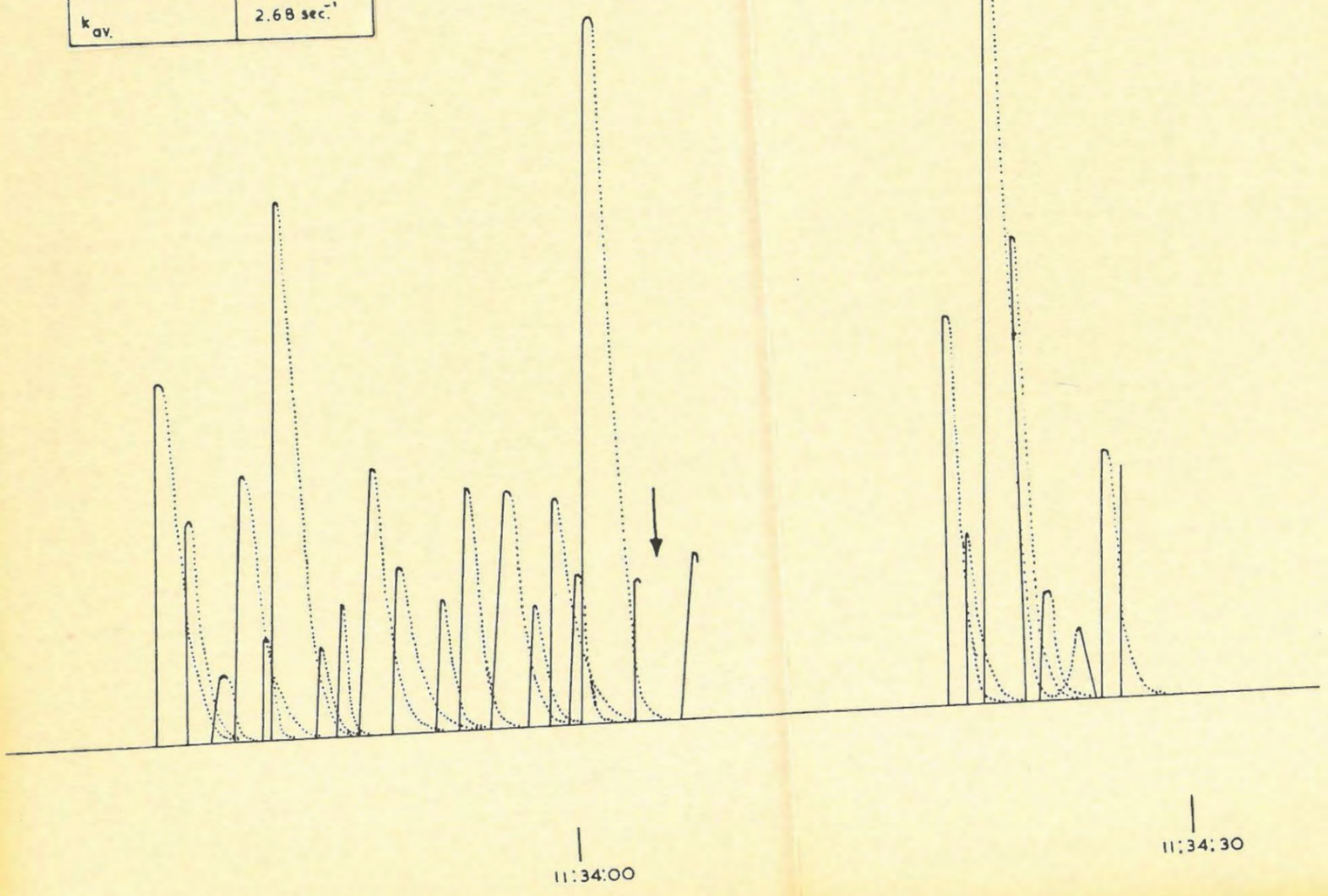

FIGURE 4:6A

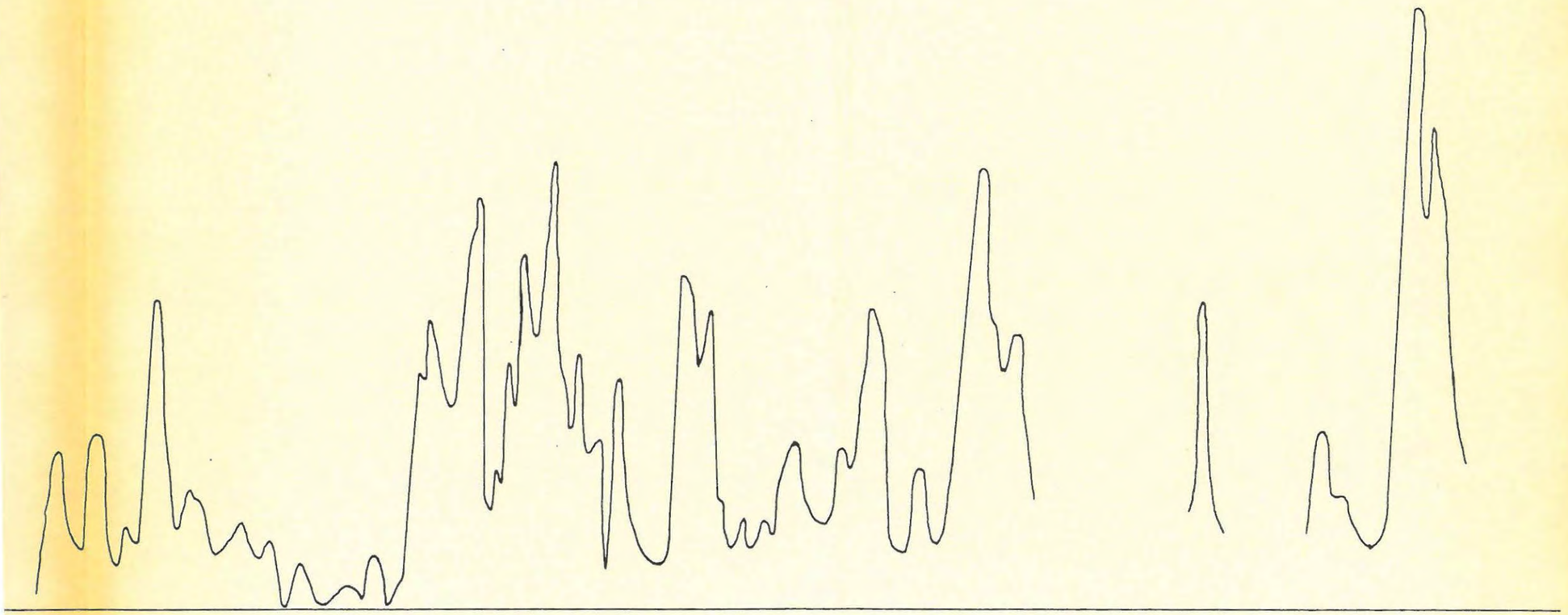

FIGURE 4:6 B

Record No.	B 33
Date	3/7/58
Time (U.T.)	10.18
Frequency	125 Mc/s.
Number of bursts.	21
$k_{av.}$	2.22 $sec.^{-1}$

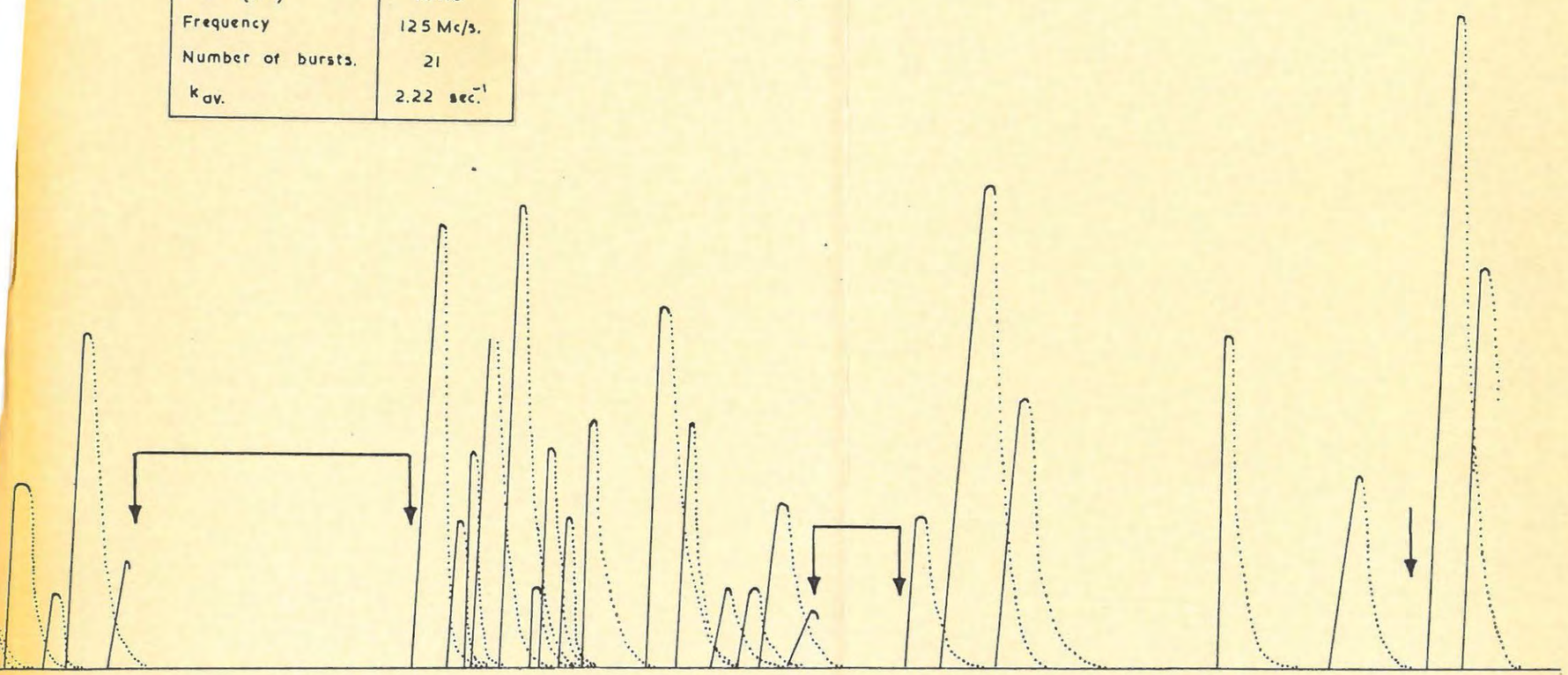

12:18:30

12:19:00

S.A.S.T.

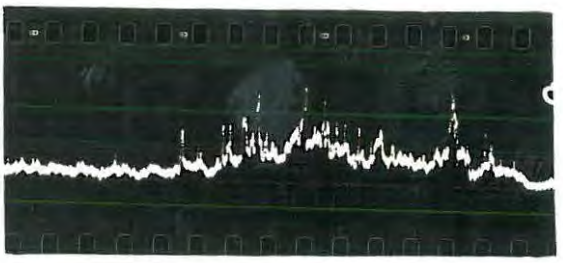

R/N. P 14
11:40
See Fig. 4:4

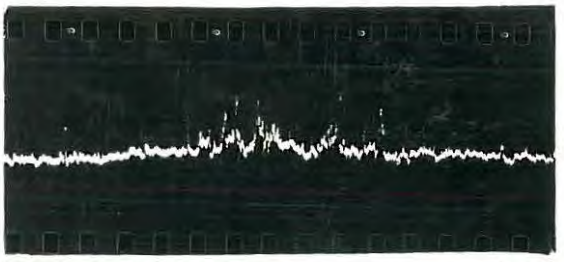

R/N. P 14
09:55
See Fig. 4:3

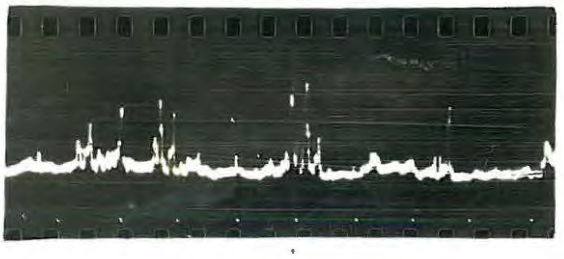

R/N. B 33
09:34
See Fig. 4:5

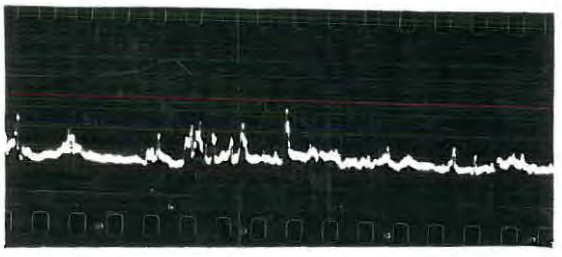

R/No. B 33
10:18
See Fig. 4:6

PLATE H

CHAPTER FIVE.

DISCUSSION OF OBSERVATIONS.

AND CONCLUSIONS.

A. COMPARISON OF OBSERVATIONS OF TYPE III (ISOLATED) BURSTS WITH THOSE MADE BY OTHER WORKERS.

(i) Decay Constants.

Summary of Author's Results	
Single-peak	$k_{av} = 1.61 \text{ sec}^{-1}$
Complex	$k_{av} = 1.27 \text{ sec}^{-1}$
Double-hump	$k_{1_{av}} = 1.71 \text{ sec}^{-1}$
Double-hump	$k_{2_{av}} = 1.71 \text{ sec}^{-1}$

Wild (32) has shown that the "normalized" decay constant appears to increase with frequency in a roughly linear fashion, for a given burst, in the range 70 - 130 Mc/s. The "normalized" decay constant is defined as $k/\bar{k}$, where k is the decay constant at a given frequency, and $\bar{k}$ is the mean value of k over the frequency band.

Wild's results are indicated in Fig. 5:1. The figure suggests that the decay constant (in the observed frequency range) may be approximately related to the frequency by an expression of the form

$$k = Kf \quad \ldots\ldots\ldots\ldots\ldots\ldots\ldots\ldots (5.1)$$

where K is of the order of 10^{-8} and is a constant

for a given burst. K varied between .62 x 10^{-8} and 1.5 x 10^{-8} for ten different bursts recorded by Wild, the average value being 0.98 x 10^{-8}.

Taking this average value of K, equation 5:1 predicts an average decay constant at 300 Mc/s of about 3 Sec^{-1}. The largest decay constant observed by the author was 3.44 sec^{-1}, but the average value of k is somewhat below that predicted by the above equation.

It must be remembered that the speed of movement of the recording film in the "x" direction limits the highest value of k that can be measured. Several peaks recorded by the apparatus decayed so rapidly that it was not possible to analyse them; three bursts with decay constants of about 6 Sec^{-1} would be sufficient to bring the mean value of k up to 3 sec^{-1}.

Thus it would seem that the curve shown in Fig. 5:1 may be extended as far as 300 Mc/s, as indicated in Fig 5:2.

A search of the literature has not revealed any observations of the decay constant at 300 Mc/s; results recorded for frequencies between 19 and 130 Mc/s are listed below.

Payne-Scott (1)	19 Mc/s: kav	= 0.3 sec^{-1}
	60 Mc/s: "	= 0.6 "
	85 Mc/s: "	= 0.6 "
Williams (7)	75 Mc/s: "	= 0.7 "

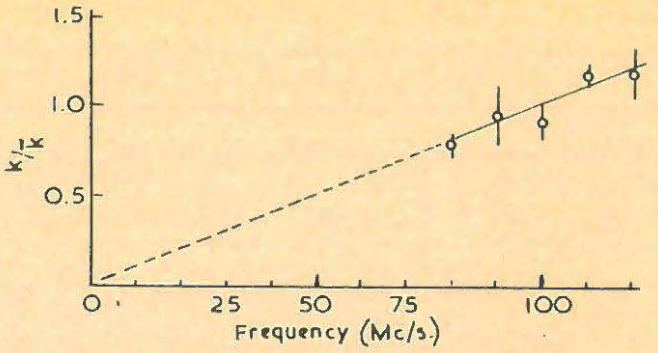

The variation with frequency of the average value of $k/\bar{k}$ for 12 observed Type III Bursts. Probable errors are indicated. (Wild (32)).

FIGURE 5:1

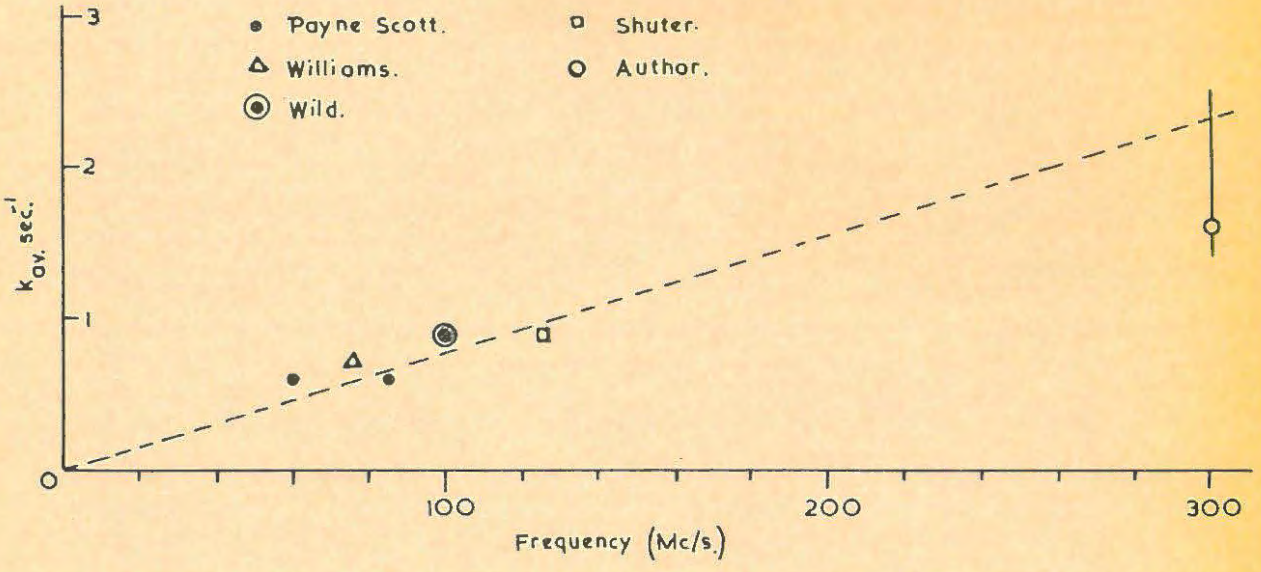

Suggested variation of $k_{av.}$ (for isolated bursts) with frequency, in the range 0 – 300 Mc/s. The large probable error indicated for the author's result is explained in the text.

FIGURE 5:2

Wild (32) 100 Mc/s: k_{av} = 1.0 sec^{-1}

Shuter (35) 125 Mc/s: k_{av} = .82 sec^{-1}

$k_1 av$ = .60 "

$k_2 av$ = .61 " .

(ii) Life-times of Isolated Bursts.

Summary of Author's Results		
Single-peak	L av = 2.04 secs.	61% of life-time spent in decay
Complex	L av = 2.29 "	57% "
Double-humped	L_1 av = 2.05 "	53% "
"	L_2 av = 2.39 "	56% "

Wild (32) observed life-times of between 2.9 and 3.8 secs. at a frequency of 100 Mc/s, a little more than half the life-time being spent in decay.

Shuter (35) observed life-times between 1.8 secs. and 8.9 secs. at a frequency of 125 Mc/s, with an average value of 4.0 secs.

Life-times observed by the author are lower than life-times measured at lower frequencies. We expect that this will be the case since the decay constant appears to increase with frequency.

(iii) Peak-Intensity ratios for double-humped bursts.

Summary of Author's Results
I_1/I_2 min. = .69
I_1/I_2 max. = 2.83
I_1/I_2 av. = 1.98

The following results are quoted for comparison.

Payne-Scott (1) 85 Mc/s (I_1/I_2) av = 4

60 Mc/s " = 4

Shuter (35) 125 Mc/s " = 1.9

The author's average value for the ratio of peak heights of double-humped bursts is very close to that recorded by Shuter and is of the same order as those measured at lower frequencies. Values at intermediate frequencies would be required to draw any conclusions as to the possible variation of this ratio with frequency; we do however notice a tendency for the ratio to decrease with increasing frequency.

(iv) Time Delays between Peaks of Double-humped Bursts.

Summary of Author's Results
"t" max. = 6.44 secs.
"t" min. = .52 "
"t" av. = 2.40 "

Payne-Scott (1) recorded time delays of between 2 and 10 secs. at frequencies of 60 and 85 Mc/s: Shuter (35) records an average value of 7.4 secs. at 125 Mc/s.

The time-delay recorded depends on the frequency, and it will be more worthwhile to compare the velocities of the burst sources as calculated from the time-delays, with velocities calculated in the same way by other investigators working at different frequencies.

We have considered the possible formation of double-humped bursts by a source travelling radially outwards through successive plasma levels in the corona.

We may thus derive the velocity of the source if we know the heights in the solar atmosphere of the 300 Mc/s and 150 Mc/s plasma levels, and if we assume that the two peaks of double-humped burst observed at 300 Mc/s correspond to the times of arrival of the source at these two harmonic levels .

Using the expression

$$f_o^2 = \frac{Ne^2}{\pi m} \quad \text{(see p. 40)} \quad \ldots (5.2)$$

to convert the natural plasma frequency f_o to the corresponding electron density N, we then use the Baumbach-Allen expression (see p. 9) to find the height of the 150 Mc/s level above the photosphere:

$$N = (1.55\ r^{-6} + 2.99\ r^{-16})\ 10^{14}\ m^{-3}$$

i.e. $$N = (1.55\ r^{-6} + 2.99\ r^{-16})\ 10^{8}\ cm^{-3} \quad \ldots(5.3)$$

Thus the height of the 150 Mc/s level above the centre of the sun, "r", in units of the radius of the photosphere (6.96×10^5 km.) may be calculated.

The Baumbach-Allen formula holds only for the corona, and since the 300 Mc/s level lies in the chromosphere, we compute the height of this level from the equation

$$N = (5.72 \times 10^{11})e^{-7.7 \times 10^{4}(h-500)} \quad \ldots(5.4)$$

where "h" is the height of the level above the photosphere in km. (This equation is given by Cillié and Menzel (33)). As before, the value of the electron density N is calculated from equation 5.2.

Height of 150 Mc/s level above photosphere	h_1	2.905×10^4 km.
Height of 300 Mc/s level above photosphere	h_2	$.050 \times 10^4$ km.
Difference in height	h_1-h_2	2.855×10^4 km.

Assuming for simplicity that the disturbance is travelling outwards along the sun-earth axis, we may make an approximate correction for the extra path travelled by the 300 Mc/s radiation. If the radiation travels with the speed of light in vaccuo, c, the time taken by it to cover the distance between

the 300 and 150 Mc/s levels will be given by

$$\frac{h_1-h_2}{c} = \frac{2.855 \times 10^4}{3.0 \times 10^5} \text{ secs.} = 0.1 \text{ secs.}$$

Thus in calculating the velocity of the source from the time delay between the peaks of a double-humped burst, we should add a correction of 0.1 secs. to the observed time delay.

Source velocities calculated in this way for individual double-humped bursts are shown in table IV.

Summary of Author's Results	
V max.	5×10^4 km/sec.
V min.	$.4 \times 10^4$ "
V av.	2.2×10^4 "

cf. Wild (32) 70-130 Mc/s: $2\times10^4 < V(\text{km/sec.}) < 10\times10^4$.

Shuter (35) 125 Mc/s: $.6\times10^4 < V(\text{km/sec.}) < 4.1\times10^4$

V av = 1.9×10^4 km/sec.

The author's values for the source velocity show close agreement, both in amount of variation and in the average value, with Shuter's results. Both sets of results are in fair agreement with velocities calculated by Wild from the drift rates of dynamic spectra in the frequency range 70-130 Mc/s.

The agreement between the source velocities calculated in this way indicates that there is no

significant acceleration or deceleration of the source as it moves through the solar atmosphere.

B. TYPE I (STORM) BURSTS.

It has been shown in Chapter IV that sections of storm profiles may be analysed into a large number of bursts having the characteristic form of isolated bursts. It should be emphasised that the importance of this result is not merely that it was possible to obtain the resultant contour by adding large numbers of bursts having a linear rise and exponential decay. It is clear that by taking a large enough number of rapidly-decaying bursts, practically any given profile could be so analysed.

The justification for assuming that received storm profiles are made up of bursts of this form lies in the fact that, in the great majority of cases, subtraction of the intensity of the "tail" of one burst from the total intensity, gave a linear rise portion for the next burst. In other cases, linear rise portions subtracted from the total intensity gave exponential "tails" for the immediately preceding burst.

Furthermore, the slopes of both the rise and decay portions of the deduced bursts are very similar to those found in isolated bursts. The decay constants

for storm bursts are on the average higher than those for Type III bursts, but the difference is small and may not be significant in view of the relatively small number of isolated bursts analysed.

C. EXTENSION OF THE MODEL OF TYPE III BURST PRODUCTION TO TYPE I BURSTS.

In the light of the results discussed in section B, it will be beneficial to review the accepted model of Type III burst-production with a view to investigating its possible application to storm bursts.

We have adopted a model of Type III burst-production involving some sort of transient disturbance travelling radially outwards through the solar atmosphere, and exciting successive plasma levels. Oscillations set up in the plasma are then responsible for the radiation of a band of frequencies around the plasma frequency fo, and of harmonic bands around the central frequencies of 2fo, 3fo, etc. We have seen how consideration of the greater absorption suffered by the fundamental may explain the fact that the fundamental and first-harmonic bands appear to have comparable intensities, while the second-harmonic band is not sufficiently intense to be recorded. We have also concluded that the rate of

decay of these bursts is determined by the reduction in the effect of the source, rather than in terms of the natural decay of plasma oscillations.

Suppose we consider a similar mechanism for the production of storm bursts. We postulate that each storm burst is produced by a transient disturbance similar to those envisaged in the case of Type III bursts.

We would therefore predict that storm bursts would have

(i) bandwidths of the same order as those of Type III bursts, i.e. about 50 Mc/s.

(ii) an average value of decay constant similar to that for Type III bursts at the same frequency.

(iii) a frequency drift to lower frequencies.

Wild (34), using a swept frequency receiver operating between 70 and 130 Mc/s, reported, inter alia, the following characteristics of storm bursts.

(i) They have a narrow bandwidth of about 4 Mc/s.

(ii) Individual bursts show no frequency drift.

(iii) Harmonic pairs are not a feature of storm bursts, as they are of Type II and III bursts.

Before attempting to explain these characteristics in terms of modifications to our postulated model of storm-burst production, we should consider

more closely the problem of the escape of radiation from the solar atmosphere.

D. ESCAPE OF RADIATION FROM THE SOLAR ATMOSPHERE.

It has been tacitly assumed in the discussion of the propagation of radiation through the solar atmosphere that radiation produced at a given level in the solar atmosphere will be propagated towards the earth even though the source is not travelling along the sun-earth axis.

This assumption is partly justifiable for the case of Type III bursts, but in the case of narrow-band Type I bursts we should re-examine the problem.

It has been shown by Smerd (unpublished data, quoted by Wild et al (4)), that the critical escape frequency "fc" from a level of natural plasma frequency "fo" is given approximately by

$$fc = f_o \sec(.87\theta) \quad \ldots\ldots\ldots (5.5)$$

for source angles θ between 0° and 80° and for frequencies around 100 Mc/s. The equation gives in effect the maximum source angle for which radiation of a given frequency fc can reach the earth if produced at the level where the plasma frequency is fo.

We see that when fc = fo, $\theta = 0$, i.e. the plasma frequency can only be received from a source exactly at

the centre of the solar disk. However, for frequencies greater than fo, θ will take on a maximum value given by

$$(fo + \delta fo) = fo \sec (.87\ \theta)$$

and the value of θ_{max} will increase as δfo increases.

In the case of Type III bursts, having received bandwidths of the order of 50 Mc/s, we may calculate the value of θ, at the plasma level of natural frequency 100 Mc/s, for the central frequency of this band.

Thus

$$(100 + 25) = 100 \sec (.87\ \theta)$$

giving $\theta \doteq 44^{o}$.

For a typical Type II burst, the central frequency of the received band will be about 6 Mc/s above the plasma frequency, since typical outburst bandwidths are of the order of 12 Mc/s.

Calculating θ as above, we have $\theta \doteq 22^{o}$.

This value of θ may be derived in another way, providing a useful check. We have noted that the ratio of central frequencies of harmonic-pair outbursts recorded by Wild et al (28) are of the order of 1.90. Thus the plasma frequency is lower than the central frequency of the escaping radiation by a factor of $\frac{1}{2}(1.90) = .95$.

Substituting this value for $\frac{fo}{fc}$ in Smerd's

equation we have $\theta = 21^{\circ}$.

We see that Type III radiation will be received from a fairly large portion of the solar disk, and Type II radiation from a smaller portion. In both cases substitution of fc = 2fo into Smerd's equation gives $\theta = 69^{\circ}$, indicating that the first-harmonic band will be received for sources situated almost anywhere on the solar disk.

The limitations described above apply even more stringently to storm bursts: a bandwidth of 4 Mc/s gives a typical value of θ of 13°. Once again the first-harmonic band will be received for source angles up to 69°.

In view of the results of Loughhead *et al* (10), who observed that solar bursts are received from practically the whole solar disk, we are led to the conclusion that a considerable proportion of radiation received at a frequency fo is in fact first-harmonic radiation generated at the fo/2 level. Bursts having no harmonic band associated with them may then be considered as being caused by sources having a relatively large source-angle; bursts with associated harmonic bands would be ascribed to sources having source angles within the limits derived above. (This hypothesis is mentioned by Wild *et al* (4) and satisfactorily explains the unusually

large source heights derived by Payne-Scott and Little (36) from their directional observations. Assuming the received band to be first-harmonic radiation, source-heights in agreement with Baumbach-Allen predictions are obtained).

On this basis we expect the occurrence of harmonic pairs in storm bursts to be very low; only for sources very near the centre of the sun would harmonic pairs be recorded.

E. POSSIBLE MODELS OF STORM-BURST PRODUCTION.

Wild et al have used Smerd's equation (5.5) to plot the variation of source angle as well as the height, of an observed outburst, with time. This particular outburst had a very slow frequency-drift with time, and we observe the following interesting characteristics:

(i) The burst has a considerably narrower bandwidth than, for example, the burst illustrated in Fig. 3:3 (behind p. 45). The latter burst has a relatively large frequency-drift with time. A study of several dynamic spectra reproduced in this paper indicates that the bandwidth may in fact be a function of the drift-rate. In Fig. 5:3 several such dynamic spectra are reproduced, and a narrowing of the bandwidth as the drift-rate decreases is clearly observed in each

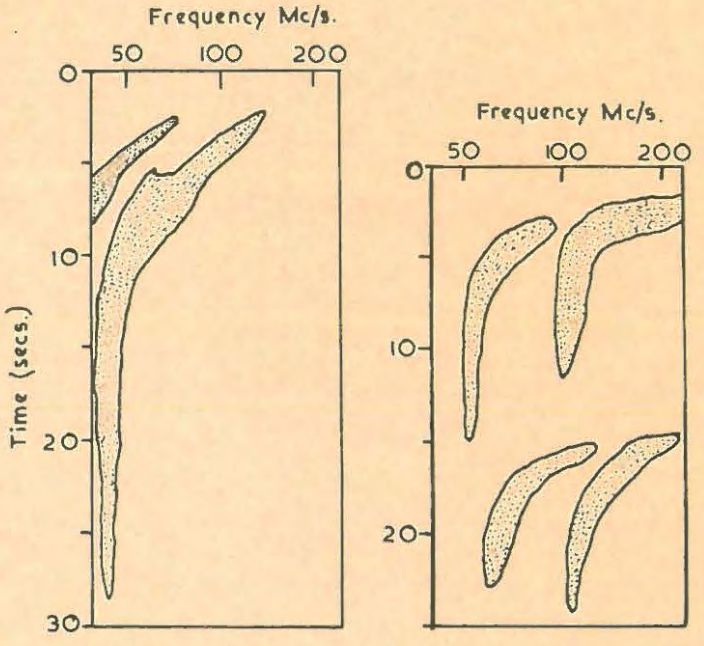

Dynamic spectra of some Type III bursts, showing the narrowing of the bandwidth with decreasing frequency drift rate.
(Wild Murray & Rowe (4)).

FIGURE 5:3

burst.

This dependence of bandwidth on frequency drift-rate is recognised by Wild (32) and by Pawsey and Smerd (37). A search of the literature has revealed no attempt to explain this phenomenon theoretically and we shall refer to it in the empirical form stated above.

Assuming then that the bandwidth of the received radiation is a function of the drift-rate, we would expect the bandwidths of bursts to be smallest for Type I (drift-rate zero), larger for Type II (slow drift) and largest for Type III (fast drift-rate). This is in good agreement with observation, since the three burst types have bandwidths of the order of 4 Mc/s, 12Mc/s and 50 Mc/s respectively.

(ii) The greater portion of the deduced motion of the outburst source was across the line of sight (see Fig. 5:4).

Suppose now we consider a source moving exactly parallel to the surface of the photosphere and exciting a narrow band of frequencies around the corresponding plasma frequency. This band of frequencies would exhibit no drift of the frequency of maximum intensity with time.

We have seen that the observed bandwidth, lack of frequency drift, and lack of associated harmonic

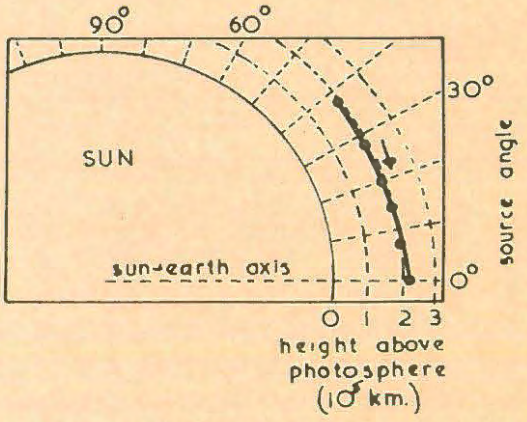

Successive positions of the source of an observed outburst at half mn. intervals. Wild Murray & Rowe (4).

FIGURE 5:4

bursts may be explained in terms of a source travelling in rather than through a level of plasma frequency f. The fundamental band of frequencies would in general not be received and the burst would be observed only at a frequency 2f.

In seeking a possible model for a source which would behave in the manner outlined above, we should consider the correlation of noise storms with the occurrence of sunspots. The most important effect on the corona of the presence of a sunspot is the existence above the sunspot of a large magnetic field. Since there is no evidence which suggests that particle streams are ejected from sunspots, and since such a stream would be expected to cause a burst with a frequency drift such as those associated with Type II and Type III bursts, we are led to the conclusion that the disturbances causing storm bursts must have the following characteristics:

(i) They must be short-lived (fraction of a second)

(ii) each disturbance must take place in a localized area.

(iii) successive disturbances should occur at random heights in the corona and should not be related to one another.

The most likely disturbance to fit all these

conditions seems to be an electrical discharge in the corona. Ryle (21) has shown (see p. 37) that such discharges are likely in the strong magnetic fields above sunspots. He has also indicated that such discharges could produce electron temperatures of sufficient magnitude to account for the intensity of the observed radiation. Such a "thermal" mechanism would not account for the similarity in shape of Type I and Type III bursts; however it is possible that such a discharge would cause a sudden discontinuity in the conditions obtaining in a small area of the corona. Such a discontinuity might well fit the conditions for a Jaeger-Westfold transient (see p. 42). It is beyond the scope of this work to justify this hypothesis theoretically.

POLARIZATION.

Since storm bursts are known to be strongly circularly polarized, while Type III bursts may be unpolarized or elliptically polarized, we should examine whether this difference can be explained on the author's model of storm-burst production.

We may explain the polarization of radiation in terms of either the generation mechanism or in terms of the propagation conditions in the medium between the source and the observer. Komesaroff (3) states

that polarization may be imposed by the medium in two ways:

(i) The radiation may pass through a region in which the refractive index for the extraordinary propagation mode is zero. In this case only the ordinary mode is transmitted, and the radiation will be completely polarized. However, the first-harmonic band will be well outside its"E stop-band" and cannot be polarized in this way.

Now in Type III harmonic-pair bursts of which the fundamental is polarized, the first-harmonic radiation exhibits similar polarization, indicating that the above mechanism does not provide the explanation for the polarization of Type III bursts. If, as the author suggests, the greater part of received storm-burst radiation is actually first-harmonic radiation, this argument applies with equal force to storm bursts.

(ii) Differential absorption of the O and E modes along the path of propagation, an effect which depends on the electron collision frequency, may cause partial polarization. Once again this effect would be virtually negligible for first-harmonic radiation, since both O and E components would be produced well away from their respective levels of zero refractive index.

Thus the absorption suffered by each component would be practically zero.

Komesaroff concludes that at least Type III bursts showing harmonic structure originate in a source which emits polarized radiation. The arguments given above show that this conclusion applies also to Type I bursts.

The author has suggested that Type I and Type III bursts are produced in much the same manner, and at similar levels in the corona. An explanation of the polarization of Type III radiation in terms of a generation mechanism would apply also to Type I radiation; the actual type of polarization produced will depend upon conditions obtaining in the localized area of the corona where the radiation is generated.

Thus radiation originating in a strong magnetic field (e.g. storm bursts) may be generated with different polarization from bursts originating in a very weak magnetic field (e.g. unpolarized Type III bursts). The occurrence of polarized Type III bursts may then be explained in terms of sources near to a sunspot group, and therefore subjected to a strong magnetic field.

F. CONCLUSION.

The production of "storm bursts" of solar radio

noise may be tentatively explained in terms of sporadic, short-lived transients of the Jaeger-Westfold type, perhaps associated with electric discharges in the solar atmosphere above sunspots.

These bursts would in general be generated at the plasma level corresponding to half the observed frequency; harmonic pairs of storm bursts should be recorded only for sources very near the centre of the solar disk.

It is suggested that polarization of both Type I and Type III radiation may best be explained in terms of a generation mechanism, the amount and type of polarization being dependent on the magnetic field to which the source is subjected.

Some methods of investigating these conclusions further are suggested in the final chapter.

CHAPTER SIX

SUGGESTIONS FOR FURTHER RESEARCH.

A. FURTHER INVESTIGATION OF THE AUTHOR'S MODEL FOR STORM-BURST PRODUCTION.

(i) The author has suggested that electric discharges in the corona might be a possible cause of storm bursts. A theoretical study of the effect on a plasma of an electric discharge in it would settle this question. The conditions in a discharge tube are not entirely analogous to those in the corona, but a study of a similar occurrence in a discharge tube should at least indicate whether this model is feasible.

(ii) The author has shown that harmonic-pair storm bursts should be recorded for sources close to the centre of the solar disk. A study of swept-frequency recordings during the occurrence of a large sun-spot near the centre of the solar disk would resolve this problem.

B. BURST PROFILES.

The author's conclusions with regard to the shapes of bursts have been limited in validity by the following considerations:

(i) the low speed of the recording film in the "x" direction has caused "bunching" of the records and has limited the accuracy of measurement of the rate of decay.

(ii) lack of time has limited the total number of records available for analysis, and the number of storm sections analysed. The variation of decay constant with frequency is still imperfectly known, and a thoroughly reliable value of "k" for 300 Mc/s can only be computed if a considerable number of bursts are available for analysis.

(iii) the lack of simultaneous recordings at another frequency, preferably harmonically related to 300 Mc/s, has severely limited the scope of the research.

The limitations (i) and (iii) mentioned above, could be overcome with relatively little modification to existing equipment and it is suggested that a more detailed study of the profiles of all three types of burst would be most rewarding. The following points would merit particular attention:

(i) The accurate determination of "kav" for a large number of Type III bursts

(ii) The accurate determination of "kav" for storm bursts and for outbursts, with resulting con-

clusions as to whether the decay constant is a property of the burst type, the frequency, or both.

(iii) The correlation of the existence or otherwise of harmonic pairs in all three types of burst with the position of the source on the solar disk, with a view to testing the limitations prescribed by Smerd's relation

$$f_c = f_o \sec (.87\theta).$$

REFERENCES.

(1)	PAYNE-SCOTT, R.	"Bursts of Solar Radiation at metre wavelengths."	Aust. J. Sci. Res. 2, p.214 1949.
(2)	WILD, J.P. McCREADY, L.L.	"Observations of the spectrum of high-intensity radiation at metre wave-lengths."	Aust.J.Sci.Res. A3,No.3,p.387 1950
(3)	KOMESAROFF, M.	"Polarization measurements of the three spectral types of Solar Radio Burst.	Aust.J.Phys. 2,No.2,p.201 1958.
(4)	WILD, J.P. MURRAY, J.D. ROWE, W.C.	Harmonics in the spectra of Solar Radio Disturbances".	Aust.J.Phys. 7,No.3,p.439 1954
(5)	MAXWELL, A. SWARUP, G.	"A new spectral characteristic in Solar Radio Emission".	Nature. 181,No.4601,p.37 1958.
(6)	ROBERTS, J.A.	"Evidence of echoes in the Solar Corona from a new type ofRadio Burst"	Aust.J.Phys. 2,No.2,p.215 1958
(7)	WILLIAMS, S.E.	"The shape of pulses of r.f. radiation from the Sun".	Nature. 162,p.108 1943
(8)	ALLEN, C.W.	"Interpretation of Electron Densities from Corona Brightness".	Mon.Not.R.Astr.Soc. 107, p.426 1947
(9)	GIOVANELLI, R.G. ROBERTS, J.A.	"Optical Observations of the solar disturbances causing Type II Radio Bursts".	Aust.J.Phys. 2,No.3,p.353 1958
(10)	LOUGHHEAD, R.E. ROBERTS, J.A. McCABE, M.K.	"Association of Solar Radio Bursts of Spectral Type III with chromospheric flares."	Aust.J.Phys. 10,No.4,p.483 1957
(11)	GIOVANELLI, R.G.	"Flare-puffs as a cause of Type III Bursts"	Aust.J.Phys. 2,No.3,p.350 1958

(12)	DODSON, H.W. HEDEMAN, E.R. CHAMBERLAIN, J.	"Ejection of hydrogen and ionized Calcium atoms at the time of Solar Flares".	Astrophys.J. 117, No.1, p.66 1953
(13)	DODSON, H.W. HEDEMAN, E.R. OWREN, L.	"Solar Flares and associated 200Mc/s radiation".	Astrophys.J. 118, No.2, p.169 1953
(14)	DODSON, H.W. HEDEMAN, E.R. COVINGTON, A.E.	Solar Flares and associated 2800 Mc/s radiation".	Astrophys.J. 119, No.3, p.541 1954
(15)	DODSON, H.W. HEDEMAN, E.R. McMATH? R.R.	"Photometry of Solar Flares".	Astrophys.J. Supp. No.20 2, p.241 1956
(16)	ROBERTS, W.K.	"A New Wide-Band Balun".	Proc.I.R.E. 45, No.12, p.1628 1957
(17)	GODFRAY, H.	"A Treatise on Astronomy".	MacMillan & Co. 1894
(18)	-	"A crystal-controlled converter for 432 Mc/s".	Radio Amateur's Handbook. p.403 1957
(19)	KELLER, J.W.	"Regulated Transistor Power Supply Design."	Electronics. p.156 Nov. 1956
(20)	RYLE, M. VONBERG, D.D.	"An Investigation of r.f. Radiation from the Sun".	Proc.Roy.Soc.A. 193, No.1032, p.98 1948
(21)	RYLE, M.	"The generation of r.f. radiation in the Sun".	Proc.Roy.Soc.A. 195, No.1040, p.32 1948
(22)	APPLETON, E.E.	"Wireless studies of the Ionosphere".	J.Inst.E.E. 71, p.642 1932
(23)	WESTFOLD, K.C.	"The Wave Equations for Electromagnetic radiation in an ionized medium in a magnetic field".	Aust.J.Sci.Res.A. 2, No.2, p.169 1949
(24)	RYLE, M.	"The significance of the observation of intense r.f. emission from the Sun".	Proc.Phys.Soc.A. 62, part8, p.483 1949

(25)	JAEGER, J.C. WESTFOLD, K.C.	"Equivalent path and Absorption for electro-magnetic radiation in the Solar Corona".	Aust.J.Sci.Res.A. 3,No.3,p.376 1950
(26)	JAEGER,J.C. WESTFOLD, K.C.	"Transients in an ionised medium with applications to Bursts of Solar Noise".	Aust.J.Sci.Res.A 2,No.3,p.322 1949
(27)	SMERD, S.F.	"A radio-frequency repre-sentation of the Solar Atmosphere".	Proc.I.E.E. 97,No.50,p.447 1950
(28)	WILD, J.P. MURRAY, J.D. ROWE, W.C.	"Evidence of Harmonics in the spectrum of a Solar Radio Outburst".	Nature. 172,p.533 1953
(29)	WILD, J.P. ROBERTS, J.A. MURRAY, J.D.	"Radio Evidence of the Ejection of very fast particles from the Sun".	Nature. 173,p.532 1954.
(30)	KRUSE, U.E. MARSHALL,L. PLATT, J.R.	"Synchrotron Radiation in the Sun's Radio Spectrum".	Astrophys.J. 124,No.3,p.601 1956
(31)	WESTFOLD, K.C.	"Magneto-hydrodynamic shock waves in the Solar Corona ....."	Phil.Mag. 2,No.23,p.1237 1957
(32)	WILD, J.P.	"Observations of the spectrum of high-intensity Solar Radiation...Part III - Isolated Bursts".	Aust.J.Sci.Res.A. 3,No.4,p.541 1950
(33)	GILLIE, D.G. MENZEL, D.H.	"Physical State of the Solar Chromosphere".	Harvard Coll.Obs. Circ.No.410 1936
(34)	WILD, J.P.	"Observations of the spectrum of High-Intensity Solar Radiation...Part IV - Enhanced Radiation".	Aust.J.Sci.Res.A. 4,No.1,p.36 1951
(35)	SHUTER, W.H.	"An investigation of Iso-lated Bursts of Solar Radio Noise".	M.Sc. thesis (Rhodes Univ.) 1958.
(36)	PAYNE-SCOTT, R. LITTLE, A.G.	"The position and move-ment on the Solar disk of sources of radiation ...III - Outbursts	Aust.J.Sci.Res.A. 5,p.32 1952

(37) PAWSEY, J.L. SMERD, S.F. "Solar Radio Emission". Chp.7 of "The Sun" Editor: Kuiper, G.P. Univ. of Chicago Press. 1953.

In addition the following books were used as general references:

(a) PAWSEY, J.L. BRACEWELL, R.N. "Radio Astronomy" Oxford Press. 1955

(b) KUIPER, G.P. (ed.) "The Sun" Univ. of Chicago Press. 1953

(c) ELLISON, M.A. "The Sun and its Influence". Routledge and Kegan Paul. 1955

(d) SCHELKUNOFF, S.A. FRIIS, H.T. "Antennas: Theory and Practice". Chapman and Hall. 1952